

**FRACTURE MODELING AND FLOW BEHAVIOR IN SHALE GAS
RESERVOIRS USING DISCRETE FRACTURE NETWORKS**

A Thesis

by

JOACHIM NWABUNWANNE OGBECHIE

Submitted to the Office of Graduate Studies of
Texas A&M University
in partial fulfillment of the requirements for the degree of
MASTER OF SCIENCE

December 2011

Major Subject: Petroleum Engineering

**FRACTURE MODELING AND FLOW BEHAVIOR IN SHALE GAS
RESERVOIRS USING DISCRETE FRACTURE NETWORKS**

A Thesis

by

JOACHIM NWABUNWANNE OGBECHIE

Submitted to the Office of Graduate Studies of
Texas A&M University
in partial fulfillment of the requirements for the degree of

MASTER OF SCIENCE

Approved by:

Chair of Committee,	David S. Schechter
Committee Members,	Jerome J. Schubert
	Yuefeng Sun
Head of Department,	Stephen A. Holditch

December 2011

Major Subject: Petroleum Engineering

ABSTRACT

Fracture Modeling and Flow Behavior in Shale Gas Reservoirs
Using Discrete Fracture Networks.

(December 2011)

Joachim Nwabunwanne Ogbechie, B.Eng., University of Benin

Chair of Advisory Committee: Dr. David S. Schechter

Fluid flow process in fractured reservoirs is controlled primarily by the connectivity of fractures. The presence of fractures in these reservoirs significantly affects the mechanism of fluid flow. They have led to problems in the reservoir which results in early water breakthroughs, reduced tertiary recovery efficiency due to channeling of injected gas or fluids, dynamic calculations of recoverable hydrocarbons that are much less than static mass balance ones due to reservoir compartmentalization, and dramatic production changes due to changes in reservoir pressure as fractures close down as conduits. These often lead to reduced ultimate recoveries or higher production costs.

Generally, modeling flow behavior and mass transport in fractured porous media is done using the dual-continuum concept in which fracture and matrix are modeled as two separate kinds of continua occupying the same control volume (element) in space. This type of numerical model cannot reproduce many commonly observed types of fractured reservoir behavior since they do not explicitly model the geometry of discrete fractures, solution features, and bedding that control flow pathway geometry. This

inaccurate model of discrete feature connectivity results in inaccurate flow predictions in areas of the reservoir where there is not good well control.

Discrete Fracture Networks (DFN) model has been developed to aid in solving some of these problems experienced by using the dual continuum models. The Discrete Fracture Networks (DFN) approach involves analysis and modeling which explicitly incorporates the geometry and properties of discrete features as a central component controlling flow and transport. DFN are stochastic models of fracture architecture that incorporate statistical scaling rules derived from analysis of fracture length, height, spacing, orientation, and aperture.

This study is focused on developing a methodology for application of DFN to a shale gas reservoir and the practical application of DFN simulator (FracGen and NFlow) for fracture modeling of a shale gas reservoir and also studies the interaction of the different fracture properties on reservoir response. The most important results of the study are that a uniform fracture network distribution and fracture aperture produces the highest cumulative gas production for the different fracture networks and fracture/well properties considered.

ACKNOWLEDGEMENTS

I would like to thank my committee chair, Dr. Schechter, and my committee members, Dr. Schubert, and Dr. Sun for their guidance and support throughout the course of this research. I would also like to specially thank Mark McCoy and Seth King of the National Energy Technology Laboratory (NETL) for their tremendous support in this project.

My gratitude also goes to Dr. Gildin for his support during the initial phase of this work. Thanks also go to my friends and colleagues and the department faculty and staff for making my time at Texas A&M University a great experience.

Finally, I want to especially thank my parents for their support and encouragement and my brothers and sister for being there for me always.

NOMENCLATURE

DFN	Discrete fracture network
DP/DK	Dual porosity/dual permeability
DP	Dual porosity
t	Time
<i>km</i>	Matrix permeability
<i>kf</i>	Fracture permeability
md	Millidarcy
nd	Nanodarcy
SD	Standard deviation
Frac	Fracture
Cv	Coefficient of variation
CI	Connectivity index
HF	Hydraulic fracture
cum	Cumulative
FA	Fracture aperture
FD	Fracture density
FL	Fracture length
HFA	Hydraulic fracture aperture
HFL	Hydraulic fracture length
NFS	Number of hydraulic fracture stages

TABLE OF CONTENTS

		Page
ABSTRACT		iii
ACKNOWLEDGEMENTS		v
NOMENCLATURE		vi
TABLE OF CONTENTS		vii
LIST OF FIGURES.....		xi
LIST OF TABLES		xviii
 CHAPTER		
I	INTRODUCTION.....	1
	1.1 Motivation.....	3
	1.2 Objective	4
	1.3 Methodology	4
II	FRACTURE LITERATURE REVIEW.....	5
	2.1 Fractured Reservoir	5
	2.2 Fracture.....	5
	2.3 Geometrical Description of Fractures	6
	2.4 Fracture Mechanisms or Origins (Nelson, 2001)	7
	2.4.1 Tectonic	7
	2.4.2 Non-Tectonic	7
	2.5 Naturally Fractured Reservoir (NFR)	7
	2.6 Classification of Naturally Fractured Reservoirs (Nelson, 2001).....	8
	2.7 Fracture Properties Definitions	10
	2.7.1 Fracture Density	10
	2.7.2 Fracture Length	10
	2.7.3 Fracture Aperture	10
	2.7.4 Fracture Systems	10
	2.7.5 Fracture Cluster	10
	2.7.6 Fracture Intensity	10

CHAPTER	Page
2.7.7 Fracture Network.....	10
2.7.8 Fracture Orientation	11
2.7.9 Fracture Spacing.....	11
2.7.10 Fracture Porosity	12
2.7.11 Fracture Permeability	13
2.8 Statistical Analysis in Fracture Characterization	13
2.8.1 Histograms	14
2.8.2 Geometrical Models	14
2.8.3 Log – Normal Distribution (Davis, 1986).....	14
2.8.4 Exponential Law (Bonnet et al., 2001).....	15
2.8.5 Gamma Law (Bonnet et al., 2001)	16
2.8.6 Power Law (Bonnet et al., 2001).....	16
2.9 Statistical Methods for Measuring Fracture Size Distributions	18
2.9.1 Frequency	18
2.9.2 Frequency Density.....	18
2.9.3 Cumulative Frequency Distributions	18
 III FRACTURE CHARACTERIZATION AND MODELLING	 20
3.1 Fracture Modeling.....	20
3.2 Fracture Modeling Approach	23
3.2.1 Continuum Model	24
3.2.1.1 Dual Porosity.....	25
3.2.1.2 Dual Porosity/Dual Permeability	25
3.2.1.3 Dual Porosity Model Types.....	26
3.2.2 Discrete-Fracture Network (DFN) Models	27
3.2.2.1 Deterministic Modeling Method	28
3.2.2.2 Stochastic Modeling Method	28
 IV ANALYTICAL APPROACH.....	 30
4.1 Study Approach.....	30
4.2 DFN Simulator (FracGen and NFlow)	31
4.2.1 FracGen: Fracture Network Generation (Boyle et al., 2010).....	31
4.2.1.1 Connectivity Control in FracGen (Hatzignatiou and McKoy, 2000).....	32
4.2.2 NFlow Natural Gas Flow Modeling	34
4.3 Ancillary Program	36
4.3.1 Fracture Aperture Reduction Model (FARM)	36
4.4 Summary of Sample Files for FracGen and NFlow	

CHAPTER	Page
(Boyle et al., 2010).....	36
4.5 Mechanism for Fracture Generation in FracGen.....	38
4.6 Drainage of Complex Fracture Network and Matrix	40
4.7 Approach: Mathematical/Numerical Model.....	40
4.7.1 Fracture Flow	43
4.7.2 Matrix Flow.....	45
4.7.3 Initial & Boundary Conditions	45
4.8 Flow Behavior Fractured Networks	46
4.8.1 Fracture Connectivity	46
4.8.2 Fracture Scalability	47
4.9 Parameters for Quantifying Connectivity in Fracture Networks	47
 V FRACTURE MODELLING OF A SHALE GAS RESERVOIR USING FRACGEN AND NFFLOW	 50
5.1 Modeling Approach.....	50
5.2 Fracture Modeling Procedure.....	51
5.3 Case 1: Uniformly Distributed Fracture Pattern of One Fracture Set	53
5.3.1 Fracture Aperture	57
5.3.2 Fracture Density	59
5.3.3 Fracture Length	61
5.3.4 Number of Hydraulic Fracture Stages.....	64
5.3.5 Hydraulic Fracture Aperture	65
5.3.6 Hydraulic Fracture Length	67
5.4 Case 2: Clustered Fracture Pattern of One Fracture Set.....	70
5.4.1 Fracture Length	73
5.4.2 Fracture Density	75
5.4.3 Fracture Aperture	76
5.4.4 Hydraulic Fracture Aperture	77
5.4.5 Hydraulic Fracture Length	78
5.4.6 Number of Hydraulic Fracture Stages	80
5.5 Case 3: Uniformly Distributed Fracture Pattern of Two Fracture Sets.....	81
5.5.1 Fracture Aperture	83
5.5.2 Fracture Density	85
5.5.3 Fracture Length	86
5.5.4 Number of Hydraulic Fracture Stages.....	87
5.5.5 Hydraulic Fracture Aperture	88
5.5.6 Hydraulic Fracture Length	90
5.6 Case 4: Two Fracture Sets With One Clustered	

CHAPTER	Page
and the Other Uniformly Distributed	91
5.6.1 Fracture Aperture	94
5.6.2 Fracture Density	96
5.6.3 Fracture Length	99
5.6.4 Number of Hydraulic Fracture Stages.....	101
5.6.5 Hydraulic Fracture Aperture	102
5.6.6 Hydraulic Fracture Length	104
5.7 Fracture/Well Properties Comparison Plots.....	106
5.7.1 Fracture Networks	106
5.7.2 Fracture/Well Property	107
5.7.3 Hydraulic Fracture Stages	108
VI CONCLUSIONS AND RECOMMENDATIONS.....	109
6.1 Conclusion.....	109
6.2 Recommendations	110
REFERENCES	111
APPENDIX 1	115
APPENDIX 2	145
VITA	152

LIST OF FIGURES

FIGURE	Page
2.1 Schematic representation of a fault and a joint (Golf-Racht, 1982).....	6
2.2 Geometric parameters associated with a discontinuity, the gap between the two surfaces is exaggerated to illustrate the aperture (Jing and Stephansson, 2007)	7
2.3 Schematic cross plot of percent reservoir porosity versus percent reservoir permeability (percent due to matrix versus percent due to fractures) for the fractured reservoir classification (Nelson, 2001)	9
2.4 Plot illustrating the four different functions (power, lognormal, exponential and gamma law) most often used to fit data sets. Data over more than 1 order of magnitude are needed before these different distributions can be easily distinguished (Bonnet et al., 2001)	17
3.1 Dual-porosity model (Warren and Root, 1963)	24
3.2 Illustration of dual porosity/single permeability and dual porosity permeability models (Schlumberger, 2010)	26
3.3 Illustration of the 3 types of dual porosity models (Reiss, 1980).....	27
4.1 Diagram showing the major features of (a) strata-bound (b) non-strata-bound joint systems (Odling et al., 1999)	30
4.2 Fundamental spatial patterns of points (1-D & 2-D) (McKoy and Sams, 1997).....	38
4.3 Fundamental distributions of spacing that arise from the fundamental spatial patterns of points (McKoy and Sams, 1997).....	40
4.4 Schematic of fracture network and flow nodes modeling (Hatzignatiou, 1999).....	41
4.5 Diagram showing fracture networks below (a) and above (b) the percolation threshold and also the backbone network (c) (Odling et al., 1999).....	48

FIGURE	Page
5.1 FracGen and NFlow simulation process	52
5.2 FracGen fracture map showing the well profile of the reservoir for case 1	54
5.3 3d representation of the well and fracture distribution.....	55
5.4 NFlow output showing the simulation result for case 1	56
5.5 Change in pressure response due to increase in fracture aperture for case 1	58
5.6 Change in cum. gas produced due to increase in fracture aperture for case 1	58
5.7 Change in pressure response due to decrease in fracture density for case 1	59
5.8 Change in pressure response due to increase in fracture density for case 1	59
5.9 Change in cum. gas produced due to decrease in fracture density for case 1	60
5.10 Change in cum. gas produced due to increase in fracture density for case 1	60
5.11 Change in pressure response due to decrease in fracture length for case 1	61
5.12 Change in pressure response due to increase in fracture length for case 1	61
5.13 Change in cum. gas produced due to decrease in fracture length for case 1	62
5.14 Change in cum. gas produced due to increase in fracture length for case 1	62
5.15 Change in cum. gas produced due to increase fracture property for case 1	63

FIGURE	Page
5.16 Change in cum. gas produced due to decrease in fracture property for case 1.....	63
5.17 Change in pressure due for different hydraulic fracture stages for case 1.....	64
5.18 Change in cum. gas produced for different numbers of hydraulic fracture stages for case 1	64
5.19 Change in pressure due to decrease in hydraulic fracture aperture for case 1.....	65
5.20 Change in pressure due to increase in hydraulic fracture aperture for case 1.....	65
5.21 Change in cum. gas produced due to decrease in hydraulic fracture aperture for case 1	66
5.22 Change in cum. gas produced due to increase in hydraulic fracture aperture for case 1	66
5.23 Change in pressure due to decrease in hydraulic fracture length for case 1.....	67
5.24 Change in pressure due to increase in hydraulic fracture length for case 1.....	67
5.25 Change in cumulative gas produced due to decrease in hydraulic fracture length for case 1	68
5.26 Change in cumulative gas produced due to increase in hydraulic fracture length for case 1	68
5.27 FracGen fracture map showing the well profile for case 2.....	72
5.28 NFflow output showing the simulation result for case 2.....	72
5.29 Change in pressure response due to increase in fracture length for case 2.....	74

FIGURE	Page
5.30 Change in cum. gas produced due to increase in fracture length for case 2	74
5.31 Change in pressure response due to increase in fracture density for case 2.....	75
5.32 Change in cum. gas produced due to increase in fracture density for case 2.....	75
5.33 Change in pressure due to increase in fracture aperture for case 2.....	76
5.34 Change in cum. gas produced due to increase in fracture aperture for case 2.....	76
5.35 Change in pressure due to increase in hydraulic fracture aperture for case 2.....	77
5.36 Change in cum. gas produced due to increase in hydraulic fracture aperture for case 2	77
5.37 Change in pressure due to decrease in hydraulic fracture length for case 2.....	78
5.38 Change in pressure due to increase in hydraulic fracture length for case 2.....	78
5.39 Change in cum. gas produced due to decrease in hydraulic fracture length for case 2	79
5.40 Change in cum. gas produced due to increase in hydraulic fracture length for case 2	79
5.41 Change in pressure response due to change in hydraulic fracture stages for case 2.....	80
5.42 Change in cum. gas production due to change in hydraulic fracture stages for case 2.....	80
5.43 FracGen fracture map showing the well profile for case 3.....	82

FIGURE	Page
5.44 NFlow output showing the simulation result for case 3	82
5.45 Change in pressure response due to increase in fracture aperture for case 3	84
5.46 Change in cum. gas production due to increase in fracture aperture for case 3	84
5.47 Change in pressure response due to increase in fracture density for case 3	85
5.48 Change in cum. gas production due to increase in fracture density for case 3	85
5.49 Change in pressure response due to increase in fracture length for case 3	86
5.50 Change in cum. gas production due to increase in fracture length for case 3	86
5.51 Change in pressure for different hydraulic fracture stages for case 3	87
5.52 Change in cum. gas production for different hydraulic fracture stages for case 3	87
5.53 Change in pressure due to decrease in hydraulic fracture aperture for case 3	88
5.54 Change in pressure due to increase in hydraulic fracture aperture for case 3	88
5.55 Change in cum. gas produced due to decrease in hydraulic fracture aperture for case 3	89
5.56 Change in cum. gas produced due to increase in hydraulic fracture aperture for case 3	89
5.57 Change in pressure due to increase in hydraulic fracture length for case 3	90
5.58 Change in cumulative gas produced due to increase in hydraulic fracture length for case 3	90

FIGURE	Page
5.59 FracGen fracture map showing the well profile for case 4.....	92
5.60 NFflow output showing the simulation result for case 4.....	93
5.61 Change in pressure response due to decrease in fracture aperture for case 4.....	94
5.62 Change in pressure response due to increase in fracture aperture for case 4.....	95
5.63 Change in cum. gas production due to decrease in fracture aperture for case 4.....	95
5.64 Change in cum. gas production due to increase in fracture aperture for case 4	96
5.65 Change in pressure response due to decrease in fracture density for case 4.....	97
5.66 Change in pressure response due to increase in fracture density for case 4.....	97
5.67 Change in cum. gas production due to decrease in fracture density for case 4.....	98
5.68 Change in cum. gas production due to increase in fracture density for case 4.....	98
5.69 Change in pressure response due to decrease in fracture length for case 4.....	99
5.70 Change in pressure response due to increase in fracture length for case 4	99
5.71 Change in cum. gas production due to decrease in fracture length for case 4.....	100
5.72 Change in cum. gas production due to increase in fracture length for case 4.....	100
5.73 Change in pressure due to increase in hydraulic fracture stages for case 4.....	101

FIGURE	Page
5.74 Change in cumulative gas production due to change in hydraulic fracture stages for case 4	101
5.75 Change in pressure due to decrease in hydraulic fracture aperture for case 4.....	102
5.76 Change in pressure due to increase in hydraulic fracture aperture for case 4.....	102
5.77 Change in cum. gas produced due to decrease in hydraulic fracture aperture for case 4	103
5.78 Change in cum. gas produced due to increase in hydraulic fracture aperture for case 4	103
5.79 Change in pressure due to decrease in hydraulic fracture length for case 4.....	104
5.80 Change in pressure due to increase in hydraulic fracture length for case 4.....	104
5.81 Change in cum. gas produced due to decrease in hydraulic fracture length for case 4	105
5.82 Change in cum. gas produced due to increase in hydraulic fracture length for case 4	105
5.83 Change in cum. gas production for different fracture networks.....	106
5.84 Change in cum. gas production for different fracture /well property.....	107
5.85 Change in cum. gas production for different hydraulic fracture stages	108

LIST OF TABLES

TABLE	Page
5.1 Fracture/well properties classification	51
5.2 Reservoir parameters for an Eagle Ford shale gas well for case 1	53
5.3 Control data fed into FracGen for case 1	54
5.4 Summary of fracture/well parameters for case 1.....	57
5.5 Summary of effect of fracture property on reservoir response for case 1	69
5.6 Reservoir parameters for an Eagle Ford shale gas well for case 2	70
5.7 Control data fed into FracGen for case 2	71
5.8 Summary of fracture/well parameters plotted for case 2	73
5.9 Reservoir parameters for an Eagle Ford shale gas well for case 3	81
5.10 Control data fed into FracGen for case 3	81
5.11 Data variation fed into FracGen for the primary fracture set for case 3	83
5.12 Reservoir parameters for an Eagle Ford shale gas well for case 4	91
5.13 Control data fed into FracGen for case 4	92
5.14 Data fed into FracGen for the different fracture properties for case 4.....	94
A2.1 Case 1 fracture length FracGen input calculation	145
A2.2 Case 1 fracture density FracGen input calculation.....	146
A2.3 Case 2 fracture length FracGen input calculation	147

TABLE	Page
A2.4 Case 2 fracture density FracGen input calculation.....	148
A2.5 Case 3 fracture length FracGen input calculation	149
A2.6 Case 3 fracture density FracGen input calculation.....	149
A2.7 Case 4 fracture length FracGen input calculation	151
A2.8 Case 4 fracture density FracGen input calculation.....	151

CHAPTER I

INTRODUCTION

As the world's conventional oil and gas fields are being depleted, the need to develop marginal and the more heterogeneous fields (fractured reservoirs) will become increasingly important.

Since the movement of hydrocarbons and other fluids in fractured reservoirs or in conventional reservoirs with significant fracture permeability often is not as expected or predicted. This behavior is due to the presence of fractures in these reservoirs which significantly affects the mechanism of fluid flow. It usually results in early water breakthroughs; reduced tertiary recovery efficiency due to channeling of injected gas or fluids; dynamic calculations of recoverable hydrocarbons that are much less than static mass balance ones due to reservoir compartmentalization; and dramatic production changes due to changes in reservoir pressure as fractures close down as conduits. These problems often lead to reduced ultimate recoveries or higher production costs.

Production experience with fractured reservoirs has repeatedly shown how understanding and exploiting the fracture connectivity at the reservoir scale is an important factor for optimizing reservoir performance (Dershowitz, 1998).

Generally, modeling flow behavior and mass transport in fractured porous media is done using the dual-continuum concept in which fracture and matrix are modeled as

This thesis follows the style of *SPE Journal*.

two separate kinds of continua occupying the same control volume (element) in space (Warren and Root 1963). This type of numerical model cannot reproduce many commonly observed types of fractured reservoir behavior since they do not explicitly model the geometry of discrete fractures, solution features, and bedding that control flow pathway geometry. This inaccurate model of discrete feature connectivity results in inaccurate flow predictions in areas of the reservoir where there is not good well control (Dershowitz et al., 2005).

The complexity of fracture networks means that a large quantity of data is required to characterize fracture systems adequately. Another modeling approach, the Discrete Fracture Network (DFN) model has been developed to aid in solving some of these problems experienced by using the dual continuum models. Discrete fracture network (DFN) models portray fractures and fracture connectivity very differently from other methods and it can lead to a more realistic representation of the fracture network in fractured reservoirs. The Discrete Fracture Networks (DFN) approach involves *“analysis and modeling which explicitly incorporates the geometry and properties of discrete features as a central component controlling flow and transport.”* (Dershowitz et al., 2005). DFN are stochastic models of fracture architecture that incorporate statistical scaling rules derived from analysis of fracture length, height, spacing, orientation, and aperture (Guohai, 2008).

1.1 Motivation

The presence of fractures in the fractured reservoir significantly affects the mechanism of fluid flow (Gilman, 2003). The impact of fractures in these reservoirs has led to exploration and development problems; this has been a major problem for both reservoir engineers developing oil and gas fields and researchers studying nuclear repository sites. With regards to the oil and gas sector the approach is to simplify the reservoir modeling process in fractured reservoir using the dual-continuum concept in which fracture and matrix are modeled as two separate kinds of continua occupying the same control volume (element) in space (Warren and Root 1963), the shortcomings of these models is that they do not explicitly model the geometry and the discrete features of the fractures. This inaccurate model of discrete feature connectivity results in inaccurate flow predictions in the reservoir which leads to lots of reservoir development issues.

Another approach uses the discrete fracture network (DFN) models for fracture modeling of the reservoir. DFN are stochastic models of fracture architecture that incorporate statistical scaling rules derived from analysis of fracture length, height, spacing, orientation, and aperture (Guohai, 2008). DFN incorporates the geometry and properties of discrete features as a central component controlling flow and transport. This leads to a better representation of the reservoir and thus produces reservoir models that give more realistic flow predictions in the reservoir.

1.2 Objective

The aim of this project is to improve the understanding of the flow behavior in shale gas reservoirs by using a Discrete Fracture Network (DFN) simulator (FracGen and NFflow) for fracture modeling of a shale gas reservoir. It also studies the interaction of the different fracture properties on reservoir response. Finally based on the understanding from this study and also learning from literature, it will aim to improve understanding on the flow behavior in shale gas reservoirs and the fracture properties and their impact on reservoir response.

1.3 Methodology

The first stage of the study is a literature review to understand the current and the past applications of discrete fracture networks in fracture modeling for both shale gas reservoirs and other types of reservoirs and also study the flow behavior in shale gas reservoir.

The next stage will be creating fracture models with the DFN simulator and running flow simulations to see the response that would be observed from the input provided. Subsequently, the results obtained from the stage above will be interpreted and sensitivity analysis done to ensure that the right parameters were fed into the models. The final stage is to make conclusions based on the results obtained and learning from other published results in the literature.

CHAPTER II

FRACTURE LITERATURE REVIEW

2.1 Fractured Reservoir

Fractured reservoirs are primarily related to their tectonic history. Fractures form due to the loading and unloading forces in the history of the rocks.

Natural fractures are believed to represent the local stress at the time of fracturing, while large scale fractures and folds can be related to differential stress over time. Both the maximum and minimum horizontal stress components increase with increasing burial. Open fractures which are of interest in fracture modeling requires stress relief in at least one direction (Nelson, 2001).

2.2 Fracture

A fracture can be defined as any discontinuity within a rock mass that developed as a response to stress. There are two forms of fracturing modes and the classification depends on the stress system that resulted in the formation of the fracture system.

In mode I fracturing, fractures are in tensile or opening mode in which displacements are normal to the discontinuity walls. This form of fracture system forms *joints* and *veins*.

In mode II fractures which results from an in - plane shear mode, in which the displacements are in the plane of the discontinuity, this fracturing system results in faults (Golf-Racht, 1982).

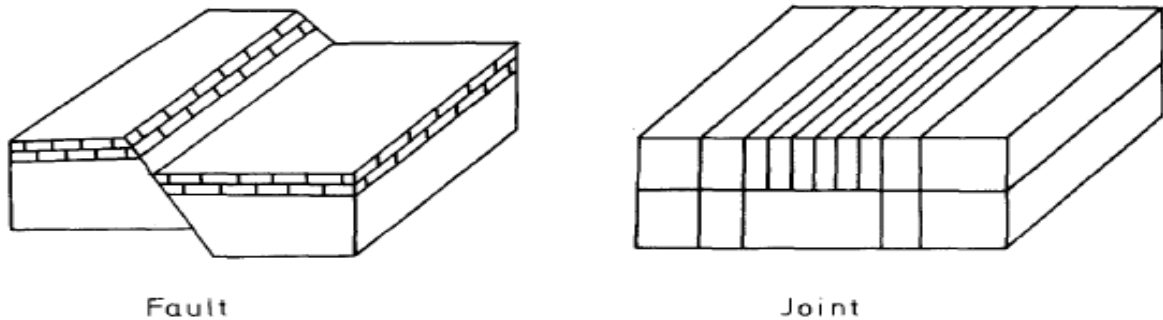


Figure 2.1: Schematic representation of a fault and a joint (Golf-Racht, 1982)

In general, a fracture in which relative *displacement has occurred* can be defined as a *fault*, while a fracture in which *no noticeable displacement* has occurred can be defined as a joint. See **Fig. 2.1**.

Fractures exist on a wide range of scales from microns to hundreds of kilometers, and it is known that throughout this scale range they have a significant effect on processes in the Earth's crust including fluid flow and rock strength (Bonnet et al., 2001).

2.3 Geometrical Description of Fractures

A fracture can be defined in a geometrical three-dimensional space with the following basic geometrical parameters (**Fig. 2.2**): dip angle, dip direction, persistence (dimension and shape) and aperture (the gap between two opposite surfaces of the discontinuity). Although there are other properties that can define a fracture these above are the basic properties that can be used to define a fracture (Jing and Stephansson, 2007).

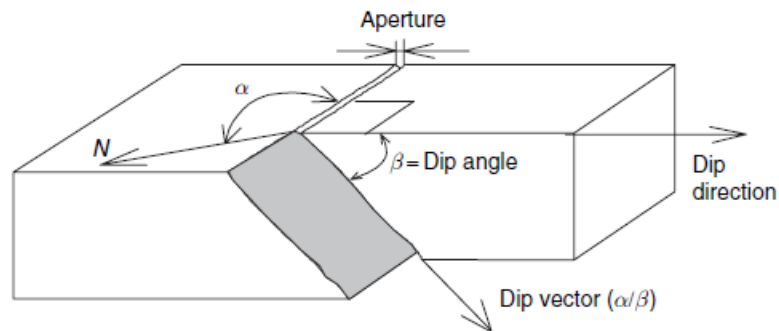


Figure 2.2: Geometric parameters associated with a discontinuity, the gap between the two surfaces is exaggerated to illustrate the aperture (Jing and Stephansson, 2007)

2.4 Fracture Mechanisms or Origins (Nelson, 2001)

2.4.1 Tectonic

- Tectonic or structure related fractures - result of tectonic events like faulting and folding.
- Regional fractures - normally covers large areas and have a pretty constant orientation. It can be difficult to unveil the exact cause of these fractures.

2.4.2 Non-Tectonic

- Contractional fractures – cause of reduction in bulk volume. Due to thermal contraction and diagenesis.
- Surface-related fractures - relate to weathering and unloading of stored stress.

2.5 Naturally Fractured Reservoir (NFR)

Natural fractures are normally generated through diagenesis or tectonic deformation and it affects most reservoirs in some way or another. This could be in a positive way - as

extra fluid conduits – or in a negative way as barriers to flow or cross-flow short-circuiting natural flow paths.

In carbonates, natural fractures typically create secondary porosity and permeability in low porosity matrix. However fractures are the fluid pathways but can also lead to early water breakthrough and inhibit secondary recovery.

In siliciclastics, they can add some permeability to existing matrix-dominated production.

Other reservoir types like basement rocks, volcanic rocks and coal-bed methane are also affected by fractures and have in later years opened the oil-companies eyes as new potential reservoirs.

2.6 Classification of Naturally Fractured Reservoirs (Nelson, 2001)

This classification is based on contribution of fractures to the total reservoir porosity and permeability (**Fig. 2.3**).

NFR's are reservoirs where naturally occurring fractures have/ are predicted to have significant effect on reservoir fluid flow and may change throughout the production history:

- Increased/decreased permeability and/ porosity
- Increased permeability anisotropy

Type 1: Fractures provide primary porosity and permeability. It requires large drainage area, typically granite or quartzite reservoirs with large fractures. Few wells needed for development, but a potential for high initial production and rapid decline (early water breakthrough). example: fractured granites.

Type 2: Fairly low matrix porosity and permeability, with good initial production given by fractures which provide essential permeability. example: carbonates.

Type 3: These reservoirs already have a high matrix porosity, with a fairly good permeability, but the fractures add an extra permeability component to productivity. example: sandstones.

Type 4: In compressional settings, folding may occur with differential strain, leading partly to extensional fractures, partly to compressional ones. In carbonates stylolites may form and in high porosity sandstones deformation bands may occur – all acting as barriers to flow, and some creating compartmentalization. Also existing open fractures may be mineralized or filled with clay.

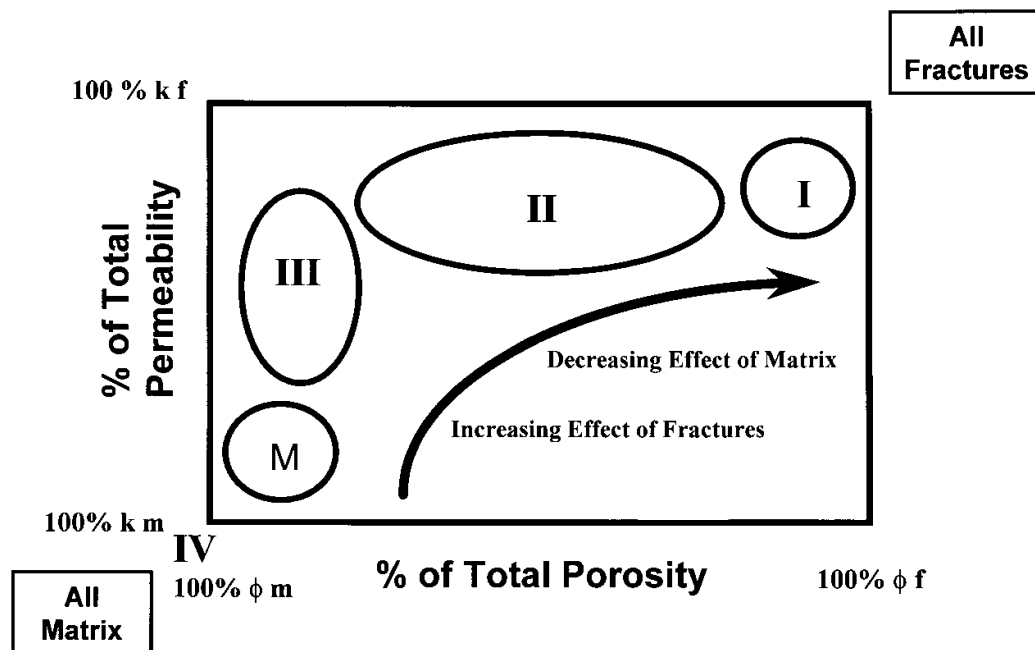


Figure 2.3: Schematic cross plot of percent reservoir porosity versus percent reservoir permeability (percent due to matrix versus percent due to fractures) for the fractured reservoir classification (Nelson, 2001)

2.7 Fracture Properties Definitions

2.7.1 Fracture Density

Fracture density is the number of fractures per unit area or volume (Davy et al., 1990).

Fracture density expresses the extent of rock fracturing.

2.7.2 Fracture Length

Fracture length, i.e., the length of the fracture, Fracture length distribution is generally taken to be a lognormal.

2.7.3 Fracture Aperture

Fracture aperture also called the fracture width (e) is the distance between the fracture walls (Bonnet et al., 2001).

2.7.4 Fracture Systems

It is defined as a set of parallel fractures.

2.7.5 Fracture Cluster

A fracture cluster is a group of linked fractures. It is a term derived from percolation theory. A cluster that links opposite sides of the study is termed a “percolating cluster.”

2.7.6 Fracture Intensity

Fracture intensity of a fracture set is measured either by the number of fractures per unit area or the summed lengths of fractures per unit area (Ghosh, 2009).

2.7.7 Fracture Network

A fracture network is generally defined as a set of individual fractures which may or may not intersect (Adler et al., 2009). It can also be defined as formed by two or several associated fracture sets.

2.7.8 Fracture Orientation

Fracture orientation gives the direction and tilt of the fracture. When characterizing the fracture orientation distribution, it is generally found that the fractures can be divided into a number of distinct fracture sets. These sets of fractures comprise fractures that can be characterized by common distributions of parameters, and which have a common origin and history. These fracture sets are often defined in terms of their orientation distributions which tend to be clustered around preferred orientations on a lower hemisphere projection of the poles to the fracture planes. This definition of the characteristic orientation is best achieved by using conventional statistical methods to identify distinct clusters. The fractures can then be separated into their distinct sets and further parameters inferred for each set independently. It is used for separation of different sets of fractures using stereographic projection techniques (Jing and Stephansson, 2007).

Fracture orientations measured for the outcrops are displayed on rose diagrams and equal-angle stereographic net projections for each of the measured locations (Ghosh, 2009). The best statistical analysis method for orientation of fractures is Fisher Distribution (Dershowitz et al., 2005).

2.7.9 Fracture Spacing

Fracture spacing (D) is the average distance between parallel regularly spaced fractures. It is the distance between two adjacent fractures of the same set following the same distribution function for their orientations. It is used for determination of the volume density of the fracture population (Jing and Stephansson, 2007).

2.7.10 Fracture Porosity

Fracture porosity is a percentage of void space in fractures compared to the total volume of the system. Fracture porosity is estimated using the following expression:

$$\phi_f = \left(\frac{e}{D+e} \right) * 100 \quad (2.1)$$

From the expression, it shows that fracture porosity is very scale-dependent. The value of ϕ_f can be 100% in a particular location of reservoir, but the value for the whole reservoir is generally less than 1%. According to (Nelson, 2001), fracture porosity is always less than 2%; in most reservoirs is less than 1% with a general value of less than 0.5%. An exception to these rules-of-thumb is vuggy fractures where porosity can vary from 0 to a very large value.

The importance of fracture porosity in reservoir performance depends on the type of fractured reservoir. If the fracture system provides an essential porosity and permeability to the reservoir, then fracture porosity is a critical parameter to be determined in early stages of development. As contribution of matrix porosity to the whole system increases, the relevance of fracture porosity decreases. Fracture porosity is one of the fracture properties that are difficult to determine. The common sources of fracture porosity estimation are:

- 1) Core analysis
- 2) Porosity-permeability relationships
- 3) Field/lab determinations
- 4) Logs
- 5) Multiple-well tests

2.7.11 Fracture Permeability

Permeability defines the ability of porous medium to transmit fluids. The presence of open fractures has a great impact in reservoir flow capacity. Therefore, fracture permeability is an important factor that determines reservoir quality and productivity. Darcy's equation that is used to model fluid flow through porous media cannot be used to represent flow through fractures. Thus, parallel plate theory was developed to model fluid flow in fractures. The parallel plate model is based on fracture width and spacing concepts (Parsons, 1966), who combined the model for fracture and matrix fluid flow and obtained the following equation for fracture permeability:

$$k_f = \frac{e^2}{12} \times \frac{\rho g}{\mu} \quad (2.2)$$

This equation assumes laminar flow between smooth, non-moving, parallel plates and homogeneous fractures with respect to orientation, width and spacing. Parson's relationship is simple but is applicable to fluid flow through fractured reservoirs.. In some cases, partially or total filled fractures can act as flow barriers. The effect of fractures on permeability depends on several factors such as morphology, orientation, and others. Fracture width and permeability are difficult to determine from direct sources such as core data or laboratory test. Well test analysis is the most common source of fracture permeability information.

2.8 Statistical Analysis in Fracture Characterization

Fracture characterization using Discrete Fracture Network (DFN) utilizes a number of statistical tools, the complexity of fracture networks means that a large quantity of data is required to characterize fracture systems adequately. These tools aid in ensuring that

the limited information provided by the various sources are applied to describe the entire well and characterize the reservoir properly.

2.8.1 Histograms

Histograms are used for the evaluation of the most frequent range of the variations of a given parameter. The data are generally collected in relation to a given criterion, such as lithology, pay interval, number of cores, types of fractures, etc. Histograms are applied to almost all parameters which define single fractures or multi-fractures characterization. From the frequency curve and cumulative frequency curve, the range of average values of a given parameter is obtained by a conventional procedure.

2.8.2 Geometrical Models

Geometrical models (especially in the case of matrix block units), using a stereographic projection approach for magnitude and shape. Polar stereogram and various other schematic representations are particularly useful in the identification of the preferential trends of certain parameters, which often help in the description of the properties for large groups of fractures.

2.8.3 Log – Normal Distribution (Davis, 1986)

The log normal distribution is closely related to the normal distribution. If the logarithm of a variable is normally distributed, then the variable itself is log normally distributed. The log-normal distribution is skewed with a long tail on the right hand side. However, after transforming the data by taking the log of the variable, the distribution becomes symmetric and normal. If we consider X to be a log normally distributed variable, then we can define $Y = \ln X$, where Y is the value of the natural logarithm of the random

variable X. If the mean of the variable Y is μ and the variance is σ^2 , we can write the probability density function for the variable X as,

$$f(x) = \frac{1}{x\beta\sqrt{2\pi}} \exp\left[-\frac{1}{2}\left(\frac{\ln x - \alpha}{\beta}\right)^2\right] \quad (2.3)$$

The mean and variance of the random variable X, is related to the mean and variance of the transformed variable Y through,

$$\alpha = \ln \mu - \frac{\beta^2}{2} \quad (2.4)$$

$$\beta^2 = \ln\left[1 + \frac{\sigma^2}{\mu^2}\right] \quad (2.5)$$

where μ is the mean of the variable X, and σ^2 is the variance of the variable X. So given a mean and variance of a variable, we can generate the log-normal values by first deriving the mean and variance from **eqn. 2.4 and 2.5**, and then standardizing this using,

$$z = \frac{\ln x - \alpha}{\beta} \quad (2.6)$$

This is similar to the normal distribution. So by choosing a range of values for z, we can generate a range of values for x.

2.8.4 Exponential Law (Bonnet et al., 2001)

This law has been used to describe the size of discontinuities in continental rocks (Cruden, 1977; Hudson and Priest, 1979; Nur, 1982; Priest and Hudson, 1981) and in the vicinity of mid-oceanic ridges (Carbotte and McDonald, 1994; Cowie et al., 1993). In these cases, fracture growth results from a uniform stress distribution (Dershowitz and Einstein, 1988), and propagation of fractures can be compared to a Poisson process (Cruden, 1977) resulting in an exponential distribution given by:

$$n(w) = A_2 \exp(-w/w_o) \quad (2.7)$$

where A_2 is a constant, The exponential law incorporates a characteristic scale w_0 **eqn. 2.7** that reflects either a physical length in the system, such as the thickness of a sedimentary layer or the brittle crust (Cowie, 1998), or a spontaneous feedback processes during fracture growth (Renshaw, 1999). Numerical simulations performed by (Cowie, 1995), and experimental results of (Bonnet, 1997) have shown that exponential distributions of fracture length are also associated with the early stages of deformation, when fracture nucleation dominates over growth and coalescence processes.

2.8.5 Gamma Law (Bonnet et al., 2001)

The gamma distribution is a power law with an exponential tail (**Fig. 2.4**) and is in common use in fault or earthquake statistics and seismic hazard assessment (Davy, 1993; Kagan, 1997; Main, 1996; Sornette and Sornette, 1999). Any population that obeys this kind of distribution is characterized by a power law exponent a , a characteristic scale w_0 (**eqn. 2.8**).

$$n(w) = A_3 w^{-a} \exp(-w/w_0) \quad (2.8)$$

The characteristic scale w_0 may be related to the correlation length in the spatial pattern, where it implies an upper bound for fractal behavior (Stauffer and Aharony, 1994), or may depend on deformation rate (Main and Burton, 1984). When w_0 is greater than the size of the system w_{max} , the gamma law reduces to a power law, and, conversely.

2.8.6 Power Law (Bonnet et al., 2001)

The power-law distribution is a straight line on a log-log plot. Numerous studies at various scales and in different tectonic settings have shown that the distribution of many fracture properties (i.e., length, displacement) often follows a power law.

$$n(w) = A_4 w^{-a} \quad (2.9)$$

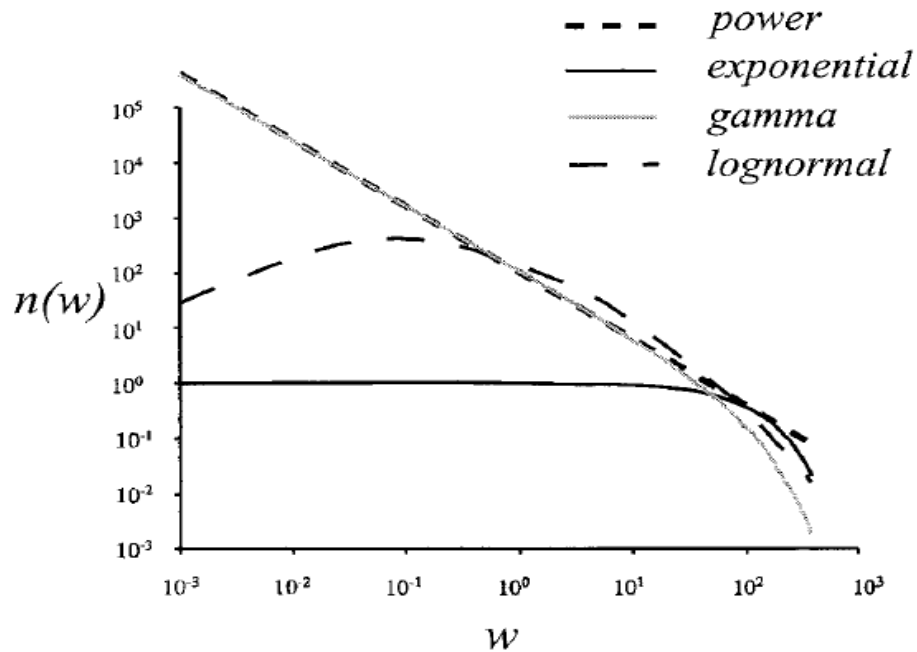


Figure 2.4: Plot illustrating the four different functions (power, lognormal, exponential and gamma law) most often used to fit data sets. Data over more than 1 order of magnitude are needed before these different distributions can be easily distinguished (Bonnet et al., 2001)

Power law distributions have the important consequence that they contain no characteristic length scale (**equation 2.9**). In nature the power laws have to be limited by physical length scales that form the upper and lower limits to the scale range over which they are valid. It is now generally recognized that resolution and finite size effects on a power law population can also result in distributions that appear to be exponential or lognormal.

But with the rise of scaling concepts in earth sciences, power law distributions have been favored over lognormal distributions because of their greater physical significance (Barton and Zoback, 1992). However, all power laws in nature must have upper and lower cutoffs.

2.9 Statistical Methods for Measuring Fracture Size Distributions

There are three different types of distribution that are commonly used to characterize fracture properties; these are:

- (a) Frequency
- (b) Frequency Density
- (c) Cumulative Frequency Distributions.

2.9.1 Frequency

The Frequency represents the occurrence of the fracture property.

2.9.2 Frequency Density

It represents the density of the occurrence of the fracture property.

2.9.3 Cumulative Frequency Distributions

The cumulative frequency distribution represents the number of fractures whose length is greater than a given length l and corresponds to the integral of the density distribution $n(l)$.

$$C(l) = \int_l^{l_{max}} n(l) dl \quad (2.10)$$

where l_{max} is the greatest length encountered in the network. Hence if $n(w)$ is a power law characterized by an exponent equal to a (**eqn. 2.9**), the cumulative distribution will be a power law for $w \ll w_{max}$ with an exponent equal to $a - 1$, the cumulative

distribution has been widely used because it is easily computed. In practice, it is constructed by summing incremental frequency data, and hence tends to give a smoother trend than the frequency or density distributions, increasing artificially the regression coefficient (Bonnet et al., 2001).

CHAPTER III

FRACTURE CHARACTERIZATION AND MODELLING

3.1 Fracture Modeling

Fractures are commonly found in most outcrops – and they affect fluid flow in most oil and gas reservoirs in the world. Natural fractures can introduce a high heterogeneity or a strong anisotropy in reservoirs, and affects fluid flow or mechanical stability. An accurate description and characterization of the fracture network is therefore of very high importance for all stages of reservoir management: drilling, well placement, stimulation, completion and production profile design.

There is an interrelationship between fractures, fluid-flow and effective stress state in the reservoir. Decisions must be made early to:

1. Identify and characterize fractures (at the exploration stage) and evaluate anisotropy etc. at the development stage for better infill drilling campaigns.
2. How does fractures (fracture network) affect fluid flow?
3. What is the effect of change in stress with production?

The purpose of fracture network modeling is to integrate geophysical, geological, petrophysical and reservoir engineering findings on fracture characterization to create a reliable fracture network model, with the aim to predict the distribution of fracture sets properties with the reservoir and build a fracture network model which will be used for flow computation and simulation.

This process aids in creating simulation properties for matrix and fractures and determines the interaction between the fracture and the matrix to be able to predict reservoir behavior. By modeling the fractures explicitly, the spatial relationships between properties in adjacent cells can be observed.

Fracture modeling is the most important aspect of the process to decipher the role of natural fractures in reservoir performance, and, eventually, it is the primary method for optimizing hydrocarbon recovery from fractured reservoir. It is a multi-step process involving several disciplines within reservoir characterization and simulation. The main idea is to build on geological concepts and gathered data such as interpretation of beds, faults and fractures from image log data, use field outcrop studies as analogs for conceptual models, seismic attributes used as fracture drivers etc. The next step is to transfer these data into a description of fracture intensity which can be populated into a geological framework model. Depending on the analysis of the fracture data, multiple sets of fractures can be identified; these can be the result of different tectonic events such as over-thrusts and extensional faults, conjugate fractures related to bending or flexure of geological layers or simply related to difference in lithology.

Once data have been identified, analyzed and categorized, the fracture model itself can be built. From our initial intensity description we need to populate the fracture intensity in the reservoir model stochastically or deterministically. The deterministic method needs to have a very good idea of where and how the fractures behave in the reservoir; if no such data exist, a stochastic method should be used.

The ultimate goal is to find reservoir grid properties which describe permeability and porosity for fractures as well as the standard permeability and porosity for the matrix they are either naturally fractured or consists of e.g. carbonates which are vugular or heavily fractured due to tectonic processes. Some of these reservoir rocks are originally dense and have little flow or storage capacity in the matrix, but once fractured, certain areas will become high flow zones. To try resolving this problem a Discrete Fracture Network (DFN) model based on intensity can be built. Up scaling properties based on a DFN model will generate a seconds set of properties of permeability, porosity and a sigma factor – describing the connectivity. This sigma/connectivity is essential in connecting ‘duplicate’ cells in a simulator describing the matrix and fracture porosities and permeabilities.

Fractures can increase effective porosity and permeability and introduce permeability anisotropy, particularly in rocks with low matrix permeability (Nelson, 2001). Faults can also function as fluid migration pathways, barriers, or a combination of both. For modeling and production purposes it is important to document directions of preferred fracture and fault orientations within primary hydrocarbon traps, such as anticlines. By understanding controls on fracture and fault orientation and distribution in a given reservoir the accuracy of flow modeling can be improved, thereby increasing primary and secondary hydrocarbon recovery.

The relationships between bed thickness, structural curvature and fracture porosity and permeability can be effective in evaluating geologic structures as

hydrocarbon reservoirs. Rocks, in general, exhibit increased fracture density with increased deformation (Nelson, 2001).

Improving the recovery from fractured reservoirs is an increasingly important focus for many oil companies. The recovery from reservoirs where fractures dominate permeability is often a fraction of the resource recovered from conventional reservoirs in which matrix permeability dominates. The lower recovery and higher risks relate to the difficulty in forecasting how various completion placements, gel treatments, surfactant injection, and tertiary recovery processes will actually perform. A reduction in risk and an improvement in understanding of reservoir behavior will lead to enhanced profitability from under-exploited fractured fields.

Fractures do more than simply increase reservoir permeability. Fractures fundamentally alter reservoir connectivity and heterogeneity. Fractured reservoirs could be modeled with the same level of confidence and success as matrix-dominated reservoirs.

More successful exploitation of fractured reservoirs has been hindered by the lack of reservoir management tools that incorporate the unique flow behavior of reservoir fracture systems.

3.2 Fracture Modeling Approach

There are two broad methods for fracture modeling that is commonly used to model field-scale fluid flow in naturally fractured petroleum reservoirs.

- (a) Continuum Model
- (b) Discrete-Fracture Network (DFN) Models

3.2.1 Continuum Model

The Continuum model (**Fig. 3.1**) is one in which fracture and matrix are modeled as two separate kinds of continua occupying the same control volume (element) in space (Warren and Root 1963).

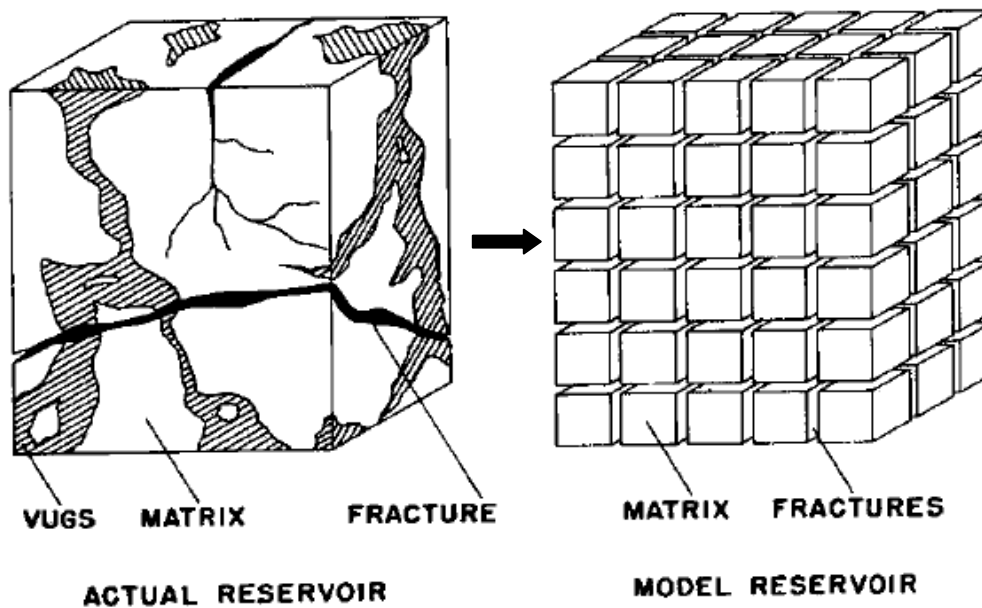


Figure 3.1: Dual-porosity model (Warren and Root 1963)

The fracture and matrix each has its own set of properties. Fluid transfer between the porous media is controlled by the pressure difference between components, fluid viscosity, matrix permeability, and a geometric factor known as shape factor. The shape factor is an important parameter in understanding the transfer function or fluid mechanism between the matrix system and fracture system vice versa. The shape factor (σ) introduced by (Kazemi et al., 1976) is given by:

$$\sigma = 4 * \left(\frac{1}{L_x^2} + \frac{1}{L_y^2} + \frac{1}{L_z^2} \right) \quad (3.1)$$

The shape factor represents the geometry of the matrix elements and controls flow between two porous media (matrix and fracture).

The continuum model is subdivided into two methods based on the nature of the fracture- matrix fluid interaction fractured reservoir (**Fig. 3.2**).

a) Dual Porosity

b) Dual Porosity/Dual Permeability

3.2.1.1 Dual Porosity

The first approach is a dual-porosity (DP) idealization of the reservoir, where a typical representative elementary volume (REV) of reservoir rock is assumed to contain a large number of equal size matrix blocks separated by interconnected fracture planes. In this method, flow to the well is only through the fracture system. Thus the fracture system acts as the primary flow path while the matrix system is the storage system and the fluid flow is from the matrix to the fracture. There is no matrix-to-matrix flow.

3.2.1.2 Dual Porosity/Dual Permeability

The second approach is the dual-porosity/dual-permeability (DP/DK) idealization of the reservoir, where, contrary to the dual-porosity case, the matrix blocks also communicate with each other; therefore, there is matrix-to-matrix flow in addition to matrix-to-fracture flow.

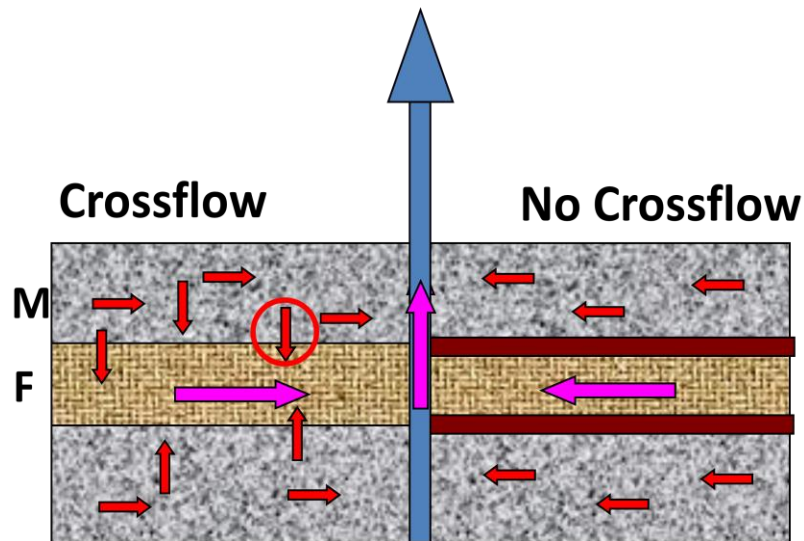


Figure 3.2: Illustration of dual porosity/single permeability and dual porosity/dual permeability models (Schlumberger, 2010)

3.2.1.3 Dual Porosity Model Types

Dual porosity idealization is a simplification of the real reservoir which is done with dual porosity model, fluid flow and transport exist in both the connected fractures and matrix blocks, there are two overlapping continua, where both are treated as porous media.

There are 3 dual porosity models that are widely used for simplification of the reservoir (**Fig 3.3**).

- Slab model (sheet of parallel fracture sets)
- Matchsticks model (2 orthogonal fracture sets)
- Sugar cube model (3 orthogonal fracture sets)

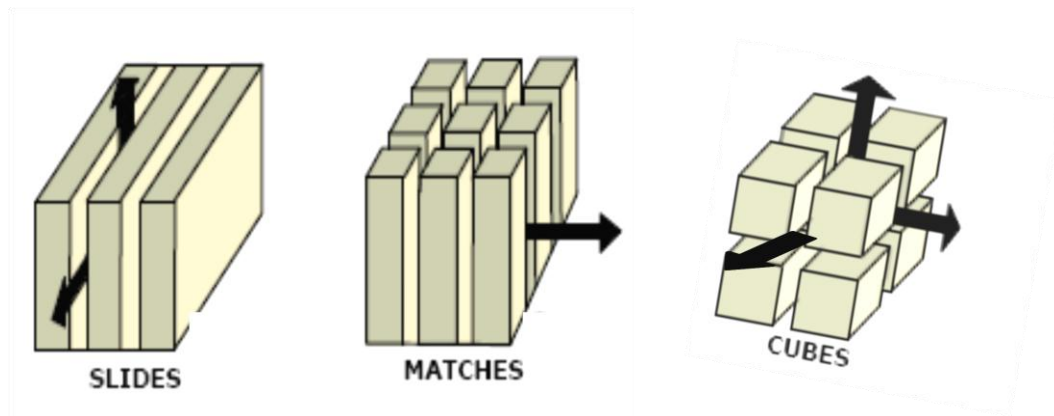


Figure 3.3: Illustration of the 3 types of dual porosity models (Reiss, 1980)

3.2.2 Discrete-Fracture Network (DFN) Models

The second fracture modeling approach is the Discrete Fracture Network (DFN) flow modeling; it is a more recent method, which relies on spatial mapping of fracture to construct an interconnected network of fracture surfaces.

The DFN model was developed to aid in solving some of these problems experienced by using the dual continuum models. The Discrete Fracture Network (DFN) approach involves *“analysis and modeling which explicitly incorporates the geometry and properties of discrete features as a central component controlling flow and transport.”* (Dershowitz et al., 2005). DFN are stochastic models of fracture architecture that incorporate statistical scaling rules derived from analysis of fracture length, height, spacing, orientation, and aperture (Guohai, 2008).

There are two methods of definition of fracture network geometry description using the DFN models.

(a) Deterministic Modeling Method

(b) Stochastic Modeling Method

3.2.2.1 Deterministic Modeling Method

In the deterministic method the fracture network system is described explicitly, with the location and orientation of all the fractures incorporated into the model. This is clearly not possible for almost all networks of interest in the reservoir scale, since the details of the fracture network in the rock away from exposures or boreholes cannot be known. In practice it is not possible to simulate using this method, where a continuum model is used this may be appropriate, and a best estimate made of the effective properties that should apply to the region. The uncertainty due to the random location of many small features is no longer considered since only larger scale average results are being predicted (Herbert, 1996).

3.2.2.2 Stochastic Modeling Method

Stochastic modeling method is based on a statistical description of the fracture system to be represented. The statistical properties of the fracture network system are measured and fracture networks are generated that exhibit the same statistics. This means that our models are not exact representations of the real physical fracture network, and one would not expect any individual model to give an accurate prediction of the detailed flow in the real network. However, if one simulates many different realizations of the fracture network flow system, each having the same statistical properties as the real network, then the range of model results should bound the behavior of the real network (if a good statistical description of the fracture network has been used). For this to be the case, it is important that sufficiently many realizations of the fracture network have been

generated and simulated. If only a few realizations are used then the distribution of possible behavior will not be accurately predicted and in particular the likelihood of more extreme behavior will not be known. Ideally, several hundred realizations may be necessary to determine this probability distribution of equally likely results and to predict, say 95% confidence limits. In practice, it is not always possible to simulate efficiently many realizations and often more qualitative bounds are estimated from a smaller sample of model results (Herbert, 1996).

CHAPTER IV

ANALYTICAL APPROACH

4.1 Study Approach

This study utilizes a set of programs that was developed by the national energy technology laboratory (NETL), to simulate gas reservoirs that consist of irregular, discontinuous or clustered strata-bound fracture networks within a tight matrix. It generates fracture networks, to simulate reservoir drainage/recharge, and to plot the fracture networks and reservoir pressures. These programs are suitable for reservoir modeling of reservoirs that produces relatively dry gas, with little interference from water or oil. The reservoir rock (matrix) has less than 1 md permeability. Variations in fracture apertures, density and connectivity are the dominant causes of heterogeneity in gas flow. Flow conductors are oriented nearly vertical and are strata-bound extending from bottom to top of beds that can be modeled individually (Boyle et al., 2010).

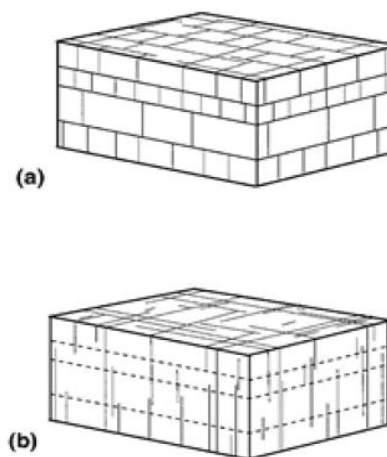


Figure 4.1: Diagram showing the major features of (a) strata-bound (b) non-strata- bound joint systems (Odling et al., 1999)

Fig. 4.1 shows a strata-bound system and a non-strata-bound joint system. In strata-bound systems, joints are largely confined to individual beds, their size is limited to a narrow range, and spacing is regular. In non-strata-bound cases, joint sizes cover a wider range, fractures cross-cut bedding and spacing tends to be clustered (Odling et al., 1999).

The five main components to the software package are:

- (1) Fracture network generator (FracGen)
- (2) Flow simulator (NFflow),
- (3) Graphical output software (Fracout),
- (4) PC-based User Interface (Fracflow)
- (5) Ancillary programs for input data analysis or manipulation.

4.2 DFN Simulator (FracGen and NFflow)

The two main components of the DFN simulator program are FracGen and NFflow.

4.2.1 FracGen: Fracture Network Generation (Boyle et al., 2010)

FracGen is a computer program that uses an input file containing parameters and statistics for fracture attributes to generate a stochastic network of lines that represent some of the patterns of fractures commonly found within thin strata-bound petroleum reservoirs and aquifers. The stochastic network is generated by in an increasing complexity through a Monte Carlo process that samples fitted statistical distributions for various network attributes of each fracture set. FracGen fracture patterns are inherently two-dimensional and single layered, although the realizations of fractured layers can be

stacked to represent multi-layer reservoirs. Within stacked single layers or multi-layer realizations, individual fractures can penetrate two or more layers.

FracGen generates fracture patterns that range across the spectrum from regular to random, to clustered. It assumes that all fractures are strata-bound and vertical also the bed thickness is constant. If the host rock unit is massive or highly variable in thickness, or if many fractures fail to extend across definable beds (i.e., average fracture height is much less than bed thickness), other models might be more appropriate. Likewise, if many fractures are not perpendicular to bedding or if low-angle faults penetrate the reservoir; other network generators should be used.

Fractures are stochastically generated using one of three models, referred to as Model 1, Model 2, and Model 3. Model 0 supports Models 1 and 2 in the generation of fractures from borehole and sample trace information. (Boyle et al., 2010)

Model 1 generates randomly located fractures, although the connectivity controls can be used to produce various degrees of clustering, including unintended clustering.

Model 2 generates fracture swarms (elongated clusters), whereby the swarms are randomly located and can overlap.

Model 3 generates fractures in a spectrum of patterns that range from regular to uniform to random to clustered.

4.2.1.1 Connectivity Control in FracGen (Hatzignatiou and McKoy, 2000)

There are three methods for controlling connectivity:

- (1) Fracture end-point shifting,
- (2) T-termination frequency control,

(3) Intersection frequency control.

The first method involves moving each fracture end-point toward or away from the center point to the first point of intersection found with another fracture. The user can specify whether this point of intersection is with pre-existing fractures, or with subsequently generated fractures, or both. Termination and intersection frequency control is implicit in the selection of the percentage of fracture length over which end point shifting is allowed.

T-termination frequency control involves moving fractures to new locations or, preferentially, swapping fracture orientation until the end-point shifting function improves the match with the user-specified percentages of fractures having zero, one or two T-terminations. The computer program controls the percentage of fracture length over which end-point shifting occurs.

Intersection frequency control is used when it is important to explicitly control the frequencies of intersections, as when modeling cross-fractures and late formed fractures, it starts with a proposed fracture of maximum allowable length and counts all fracture intersections with the proposed fracture. If an acceptable number of intersections are found, it truncates the proposed fracture at the optimal number of intersections needed to improve the match with the user-specified distribution of intersection frequencies. If too few intersections are found, it swaps the proposed fracture orientation or location and repeats the process until the desired number of intersections is found. The user-specified frequency of T-terminations is matched also, but this is of lower priority. To control the resulting fracture length distribution,

maximum and minimum acceptable fracture lengths are established and varied by the computer program to produce a distribution with lognormal statistics that match those specified by the user.

Another useful connectivity control mechanism is the synthetic annealing process which can be used in all three models to move fractures to locations where user-specified terminations or intersections are achieved. Both the second and third methods of connectivity control use a type of synthetic annealing in which the user specifies the frequency for swaps of location, the total number of swaps allowed per fracture, and the percentage of fractures generated in a set before synthetic annealing begins. These controls limit unintended parent-daughter clustering.

The user has the option to specify the locations of individual fractures and individual clusters. Therefore, it is possible to include within a generated network, known fault/fracture locations, seismically interpreted faults and fractures, and interpreted regional or local variations in fracture density or orientation.

4.2.2 NFflow Natural Gas Flow Modeling

NFflow is a numerical model for simulating naturally fractured tight gas tight (< 1 md matrix permeability) fractured reservoirs based on stochastically derived fracture patterns that mimic a complex system of interconnected natural fractures in the reservoir (Sams, July 1995.). NFflow is for single-layer and multi-layer reservoirs with the possibility of tilt and curvature. This approach permits a more accurate and realistic representation of fractured porous media fluid flow compared to traditional deterministic naturally fractured reservoir formulations.

The NFflow simulator is a single-phase (dry-gas), two-dimensional numerical model that solves fluid flow equations in both matrix and fracture domains sequentially for strata bound naturally fractured reservoirs. The mathematical model decouples fluid flow in fractures and matrix, and solves a one-dimensional un-steady state flow problem in the matrix domain to compute the volumetric flow rates from matrix into fractures and wellbores. Subsequently, the model uses the computed recharge fluid rates entering the fractures at the middle point of each fracture segment to compute the pressure and flow rate distributions at each node of the system by solving a two-dimensional fluid flow problem in the fracture domain (Sams, 1995). Flow through the rock is modeled with Darcy's Law, while flow along fractures is modeled as a linear (cubic law) function of the pressure difference between the recharge points and the fracture intersections. It assumes that there is no flow from matrix block to matrix block.

NFflow can operate in either rate-controlled mode or pressure-controlled mode. NFflow is designed to work with the fracture network files from FracGen but can be used with any fracture network descriptions having the proper format regardless of the source (Hatzignatiou and McKoy, 2000).

The flow simulator requires two input files, a run control file (*.RES) and fracture network description file (*.FLO). The *.RES file contains all data except the flow network description, which is contained in *.FLO. The flow network description consists of the fracture network plus the user-specified well descriptions (Boyle et al., 2010).

4.3 Ancillary Program

There are a number of ancillary programs but the one that was utilized most for this study is the fracture aperture reduction model (FARM).

4.3.1 Fracture Aperture Reduction Model (FARM)

It aids the user to reduce the hydraulic apertures within a specified distance around the well bore by running the ancillary program FARM.EXE. This program may be used in a trial-and-error process until the best possible match with production data or well test data is obtained for each of one or more networks (Boyle et al., 2010). Thus, the user estimates the amount and distance of fracture obstruction by drilling fluids, stimulation fluids, condensates, precipitates, or bio-fouling. It aids in reducing the flow from one or more fracture networks, this is done by shrink the apertures of the fractures nearby the well to account for the drilling damage. This adjustment is done on the fracture apertures in *.FLO file.

4.4 Summary of Sample Files for FracGen and NFflow (Boyle et al., 2010)

The list below is a summary of different FracGen and NFflow files.

- a) DAT File is the Input data file for FracGen; it is used to create fracture network realizations.
- b) FLO file is an output file from FracGen.
- c) DIA file is the output file from FracGen. It contains the diagnostics for the fracture network in the FLO file. It contains information on how many fractures are in the network, the connectivity of the fractures, and other

statistics. It aids the user to see if the network generated is what was desired and what inputs should be changed to generate better networks.

- d) RES file is the Input file for NFflow. It contains the reservoir parameters, PVT data, recurrent data for the flow simulation and the well performance schedule.
- e) BHP file contains the field data file for the performance of well. The file is can be produced by the ancillary program BHP.EXE, which calculates bottom-hole pressures using the Cullender and Smith method. This file contains a number of lines of information related to the calculation of bottom-hole pressures. At the bottom of the file is a table of well head flowing pressures and calculated bottom-hole flowing pressures for various times indicated. This file's specification must be listed in the *.RES file if the historical data is to be shown on any pressure versus time plots made by NFflow.
- f) LDF file is the file that gives the layer depths across the reservoir. This is the input needed to describe the upper and lower bounds of each layer and properties that are allowed to vary across the layer. The layer boundary definition is designed to allow the user to add continuous, smooth features to a reservoir (i.e. tilt, curvature); describing discontinuous features (i.e. faults) may produce unexpected results.

4.5 Mechanism for Fracture Generation in FracGen

Fractures are generated by randomly selecting fracture center-points and then assigning a length, aperture, and orientation to each center-point to define each fracture. Fracture attributes are defined by fixed variables and statistical distributions.

We begin to derive our fracture network models by assuming that an investigator can treat fractures as straight line segments (or rectangles in three-dimensional space) that are defined by a center point, a length, and an azimuth (all fractures are perpendicular to bedding).

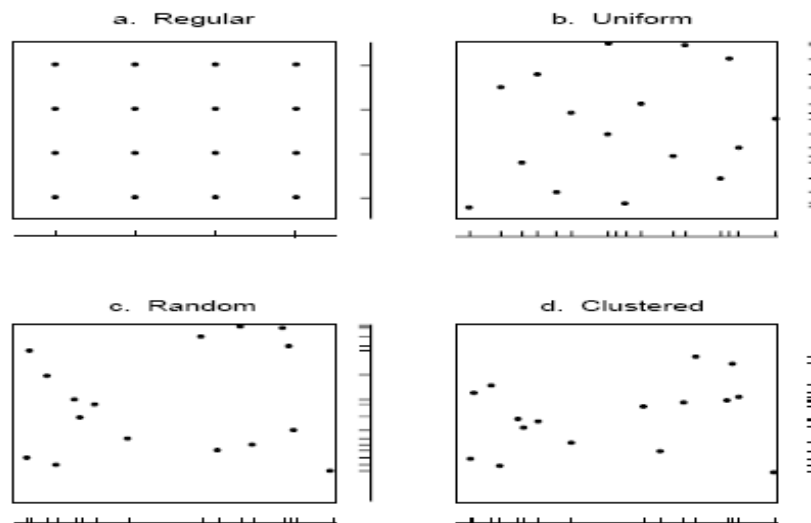


Figure 4.2: Fundamental spatial patterns of points (1-D & 2-D) (McKoy and Sams, 1997)

Fig. 4.2 illustrates the fundamental two-dimensional patterns of points in space. These patterns and are associated with different probability distributions. On the bottom and right sides of each two-dimensional illustration, **Fig. 4.2** shows the equivalent one

dimensional pattern of point locations. The one-dimensional pattern is similar to the patterns that would arise if the points in the two-dimensional illustrations were converted into lines (fractures) oriented perpendicular to the one-dimensional illustrations.

Fig. 4.3 represents relative frequency histograms for the fundamental distributions of spacing, as observed along a sample line. These distributions of spacing arise from the fundamental patterns of point location. The pattern of points on a map is "random" (**Fig. 4.2c**) if each quadrant has the same probability of containing a center point as all other quadrants of equal size and if all points are placed without regard to the placement of other points. The distribution of spacing between random points along a sample line is exponential (**Fig. 4.2c**), with more short spacing's than long spacing's. The pattern of points on a map is "clustered" (**Fig. 4.2d**) if equal-size quadrants have different probabilities of containing a center point and if any points are placed in relation to the placement of other points.

In nature, things tend to be related, and fractures develop more closely together in some areas because of stress variations around primary or structural features in the rock or because of local stress variations originating in the underlying rock. In other areas, fractures are more uniformly spaced because each fracture relieved the ambient stress as it formed. Consequently, truly random fracture locations in rock are probably rare. Locations that appear random probably result from a combination of a uniform distribution and a clustered distribution.

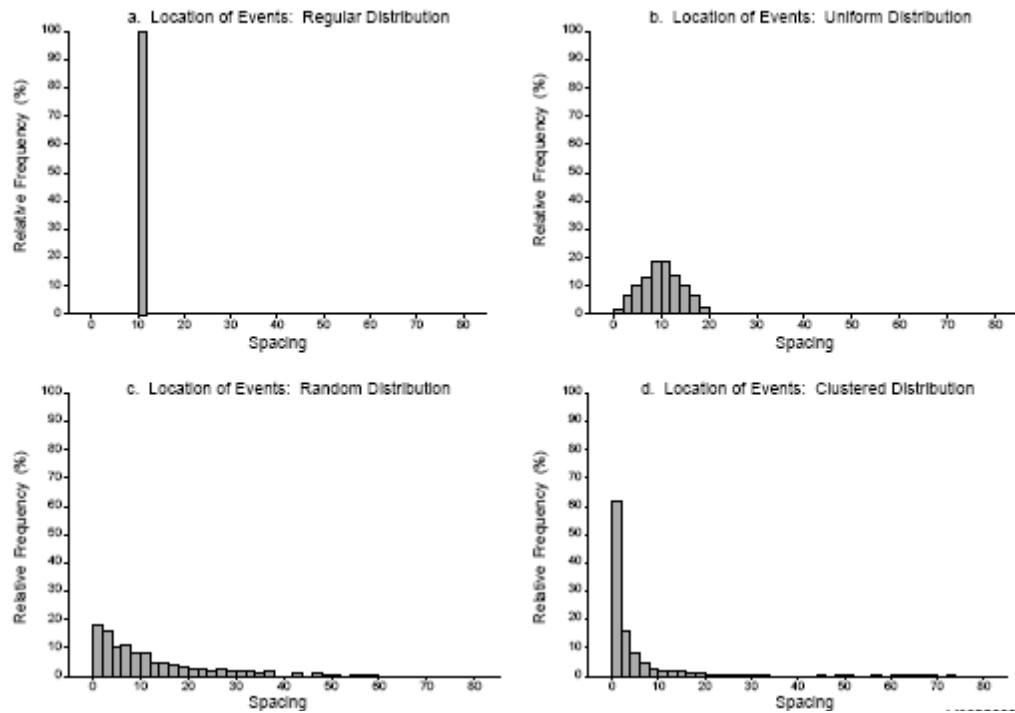


Figure 4.3: Fundamental distributions of spacing that arise from the fundamental spatial patterns of points (McKoy and Sams, 1997)

4.6 Drainage of Complex Fracture Network and Matrix

The mathematical model described below was developed to study reservoir performance as a function of fracture pattern, fracture network connectivity, and variations in matrix block size populations and locations. To this end, the model characterizes the reservoir in terms of the fluid carrying capacity of fractures, fluid flow paths, and the effective volumes drained by fracture segments (McKoy and Sams, 1997).

4.7 Approach: Mathematical/Numerical Model

The material balance and flow equations that constitute the mathematical model for the gas reservoir simulator is developed below.

The cubic law which is a linear function of the pressure difference between the recharge points and the fracture intersections shown in **eqn. 4.1**.

$$Q_v = -\frac{hw^3}{12\mu} \frac{dp}{ds} \quad (4.1)$$

where h is the formation thickness, w is the fracture aperture, μ is the gas viscosity, and $\frac{dp}{ds}$ is the gas pressure gradient. The molar gas density is given by the real gas equation of state.

$$\rho = \frac{1}{RT} \frac{p}{z} \quad (4.2)$$

where R is the gas constant, T is the temperature, and Z is the Z factor which is a function of T and p . The reservoir is assumed to be isothermal so the temperature dependence of Z is suppressed in the derivation.

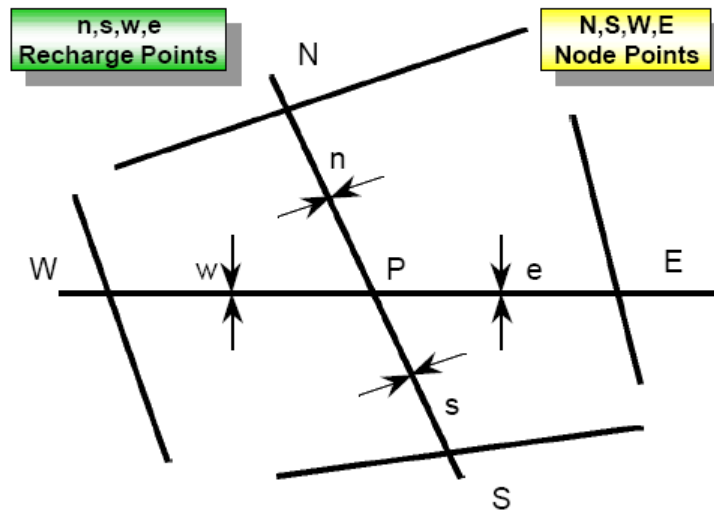


Figure 4.4: Schematic of fracture network and flow nodes modeling (Hatzignatiou, 1999)

Writing the material balance at P (Figure 4.4) yields,

$$-\left(\frac{hw^3}{12\mu}\right)_w \left(\frac{1}{RTZ} \frac{p}{ds}\right)_{P-w} + \left(\frac{hw^3}{12\mu}\right)_e \left(\frac{1}{RTZ} \frac{p}{ds}\right)_{P-e} - \left(\frac{hw^3}{12\mu}\right)_s \left(\frac{1}{RTZ} \frac{p}{ds}\right)_{P-s} + \left(\frac{hw^3}{12\mu}\right)_n \left(\frac{1}{RTZ} \frac{p}{ds}\right)_{P-n} = 0 \quad (4.3)$$

By defining the real-gas pseudopotential (potential for short) as

$$\Phi = \int_0^p \frac{p' dp'}{\mu(p')Z(p')} \quad (4.4)$$

The primary nodes of the finite difference numerical system are placed in active fractures (fractures intersecting other fractures or wells), whereas nodes are not assigned in the matrix volume of the reservoir. **Fig. 4.4** illustrates two main fractures with north-south and west-east directions intersected at point P, and four additional fractures intersecting with the two main ones defining the intersection points W, E, N, and S. In this system there are five nodes (P, W, E, N, S) and four fracture segments WP, EP, NP, and SP. Fluid is allowed to flow from a matrix element into a fracture segment in both directions and at recharge points w (west), e (east), n (north) and s (south) defined at the middle of the four fracture segments. Note that any fracture which does not intersect another fracture or a well is considered as inactive and not a part of the fluid transportation network (Hatzignatiou, 1999).

The recharge fluid volumes from matrix into active fractures are computed by discretizing the matrix volume drained by each fracture segment and solving a one-dimensional, linear, unsteady-state, porous media flow problem. The grid blocks in the matrix volumes, generated internally by the simulator, are non-uniform (grids located next to the fracture or wellbore are small and become progressively larger as a function

of distance). The matrix block volumes are essentially "effective pore volumes" computed by NFFlow to preserve fluid in place. The matrix of the system is considered homogeneous and isotropic and gravitational forces are neglected. The compressibility of both fracture and matrix is considered to be negligible, i.e., the matrix and fracture porosities are pressure independent (Hatzignatiou, 1999).

4.7.1 Fracture Flow

The flow in the fracture network is described by Poiseuille's law. The numerical model is developed based on the gas pseudo pressure function which for convenience is defined as the half of the well-known gas pseudo pressure function. The finite difference approximation of the material balance equation at node P (see **Fig. 4.4**) (Sams, July 1995.):

$$(R_p^f)^l + 2 \sum_j TX_j (\delta \phi_j^f - \delta \phi_j^f) = 0 \quad ; \quad j = w, e, n, s \quad (4.5)$$

where R_p^f denotes the residual function,

$$\delta \phi_j^f = (\phi_j^f)^{n+1} - (\phi_j^f)^k \quad ; \quad j = w, e, n, s \quad (4.6)$$

The gas pseudo pressure function difference, and

$$TX_j = \left(\frac{hw^3}{12\Delta x} \right)_j \quad ; \quad j = w, e, n, s \quad (4.7)$$

Equation 4.7 defines the transmissibility in the fracture at fracture segment midpoints w, e, n and s. A material balance in a control volume in the fracture segment network expressed in a finite difference form yields relationships that relate pseudo pressure function values at fracture segment mid-points and node points (P, W, E, N and S):

$$\delta \phi_j^f = \frac{r_j (R_j^m)^l}{2TX_j} + r_j (\delta \phi_j^f - \delta \phi_p^f) \quad ; \quad j, i = w, W, e, E; N, n, S, s \quad (4.8)$$

With the residual function at recharge points in fracture segments expressed as

$$(R_j^m)^l + 2TX_j(\delta\phi_j^f - \delta\phi_p^f) - 4TX_j\delta\phi_j^f + T_j^m \left[\left(\frac{\partial\phi^m}{\partial\phi^f} \right)_j - 1 \right] +$$

$$-\delta\phi_j^f - \frac{V_f}{\Delta t} \left[\frac{d}{d\phi^f} \left(\frac{p}{z} \right) \right]_j \delta\phi_j^f = 0 ; j = w, e, n, s \quad (4.9)$$

In **eqn. 4.8**, r_j at recharge point j is equal to,

$$r_j = 2 \left(\frac{TX}{4TX+Tc} \right)_j ; j = w, e, n, s \quad (4.10)$$

With the matrix transmissibility at j defined as

$$T_j^m = 2 \left(\frac{A_m k_m}{\Delta x_m} \right)_j ; j = w, e, n, s \quad (4.11)$$

and

$$T_j^c = T_j^m \left(1 - \frac{\partial\phi^m}{\partial\phi^f} \right)_j + \frac{V_f}{\Delta t} \left[\frac{\partial}{\partial\phi} \left(\frac{p}{z} \right) \right]_j ; j = w, e, n, s \quad (4.12)$$

The expressions for fracture segments WP, EP, NP and SP from **eqn. 4.8** can be substituted into the nodal material balance expression, **eqn. 4.17**, to obtain the following finite difference equation:

$$(R_p^f)^l + \sum_j r_j (R_j^m)^l + 2 \sum_{j,i} TX_j r_j \delta\phi_j^f + 2\delta\phi_p^f \sum_j TX_j (r_j - 1) = 0 ; \quad (4.13)$$

$$j, i = w, We, E; N, n, S, s$$

This expression applied to the fracture and wellbore flow nodes yields a system of equations with unknowns the flow nodes gas pseudo pressure function difference. The solution of this system is obtained via the Gauss-Seidel over-relaxation method (Aziz and Settari, 1985; Sams, July 1995.)

4.7.2 Matrix Flow

The flow in matrix is governed by Darcy's equation provided that turbulence flow effects are not present; the fluid flow problem in the matrix is solved numerically as a one-dimensional problem with the grid block system drained into a well or a fracture. Following standard techniques, a fully-implicit, finite difference formulation of the material balance equation for dry-gas flow in porous media and in residual form yields:

$$R_m^k = T_{m,i+1/2} \Delta \phi_{m,i+1} - \left(\left(\frac{PV_m \mu C}{\Delta t} \right)_i^k + T_{m,i+1/2} + T_{m,i-1/2} \right) \Delta \phi_{m,i} + T_{m,i-1/2} \Delta \phi_{m,i-1} \quad (4.14)$$

where

$$R_m^k = T_{m,i+1/2} (\phi_i^k - \phi_{i+1}^k) - T_{m,i-1/2} (\phi_{i-1}^k - \phi_i^k) + \left(\frac{PV_m \mu C}{\Delta t} \right)_i^k (\phi_i^k - \phi_i^n) \quad (4.15)$$

A_m denotes the matrix block area, Note that the matrix transmissibility for describing the fluid flow among matrix grid blocks is defined as

$$T_{m,i\pm 1/2} = 1/2 T_i \quad (4.16)$$

The solution of **eqn. 4.15** can be obtained iteratively by solving a tri-diagonal matrix, using Thomas algorithm (Aziz and Settari, 1985), to obtain the values of in the reservoir matrix which are then used to compute the pseudo pressure function at each time step.

4.7.3 Initial & Boundary Conditions

The conditions applied to obtain the numerical solution are presented in this subsection.

Inner boundary condition: The two types of inner boundary conditions considered are

the constant surface gas production rate and constant bottomhole production pressure. For the constant surface gas production rate the model allows gas to flow into the wellbore from both matrix blocks and fractures. Therefore, the gas production rate at the well is the summation from both these contributions, i.e.

$$q_{gsc} = \sum_{i=1}^{NS} J_i [\phi_{mi} - \phi(P_{wf})] + 2 \sum_{j=1}^{NF} TX_j [\phi_{fj} - \phi(P_{wf})] \quad (4.17)$$

4.8 Flow Behavior Fractured Networks

The two important factors that affect flow behavior in fractured reservoirs are:

- 1) Fracture connectivity.
- 2) Fracture scaling.

4.8.1 Fracture Connectivity

Fracture connectivity refers to how individual fractures link to form coherent networks. Another definition of connectivity defines in terms of fracture clusters defines it quantitatively as the proportion of the total trace length that belongs to the largest cluster. It is sensitive to network geometry and fracture characteristics such as length, size distributions, orientation, density and aperture of individual fractures. Connectivity also depends on the spatial distribution and interaction of different fracture sets to form a continuous network (Odling et al., 1999). Clustering of fractures into swarms is a key factor affecting the fracture interconnectivity and it is used as a measure for assessing flow transport in rocks (Xu et al., 2006).

In general, connectivity increases as:

- 1) An increasing number of fractures of the same set are added to the system resulting in an increase in fracture density.

- 2) The length of the fractures increases.
- 3) The orientation of fractures in a set exhibits a higher degree of dispersion.
- 4) Fractures of multiple sets are added to the system.

4.8.2 Fracture Scalability

Fracture scalability refers to how small features are related to large (Odling et al., 1999). The scalability of fracture system is an important parameter that affects the properties of the fractures and ultimately the flow behavior of a reservoir. Considering that access to the reservoir is usually limited to just the area where the wellbore is exposed, this is usually a small area compared to the overall area of the reservoir so different schemes will be employed to be able to estimate what the fracture network will be in the entire reservoir scale from the information that is obtained from the wellbore region.

4.9 Parameters for Quantifying Connectivity in Fracture Networks

Three parameters from literature that can be used to quantify the connectivity of a fracture system are:

- 1) Percolation Threshold
- 2) Connectivity Index
- 3) Coefficient of Variation (C_v)

Percolation theory is a general mathematical theory of connectivity and transport in geometrically complex systems (King et al., 2002). It describes the effect of the connectivity of the small-scale, or microscopic, parts of a disordered system on its large-scale, or macroscopic, properties, (Hunt, 2005). From percolation theory which is applied to fracture systems. When fracture density is low, clusters of connected fractures

are small and no cluster spans the entire area with increasing fracture density, clusters grow and at the '*percolation threshold*' the largest cluster spans the sample area (Odling et al., 1999).

Thus the '*percolation threshold*' is a value once reached the fracture network changes from fracture clusters to fracture networks, it is an important parameter, since it gives us information about the state of the fracture network.

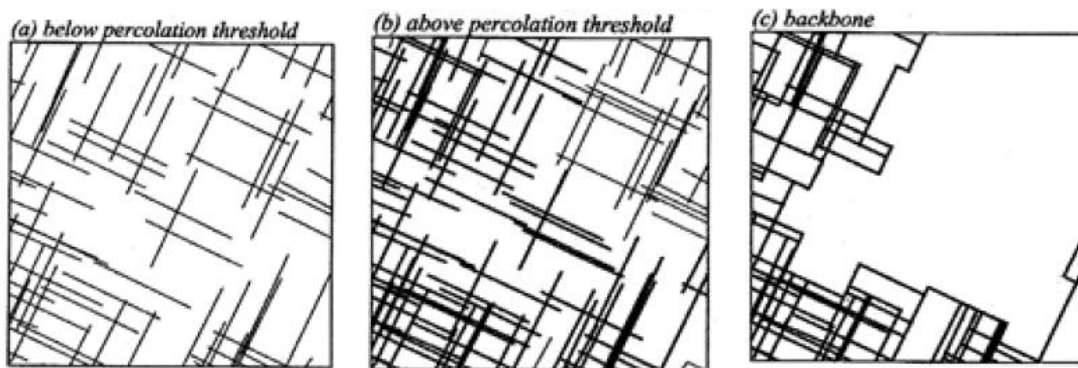


Figure 4.5 Diagram showing fracture networks below (a) and above (b) the percolation threshold and also the backbone network (c) (Odling et al., 1999)

In **Fig. 4.5a** isolated fractures with few interconnections can be observed below the percolation threshold while in **Fig. 4.5b** a fracture network spanning the entire area can be seen above the percolation threshold. **Fig. 4.5c** shows the 'backbone'; defined as all direct routes through the fracture network across the sample area. This is the largest cluster with all 'dead-ends' removed. The backbone is the part of the spanning cluster which can conduct fluid.

The connectivity index (CI) quantifies the connectivity between any two points in space. Monte Carlo simulation is used to evaluate the connectivity index for stationary cases and relationships between the connectivity index and the parameters of the discrete fracture model are analyzed.

The CI is the probability that two arbitrary points within the region are connected. The CI is, therefore, local and independent of the scale of the region. The CI can, however, be used to evaluate the percolation thresholds when combined with percolation criteria and the scale of the system. Monte Carlo simulation is used to evaluate the connectivity index and to assess the influence on connectivity of different fracture network models (Xu et al., 2006).

A more practical approach at understanding fracture connectivity in the reservoir is using the coefficient of variation, C_v which is a measure of the spatial distribution. It is defined as the standard deviation divided by the mean spacing (Cox and Lewis, 1966). If the fractures are located randomly, the intersections with line sampling define a Poisson point process and spacing's have a negative exponential distribution where $C_v = 1$. If the traces are regularly spaced the standard deviation of spacing is small and $C_v < 1$. If however, fractures are clustered, the standard deviation is large and $C_v > 1$ (Xu et al., 2006).

CHAPTER V
FRACTURE MODELLING OF A SHALE GAS RESERVOIR
USING FRACGEN AND NFFLOW

5.1 Modeling Approach

From the previous chapter the principle of operation of FracGen and Nfflow has been discussed at length, in this chapter the application of FracGen and Nfflow for fracture modeling of a shale gas reservoir in the Eagle Ford shale will be highlighted.

From the well information and also from basin information for an Eagle Ford shale gas reservoir an input data for FracGen was created and fed into it to create the fracture map that represents the reservoir. This study will utilize data from an Eagle Ford shale gas reservoir data obtained from SPE 138425.

The focus is to study the interaction of different fracture/well properties on reservoir response, four cases will be considered for this analysis and they represent the following fracture sets.

- 1) Uniformly distributed fracture pattern of one fracture set.
- 2) Clustered fracture pattern of one fracture set.
- 3) Uniformly distributed fracture pattern of two fracture sets.
- 4) A uniform distributed fracture pattern of one fracture set and a clustered fracture set.

The fracture/well properties are subdivided into two broad categories.

- 1) Controllable
- 2) Non-Controllable

Table 5.1: Fracture/well properties classification

Fracture/Well Properties	
Controllable Well Properties	Non-Controllable Geological
Hydraulic Fracture Aperture	Natural Fracture Aperture
Number of Stages Hydraulic Fracture	Natural Fracture Length
Hydraulic Fracture Length	Natural Fracture Density

This classification of the fracture\well properties (**Table 5.1**) is based on their nature; natural fracture and hydraulic fracture. Natural fractures are fractures that are created by forces of nature, while hydraulic fracture are fractures created by human influences on the reservoir either by hydraulic fracturing or other well activities, for example drilling. For this study the focus of the hydraulic fractures are fractures created by hydraulic fracturing process in shale gas reservoir.

5.2 Fracture Modeling Procedure

The steps below are the procedure taken for fracture modeling of the shale gas reservoir using FracGen and NFflow.

- (1) A FracGen input file was created from the well/reservoir parameters and fed into FracGen.
- (2) An output FLO file is created from FracGen and then well parameters are added before it is fed into the NFflow for flow simulation.
- (3) Also from FracGen the layer description file (LDF) is also created which specifies the depths, porosity & permeability of the layers.

- (4) After that the BHP files is created from the rate versus time data as well as the pressure versus time data. The BHP file contains data that is used for history matching while running the NFlow.
- (5) Then the RES file is created to aid in running the flow simulation in NFlow. The RES file contains the PVT properties and also the file directory paths of both the LDF and the BHP file.

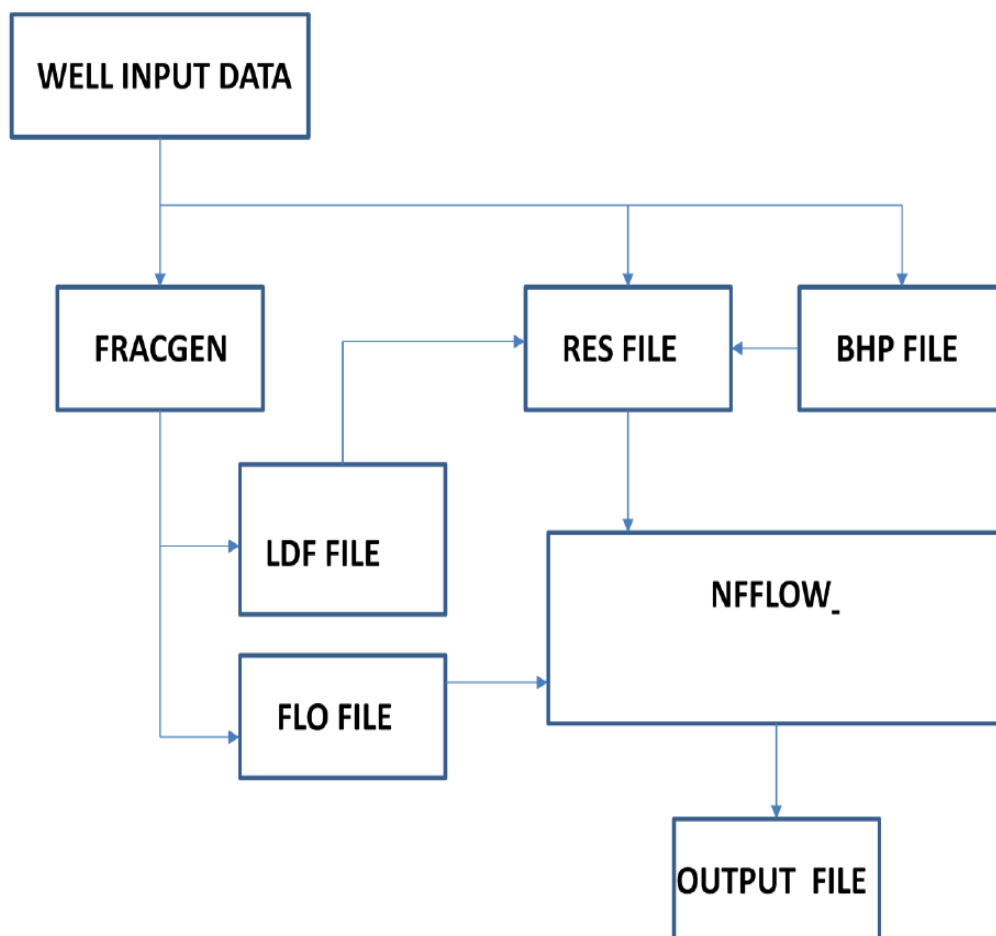


Figure 5.1: FracGen and NFlow simulation process

5.3 Case 1: Uniformly Distributed Fracture Pattern of One Fracture Set

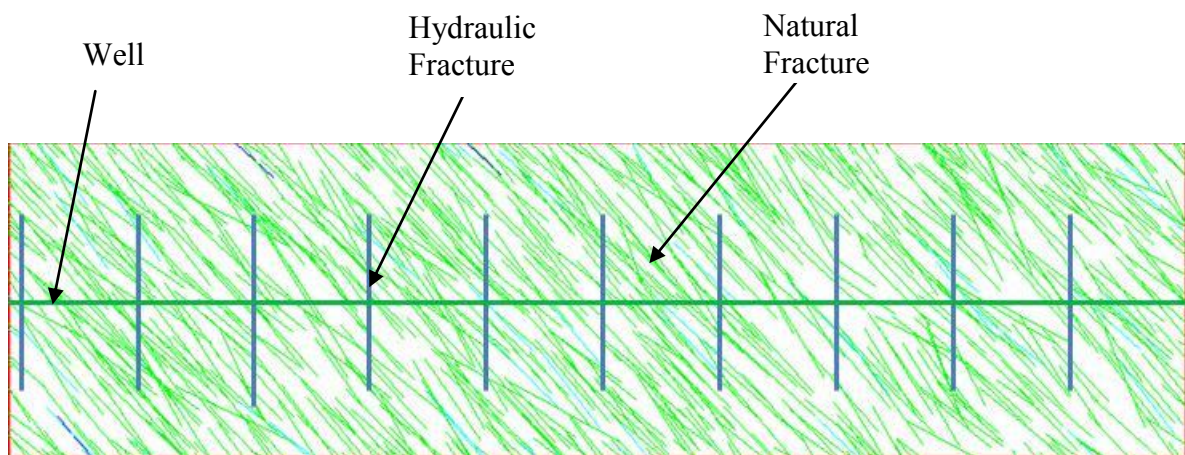
Table 5.2: Reservoir parameters for an Eagle Ford shale gas well for case 1

Reservoir and Fracture Properties for Well A	
Parameter	Value
Wellbore Radius (ft)	0.33
Wellbore Lateral Length (ft)	3710
Number of Fracture Stages	10
Depth (ft)	10875
Pay Zones Thickness (ft)	283
Reservoir Pressure	7000
Specific Gravity	0.621
Temperature (F)	285
BHFP (psi)	3600
Drainage Area (Acres)	80
Reservoir Size (ft)	(933.38 , 3733.52)
Reservoir Permeability (nd)	55
Reservoir Porosity (%)	4

From the FracGen and NFlow procedure shown in **Fig. 5.1**, a FracGen input **A1.1** (**Appendix 1**) was created from the fracture properties and other reservoir parameters for the Eagle Ford Shale gas (**Table 5.2**) and fed into FracGen to generate a fracture map **Fig. 5.2**, the well control data is shown in **Table 5.3**.

Table 5.3: Control data fed into FracGen for case 1

Fracture Property	Value	Source
Fracture Aperture (ft)	2.E-04	Assumed
Mean Fracture Length (ft)	280	Assumed
Fracture Orientation (degree)	N 45° E	Assumed
Fracture Density (ft/ft ²)	0.056	Assumed
Hydraulic Fracture Aperture (ft)	2.E-04	Assumed
Hydraulic Fracture Length (ft)	400	Well Data
Hydraulic Fracture Orientation	E-W	Assumed
Number of Hydraulic Fracture Stages	10	Well Data

**Figure 5.2: FracGen fracture map showing the well profile of the reservoir for case 1**

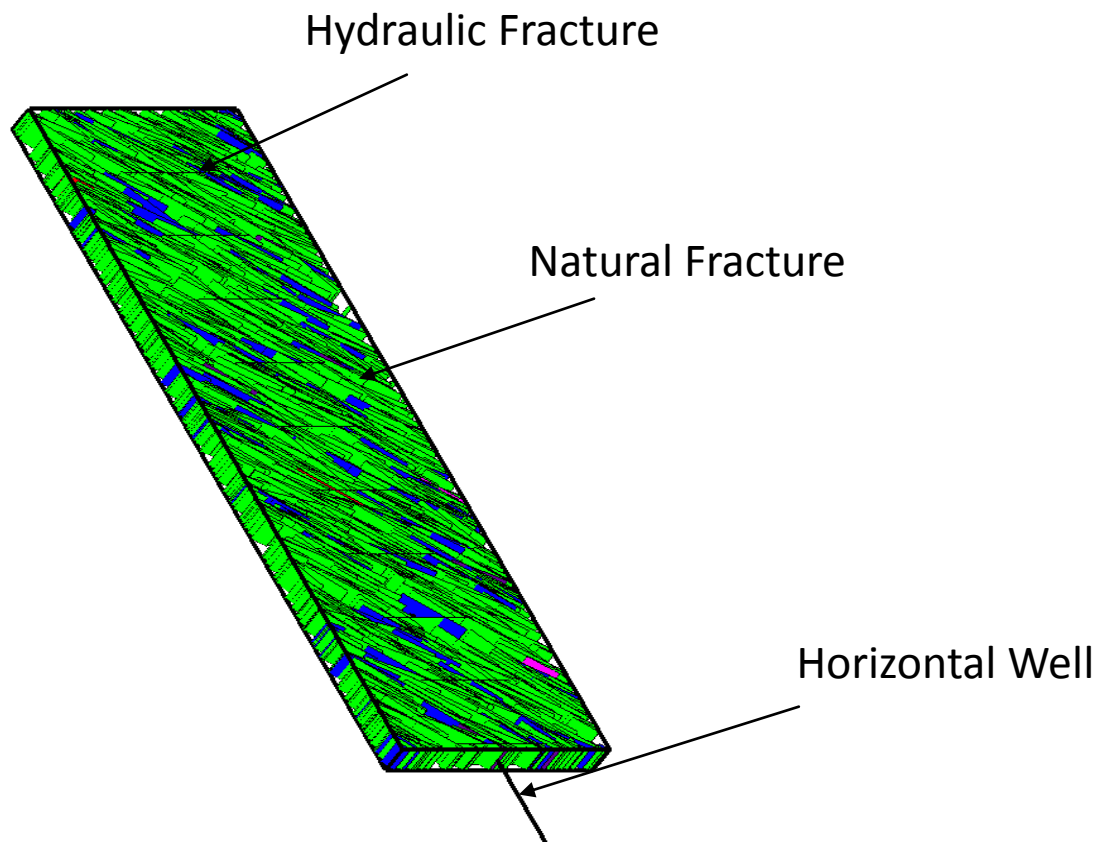


Figure 5.3: 3d representation of the well and fracture distribution

The FLO file **A1.2** and LDF file **A1.3** are used to run the flow simulation. The next step is to add well parameters to the FLO file; this basically involves the well location, well radius and some key words that identify it as a well. Then a BHP file **A1.4** and RES file **A1.5** is created. The file path to the LDF and BHP files are added to the RES file to enable NFlow access them during the flow simulation. Another important process carried out before flow simulation is to apply a FARM factor if necessary to the FLO file which represents damage around the well due to drilling activities, it can also

represent a skin factor. Then the RES and FLO file is fed into Nfflow and the flow simulation is run and the reservoir parameter is adjusted to obtain a match for the reservoir data.

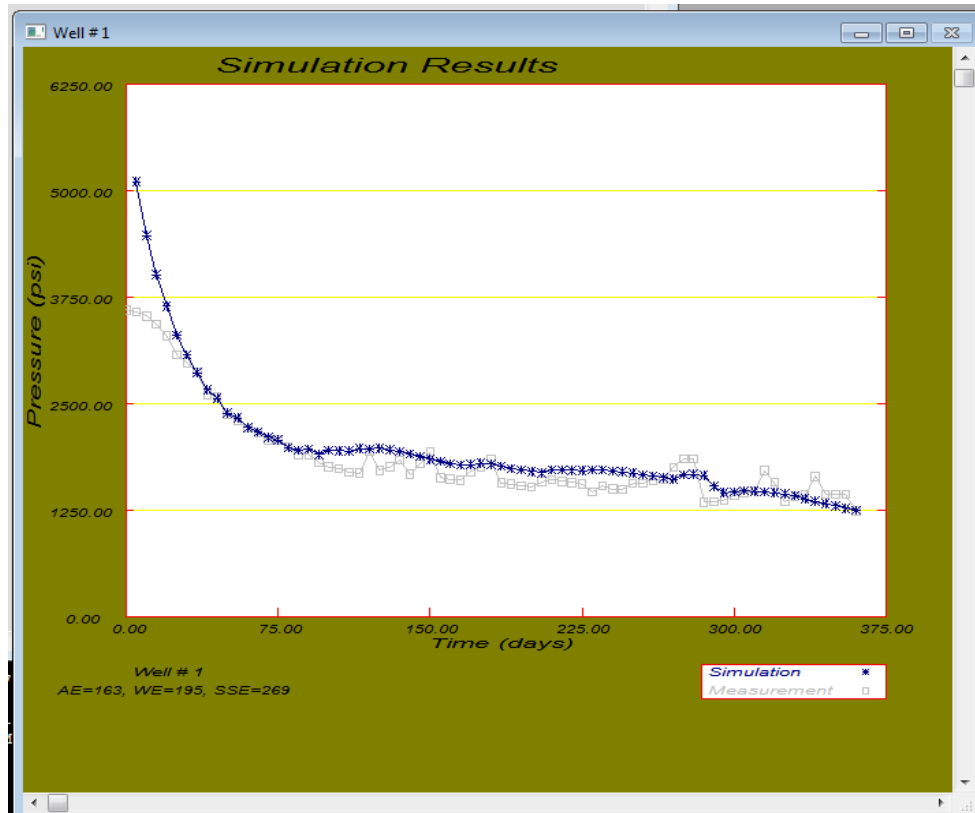


Figure 5.4: Nfflow output showing the simulation result for case 1

Fig. 5.3 is a 3d representation of the well and fracture distribution while **Fig. 5.4** shows the simulation result for the case run above and is taken to be the control case as we have a match with the observed data. The next step is to vary the fracture/well control properties stated in **Table 5.3** and observe the changes to the reservoir response. The values in **Table 5.4** are used as input parameters for the flow simulation.

Table 5.4: Summary of fracture/well parameters for case 1

Fracture/well Prop.	-50%	-25%	Control	+25%	+50%
Fracture Aperture (ft)	0.00001	0.00015	0.00002	0.000025	0.00003
Fracture Density (points/ft ²)	0.0001	0.00015	0.0002	0.00025	0.0003
Mean Fracture Length (ft)	140	210	280	350	420
Hydraulic Fracture Aperture (ft)	0.00001	0.000015	0.00002	0.000025	0.00003
Hydraulic Fracture Length(ft)	200	300	400	500	600

Some preliminary calculations were carried out shown in **Appendix 2**, this is to ensure that the 2d- fracture density is either kept constant or varied when altering fracture properties by using the relationship relating 2d-fracture density with the other properties.

It is important to note that for all cases in this project, 2 simulation runs were carried out for each input parameter, one is for the pressure response using a rate controlled RES & BHP files and the other uses a pressure controlled file for cumulative gas produced.

5.3.1 Fracture Aperture

This represents the width of the fracture opening; the value in the control file is 0.00002 ft, this value is varied in steps and the values obtained are used for running simulations **Figs. 5.5-5.6** shows summaries of the responses observed.

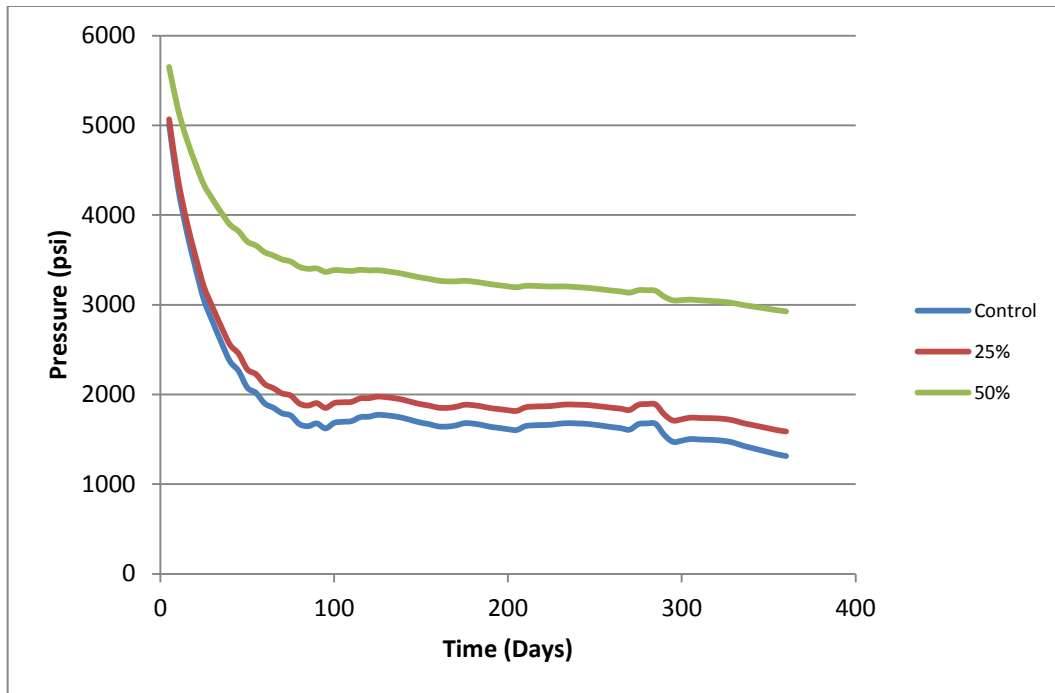


Figure 5.5: Change in pressure response due to increase in fracture aperture for case 1

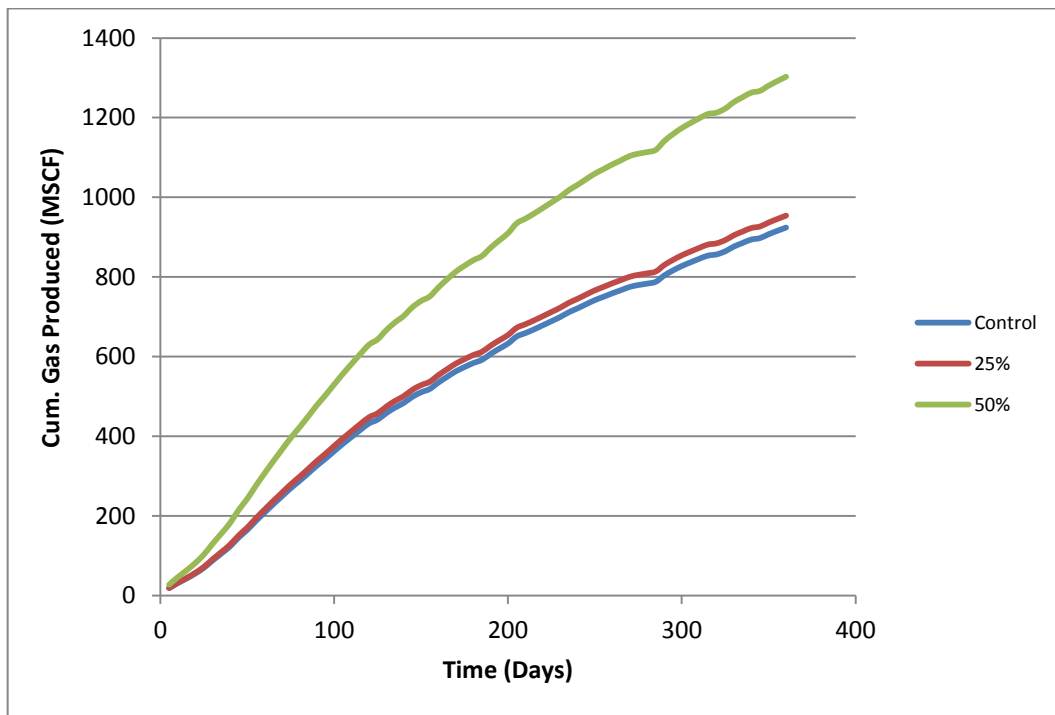


Figure 5.6: Change in cum. gas produced due to increase in fracture aperture for case 1

5.3.2 Fracture Density

The fracture density represents the number of fractures per unit area/volume, the value in the control file is 0.0002 points/ft², this value is varied in steps from the control and the values obtained were used to run simulations and results are shown in **Fig. 5.7 - 5.10**.

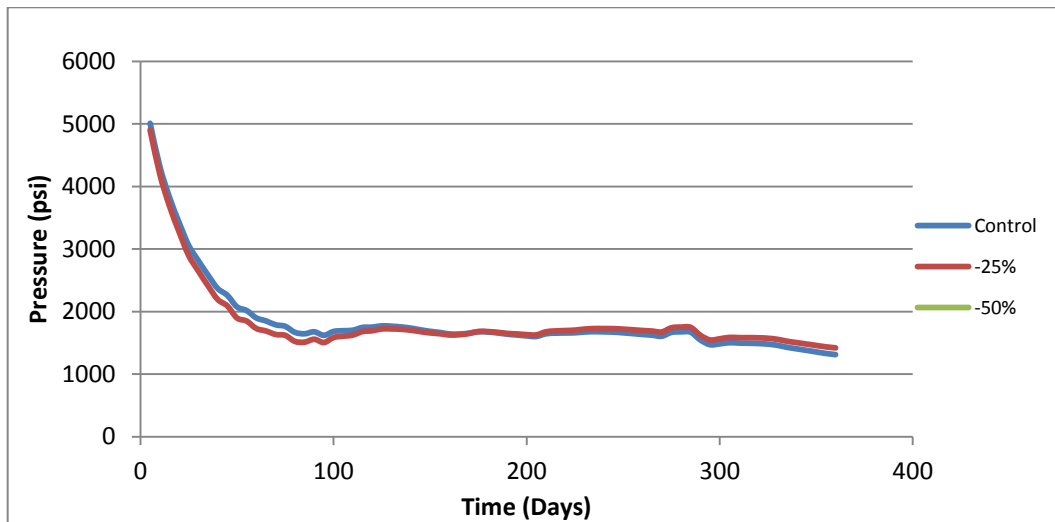


Figure 5.7: Change in pressure response due to decrease in fracture density for case 1

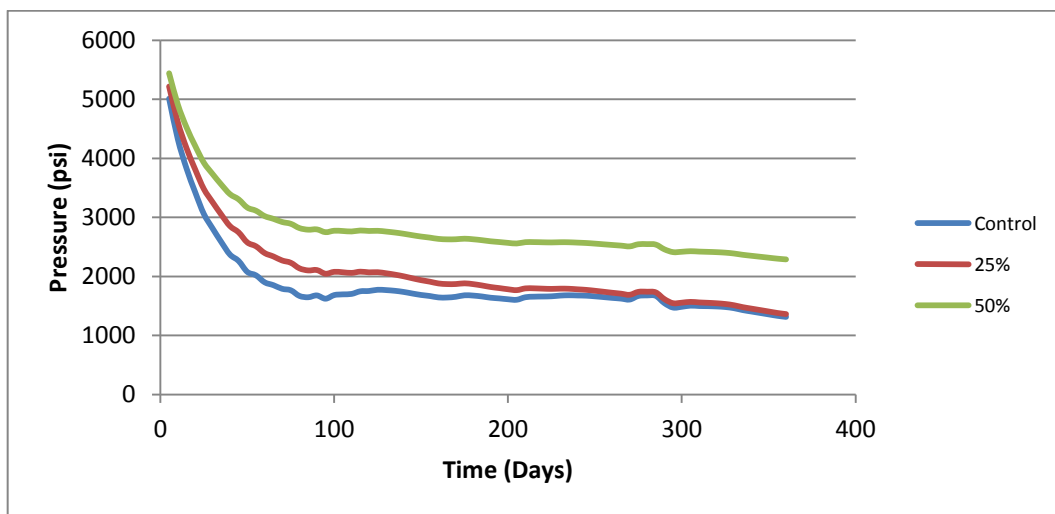


Figure 5.8: Change in pressure response due to increase in fracture density for case 1

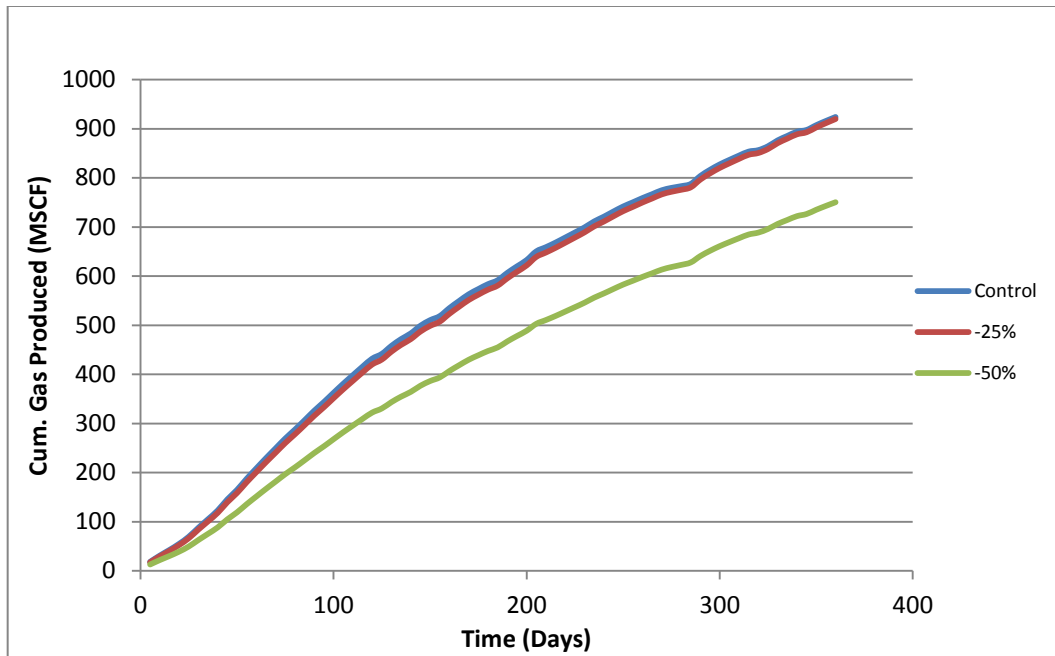


Figure 5.9: Change in cum. gas produced due to decrease in fracture density for case1

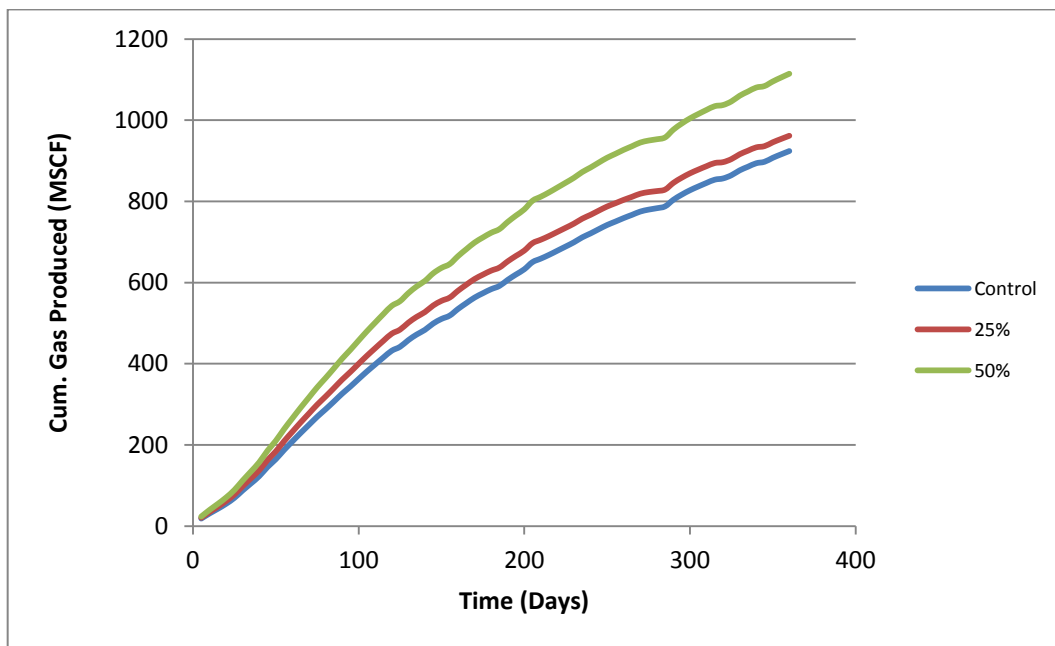


Figure 5.10: Change in cum. gas produced due to increase in fracture density for case1

5.3.3 Fracture Length

This represents the mean length of the fracture with a fracture set, the value in the control file is mean of 280 ft, this value is varied in steps and values obtained were used to run simulations and results obtained are shown in **Fig. 5.11 - 5.14**.

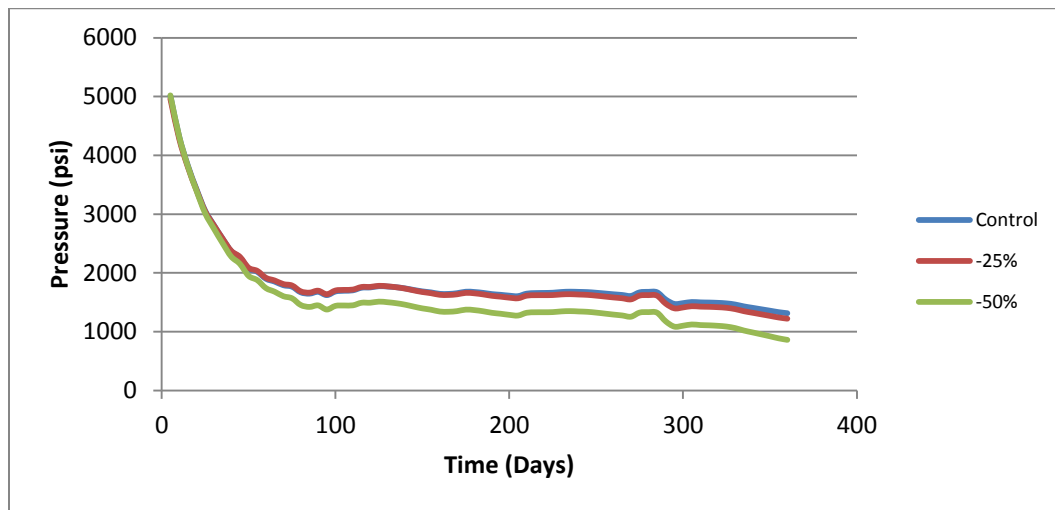


Figure 5.11: Change in pressure response due to decrease in fracture length for case 1

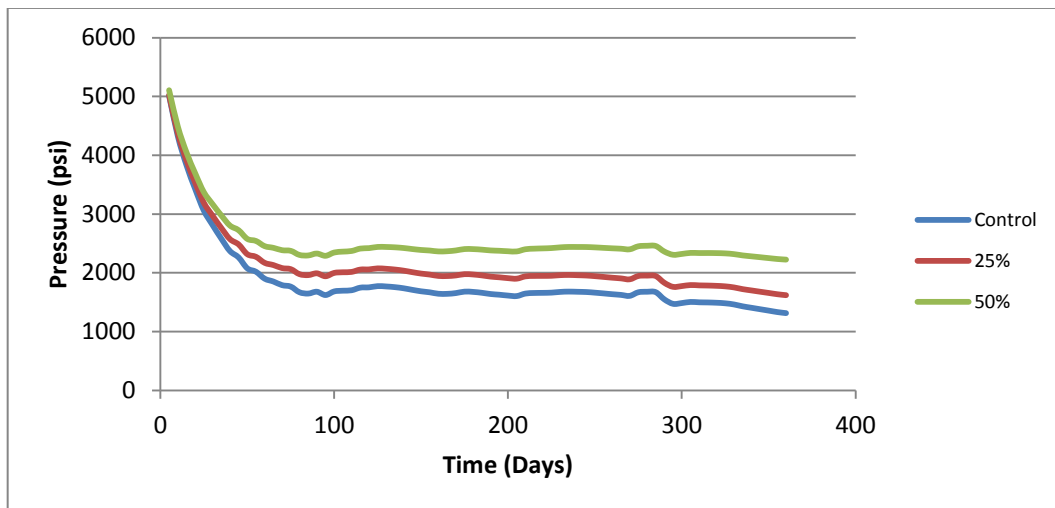


Figure 5.12: Change in pressure response due to increase in fracture length for case 1

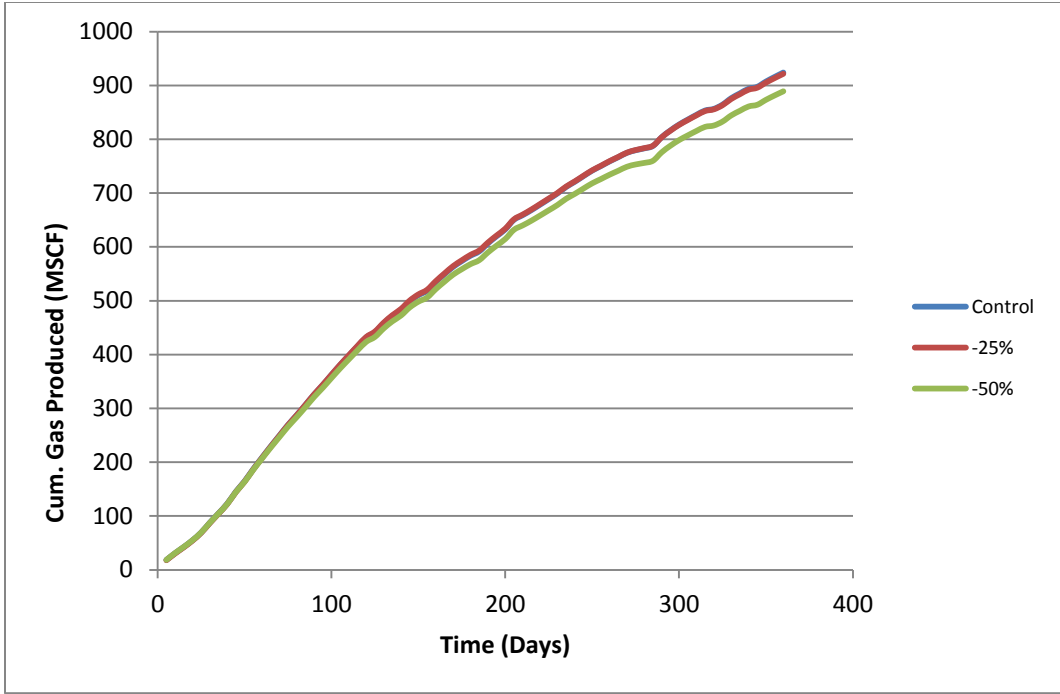


Figure 5.13: Change in cum. gas produced due to decrease in fracture length for case 1

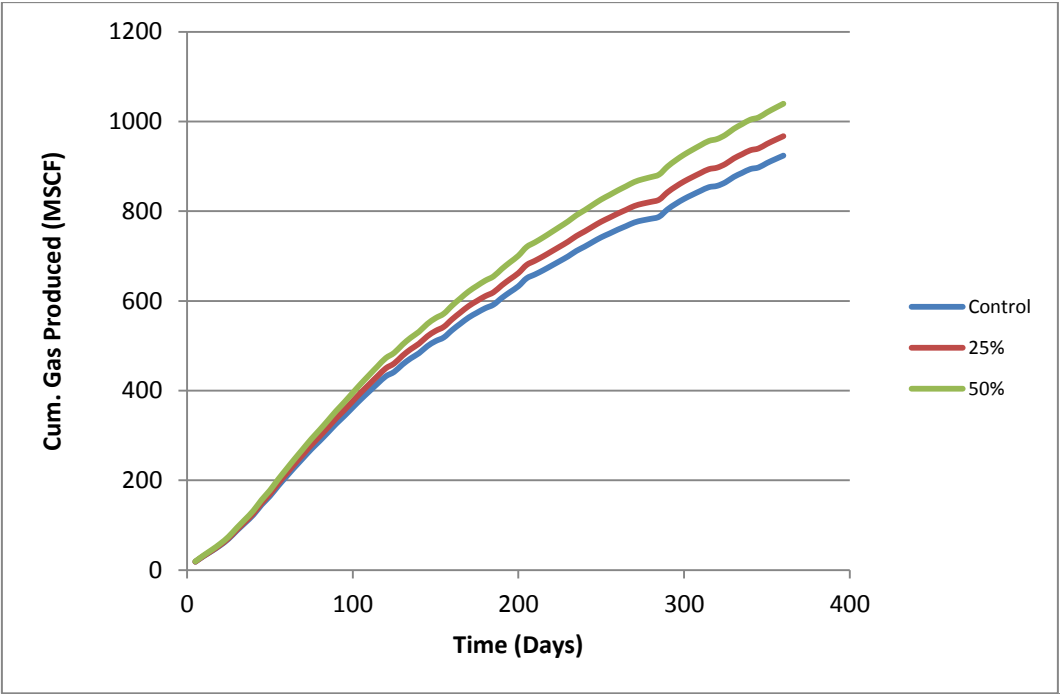


Figure 5.14: Change in cum. gas produced due to increase in fracture length for case 1

The summary plots (**Fig.5.15 &5.16**) for the non-controllable fracture properties for the change in cumulative gas production.

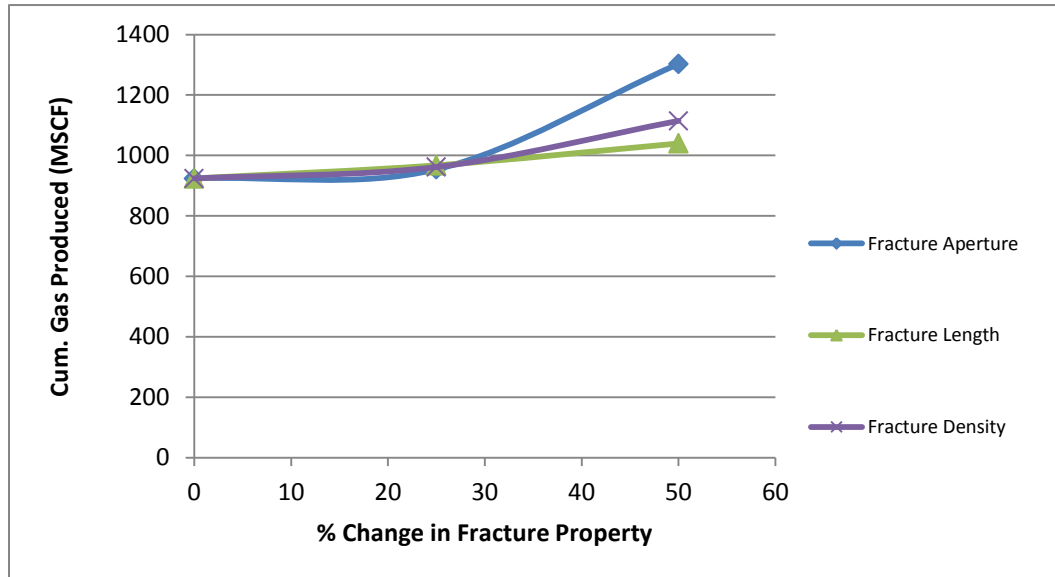


Figure 5.15: Change in cum. gas produced due to increase fracture property for case 1

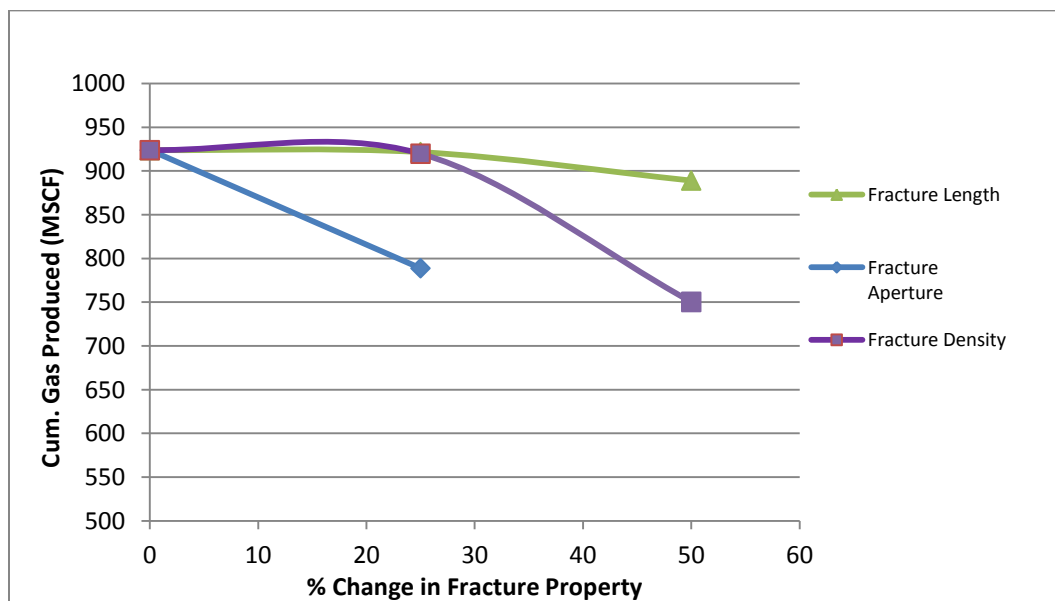


Figure 5.16: Change in cum. gas produced due to decrease in fracture property for case 1

5.3.4 Number of Hydraulic Fracture Stages

This represents the number of fracture stages; it is 10 in the control file. This number is varied and was used to run flow simulation and results are shown in **Fig. 5.17 & 5.18**.

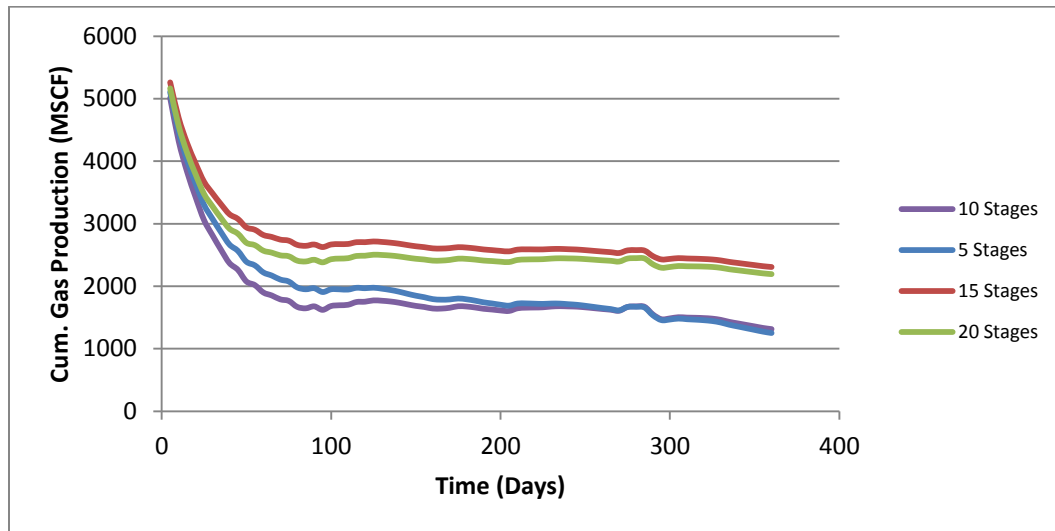


Figure 5.17: Change in pressure for different hydraulic fracture stages for case 1

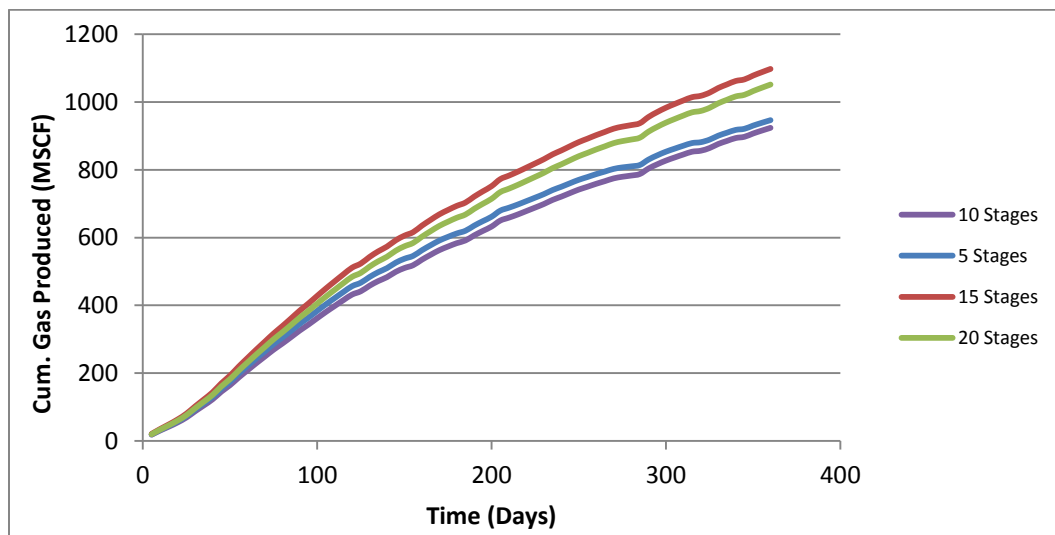


Figure 5.18: Change in cum. gas produced for different numbers of hydraulic fracture stages for case 1

5.3.5 Hydraulic Fracture Aperture

This represents the aperture of the hydraulic fracture, the value in the control file is 0.00002 ft, this value is varied in steps from the control and were used to run flow simulation and results obtained is shown in **Fig. 5.19 -Fig. 5.22**.

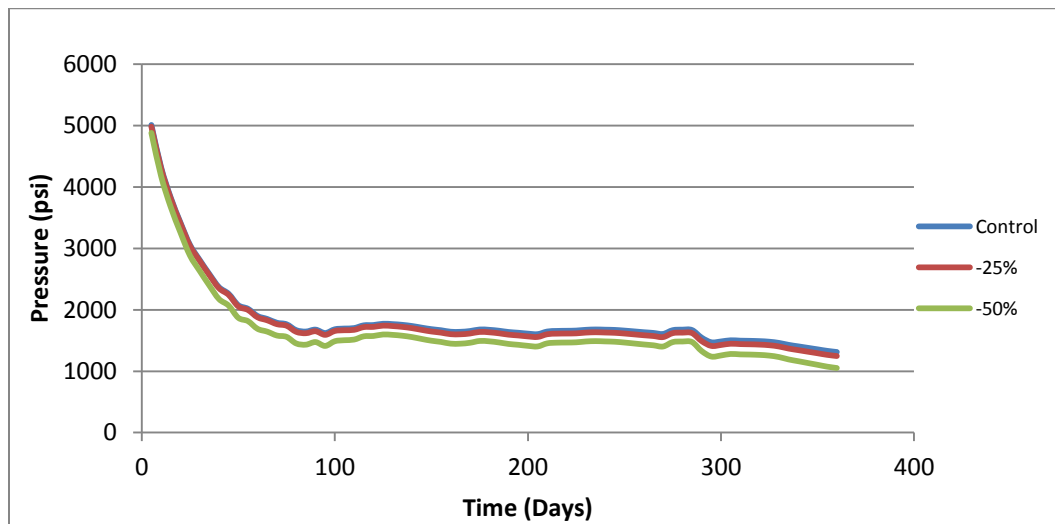


Figure 5.19: Change in pressure due to decrease in hydraulic fracture aperture for case 1

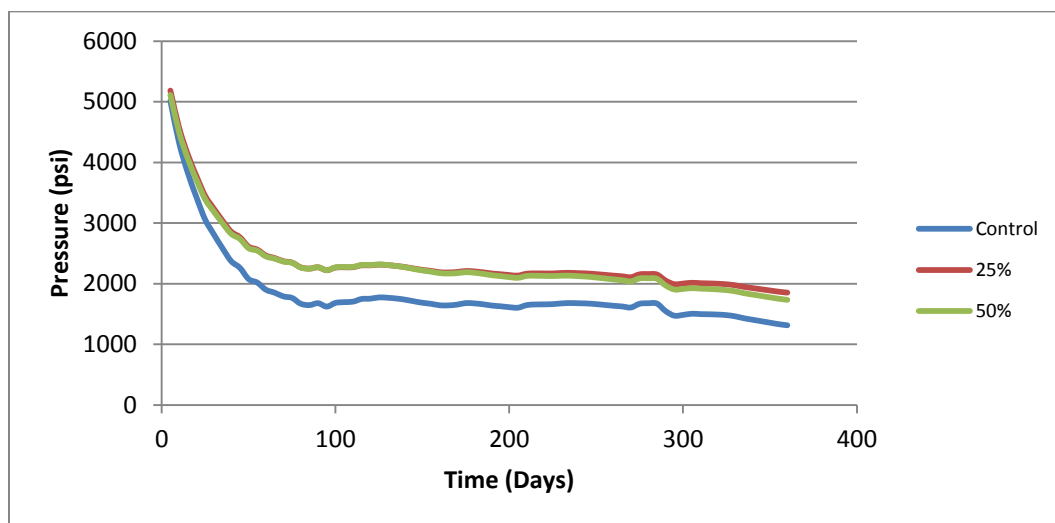


Figure 5.20: Change in pressure due to increase in hydraulic fracture aperture for case 1

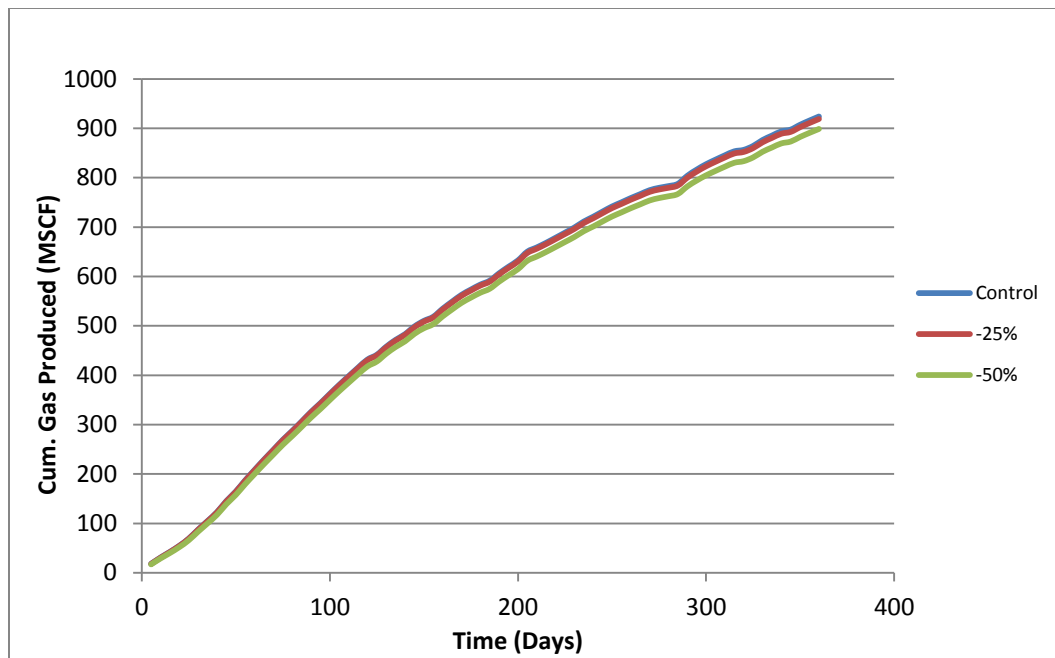


Figure 5.21: Change in cum. gas produced due to decrease in hydraulic fracture aperture for case 1

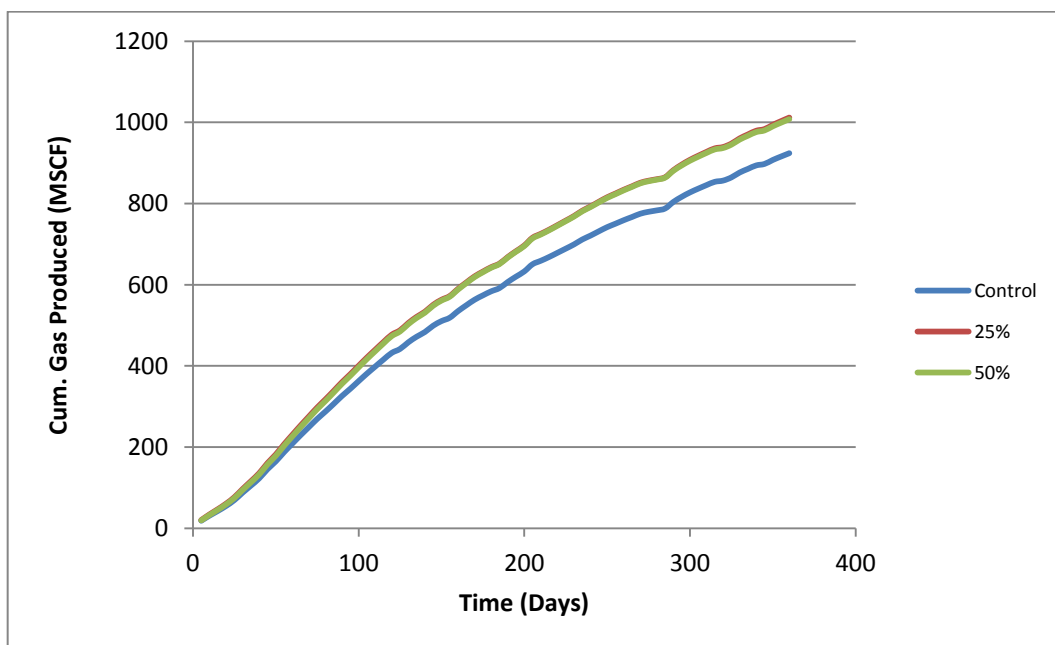


Figure 5.22: Change in cum. gas produced due to increase in hydraulic fracture aperture for case 1

5.3.6 Hydraulic Fracture Length

This represents the length of the hydraulic fracture; the value is 400 ft. in the control file. This value is varied in steps from the control and the values obtained were used to run flow simulation and results are shown in **Fig. 5.23 - 5.26**.

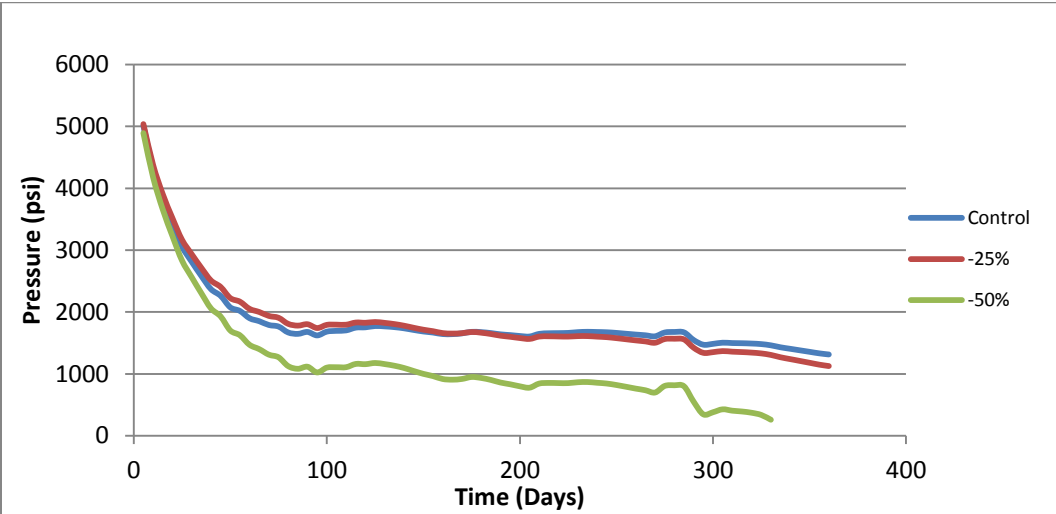


Figure 5.23: Change in pressure due to decrease in hydraulic fracture length for case 1

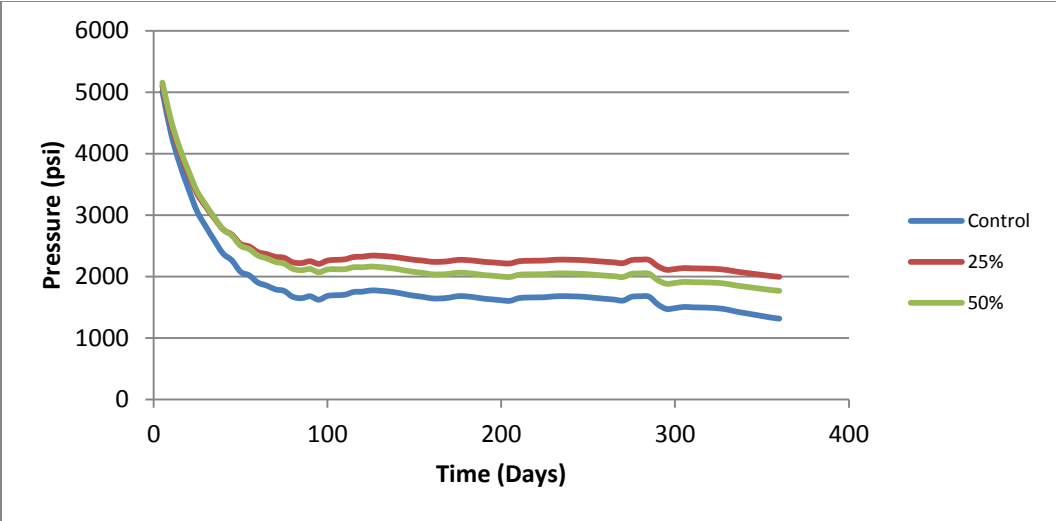


Figure 5.24: Change in pressure due to increase in hydraulic fracture length for case 1

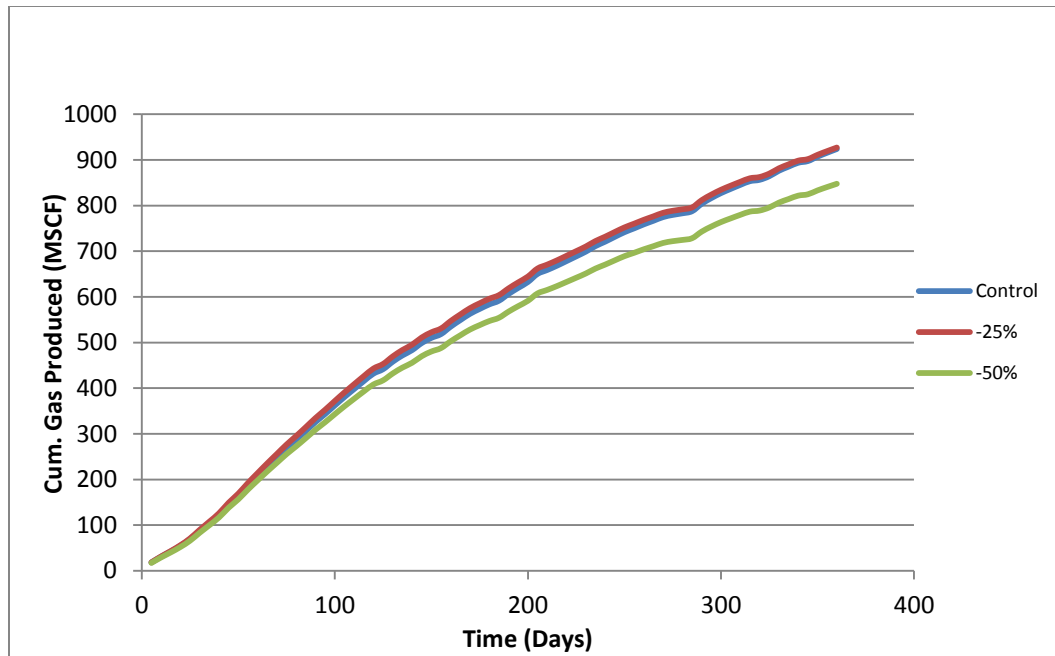


Figure 5.25: Change in cumulative gas produced due to decrease in hydraulic fracture length for case 1

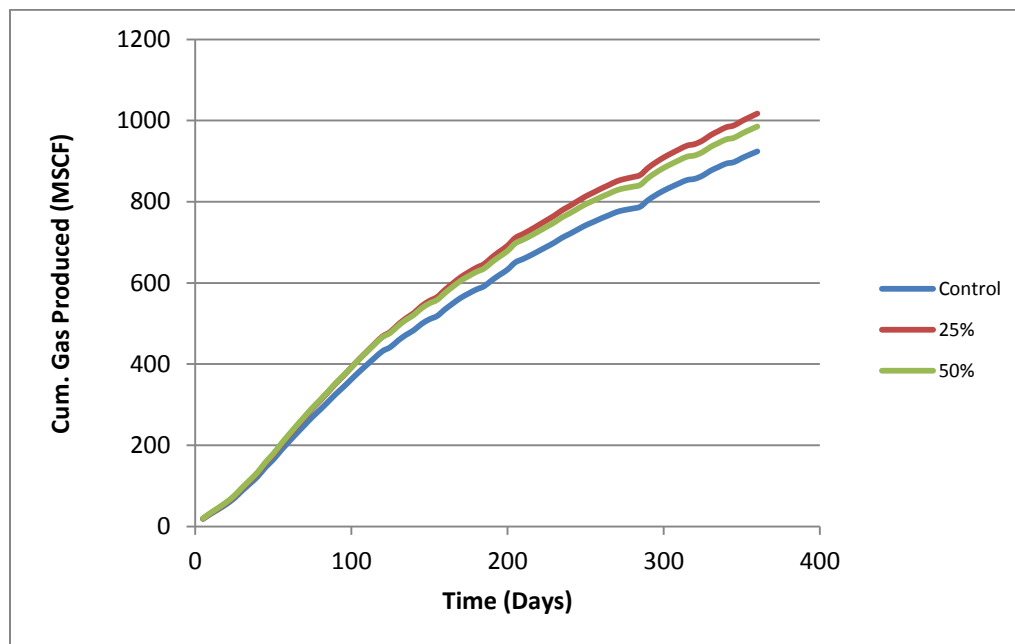


Figure 5.26: Change in cumulative gas produced due to increase in hydraulic fracture length for case 1

The chart (**Table 5.5**) is a summary of the different effects on reservoir response observed.

Table 5.5: Summary of effect of fracture property on reservoir response for case 1

Fracture Property	Increasing Property	Decreasing Property
Fracture Length	The bottomhole pressure increases and the cum. gas produced increases	The bottomhole pressure decreases. The Cum. Gas produced decreases steadily.
Fracture Aperture	The bottomhole pressure increases. The Cum. Gas produced remains increases.	
Fracture Density	The bottomhole pressure increases and the cum. gas produced increases	The bottomhole pressure decreases. The Cum. Gas produced decreases steadily.
Hydraulic Fracture Stages	The bottomhole pressure increases and cum. gas produced increases till it reaches an optimum value	The bottomhole pressure decreases and cum. gas produced decreases.
HF Fracture Aperture	The bottomhole pressure remain largely constant at lower values but increases with larges values in hydraulic fracture Aperture and cum. gas produced follows the same trend	The bottomhole pressure and cum. gas produced remain constant
HF Fracture Length	The bottomhole pressure increases steadily and cum. gas produced increases till it reaches an optimum value	The bottomhole pressure decreases steadily and cumulative gas produced decreases.

5.4 Case 2: Clustered Fracture Pattern of One Fracture Set

For the analysis due to the highly stochastic nature of the clustered fracture network, we considered more increments and also for each case considered a number of simulation runs and the output were averaged to improve the accuracy of the solution and reduce the effect of the stochastic distribution of parameters.

Some preliminary calculations were carried out shown in **Appendix 2**, this is to ensure that the 2d- fracture density is either kept constant or varied when altering fracture properties by using the relationship relating 2d-fracture density with the other properties. **Table 5.6** shows the reservoir parameters for the Eagle Ford shale gas.

Table 5.6: Reservoir parameters for an Eagle Ford shale gas well for case 2

Reservoir and Fracture Properties for Well A	
Parameter	Value
Wellbore Radius (ft)	0.33
Wellbore Lateral Length (ft)	3710
Number of Fracture Stages	10
Depth (ft)	10875
Pay Zones Thickness (ft)	283
Reservoir Pressure	7000
Specific Gravity	0.621
Temperature (F)	285
BHFP (psi)	3600
Drainage Area (Acres)	80
Reservoir Size (ft)	(933.38 , 3733.52)
Reservoir Permeability (nd)	55
Reservoir Porosity (%)	4

The list outlines properties used to describe a clustered fracture network in FracGen, listed in **Table 5.7** and used as input to produce the fracture map **Fig. 5.27**.

- 1) Cluster length
- 2) Fracture length
- 3) Intra-cluster fracture density/spacing
- 4) Density of cluster center-points
- 5) Fracture aperture
- 6) Hydraulic fracture aperture
- 7) Hydraulic fracture length
- 8) Hydraulic fracture stages

Table 5.7: Control data fed into FracGen for case 2

Fracture Property	Value	Source
Fracture Aperture (ft)	0.00002	Assumed
Mean Fracture Length (ft)	280	Assumed
Fracture Orientation (deg.) (Mean, SD.)	N 45° W, 8.0	Assumed
2d Fracture Density (ft/ft ²)	0.056	From Case 1
Hydraulic Fracture Aperture (ft)	0.00002	Assumed
Hydraulic Fracture Length (ft)	400	Well Data
Hydraulic Fracture Orientation	E-W	Assumed
Number of Hydraulic Fracture Stages	10	Well Data
Cluster Orientation (deg.) (Mean, STD)	N 40° W, 10.0	Assumed
Mean cluster Length (ft)	1500	Assumed
Mean Intra-cluster Fracture spacing (ft)	40	Assumed
Mean Intra-cluster Fracture density (ft)	0.00006	Assumed
Density of cluster center-point (pts/ft ²)	0.0000057	Assumed

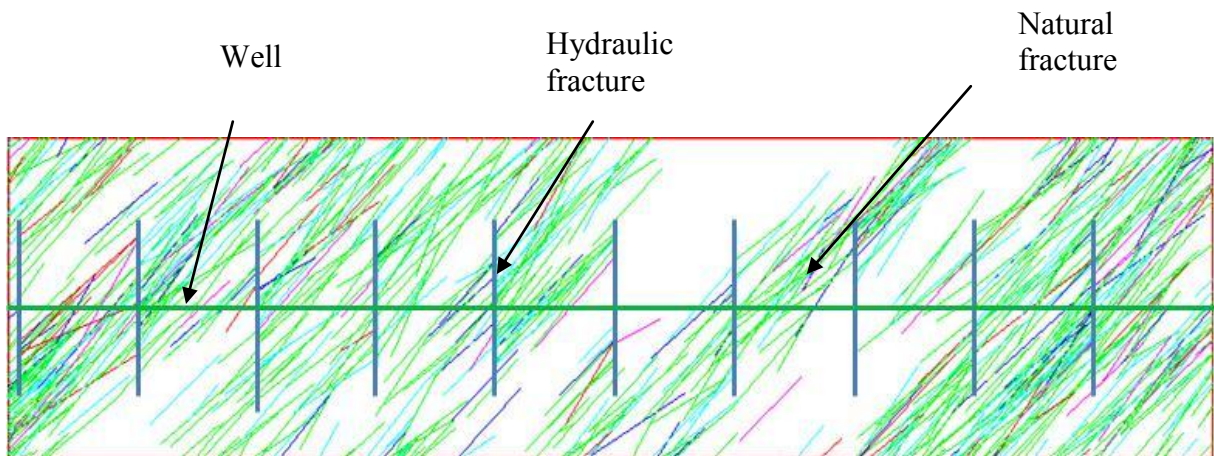


Figure 5.27: FracGen fracture map showing the well profile for case 2

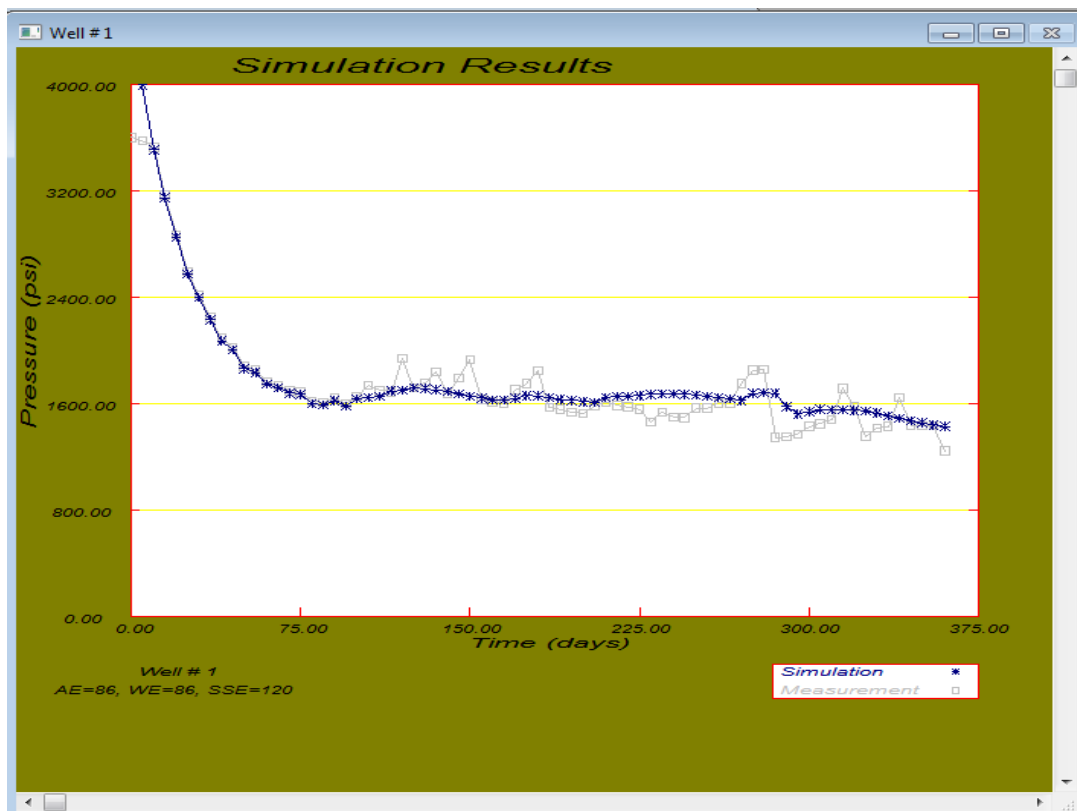


Figure 5.28: Nflow output showing the simulation result for case 2

Using the same procedure described in case 1 the simulation output is obtained and shown in **Fig. 5.28**.

Fig. 5.28 shows the simulation result for the case run above and is taken to be the control data. The next step is to vary the control fracture/well properties stated in **Table 5.8** and observe the changes to the reservoir response.

Table 5.8: Summary of fracture/well parameters plotted for case 2

Fracture/well Prop.	-50%	-25%	Control	25%	50%	100%
Fracture Aperture (ft)	0.000010	0.000015	0.000020	0.000025	0.000030	-
Fracture Density (ft/ft ²)	0.028	0.042	0.056	0.070	0.084	0.112
Fracture Length (ft)	140	210	280	350	420	560
Hydraulic Fracture Aperture (ft)	0.00001	0.000015	0.00002	0.000025	0.00003	0.00004
Hydraulic Fracture Length(ft)	200	300	400	500	600	800
Density of cluster center point (pts/ft ²)	1.030E-05	7.241E-06	5.742E-06	4.874E-06	4.324E-06	3.726E-06

5.4.1 Fracture Length

This represents the mean length of the fracture within a fracture set, the value in the control file is 280 ft, this value is varied in steps from the control and values obtained were used to run simulations and results obtained are shown in **Fig. 5.29 & 5.30**.

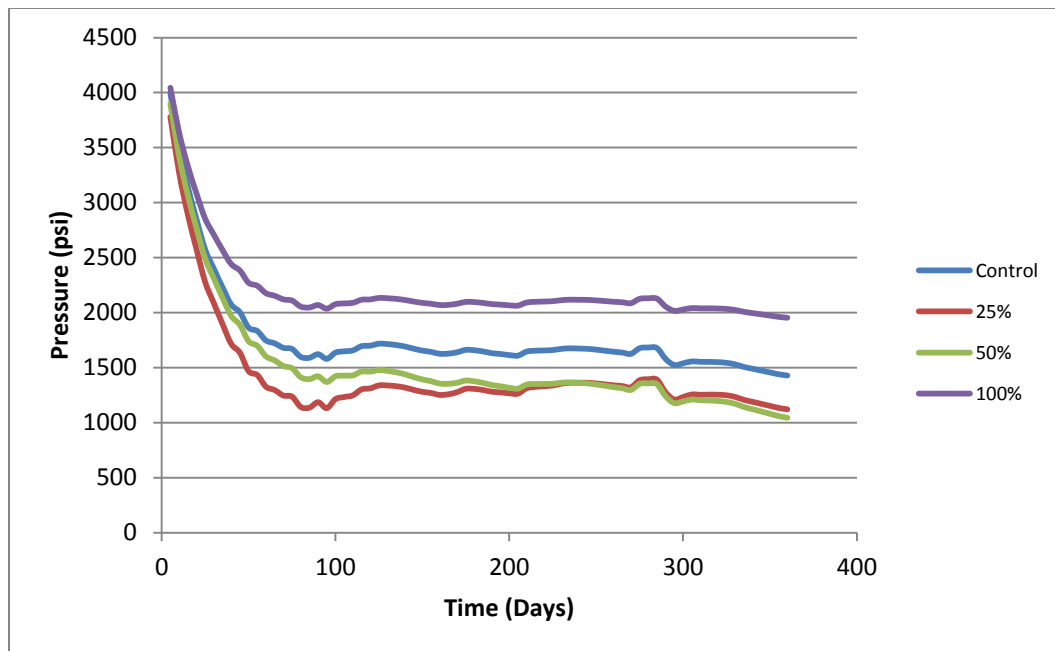


Figure 5.29: Change in pressure response due to increase in fracture length for case 2

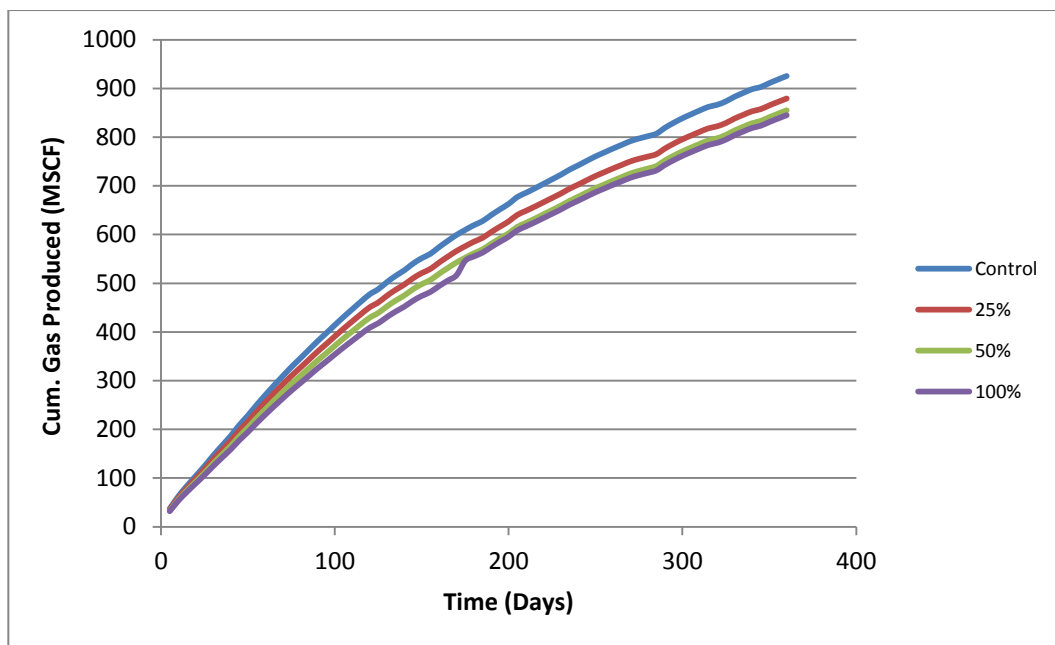


Figure 5.30: Change in cum. gas produced due to increase in fracture length for case 2

5.4.2 Fracture Density

This represents the density of fractures within the clusters, the control value is 0.0000057 pts/ft and it is varied in steps. The simulation results shown **Fig. 5.31 - 5.32**.

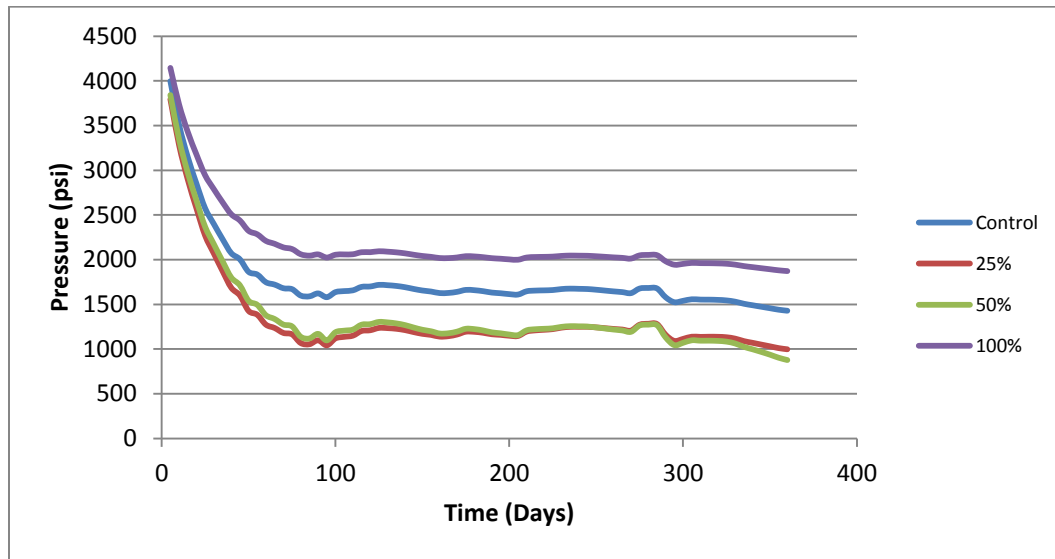


Figure 5.31: Change in pressure response due to increase in fracture density for case 2

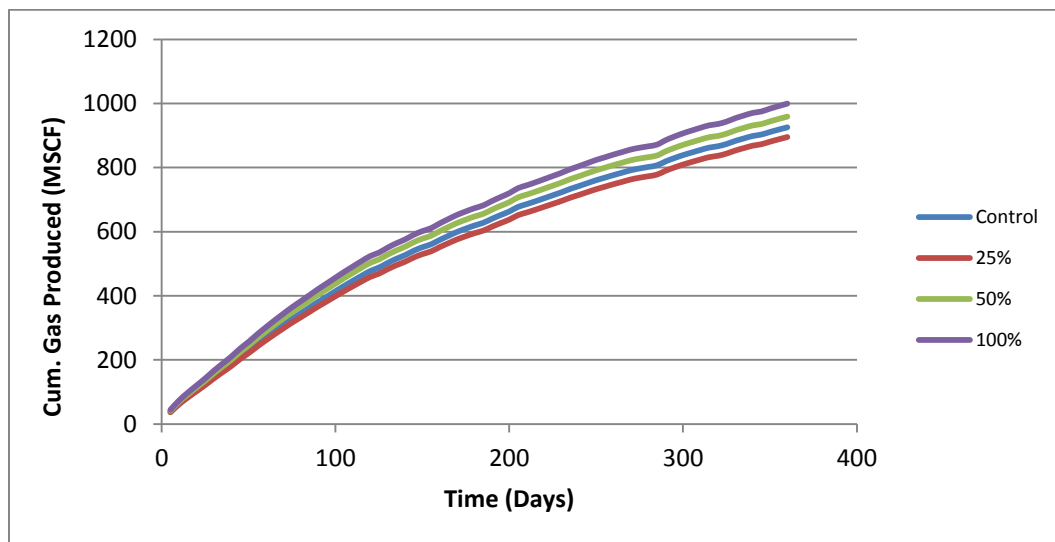


Figure 5.32: Change in cum. gas produced due to increase in fracture density for case 2

5.4.3 Fracture Aperture

This represents the aperture of the fractures, the value in the control file is 0.00002 ft, and simulation results obtained are shown in **Fig. 5.33 – 5.34**.

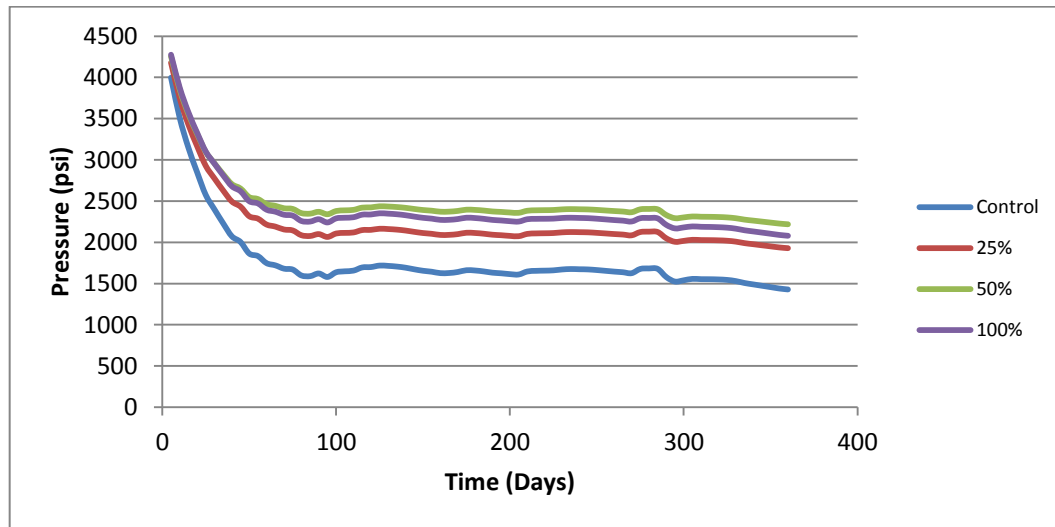


Figure 5.33: Change in pressure due to increase in fracture aperture for case 2

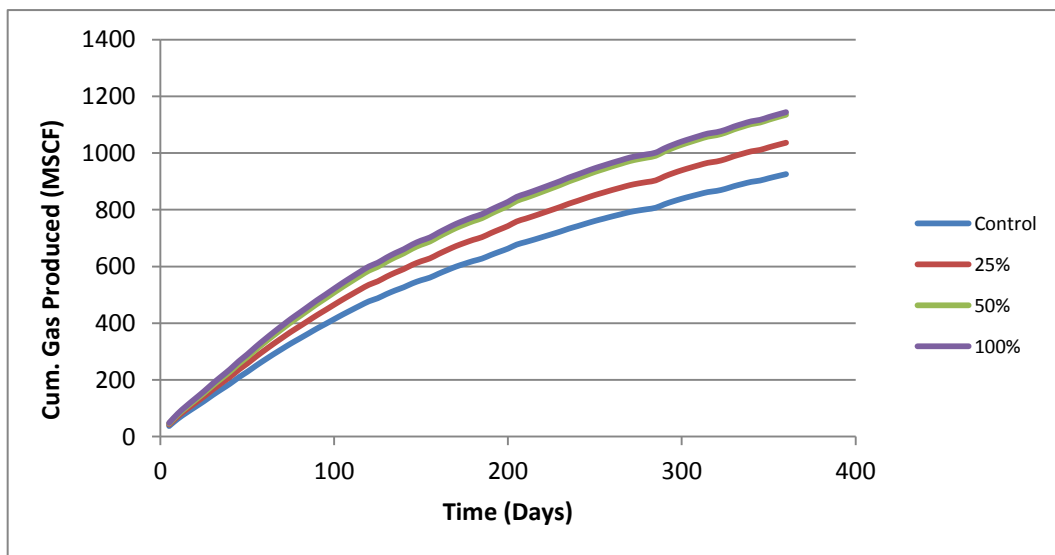


Figure 5.34: Change in cum. gas produced due to increase in fracture aperture for case 2

5.4.4 Hydraulic Fracture Aperture

This represents the aperture of the hydraulic fractures, the value in the control file is 0.00002 ft and simulations results obtained are shown in **Fig. 5.35 – 5.36**.

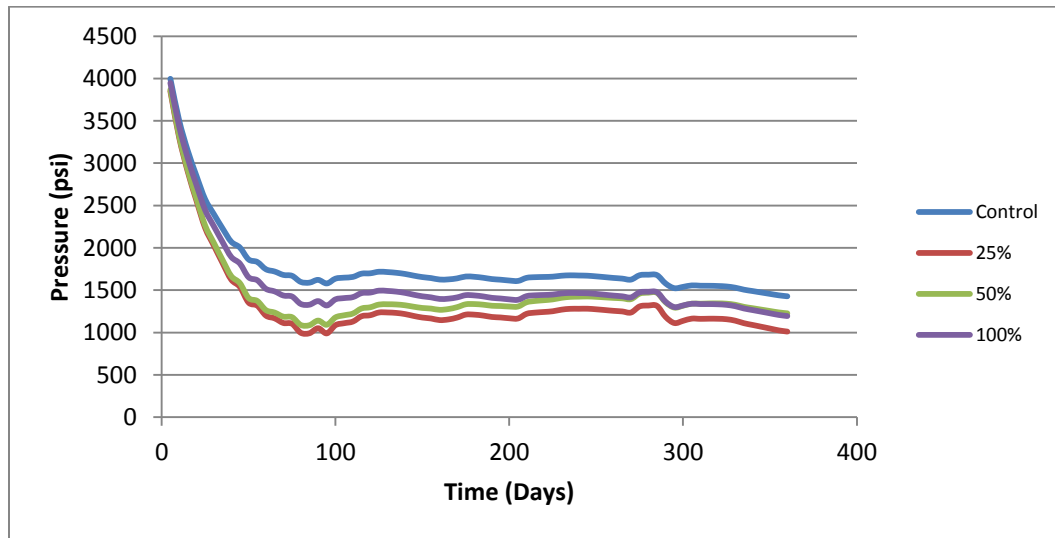


Figure 5.35: Change in pressure due to increase in hydraulic fracture aperture for case 2

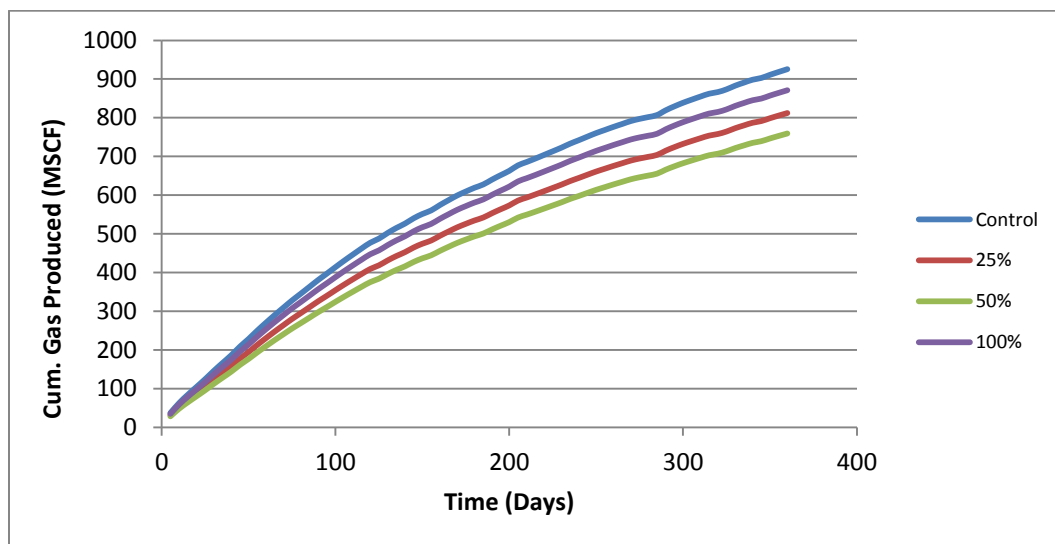


Figure 5.36: Change in cum. gas produced due to increase in hydraulic fracture aperture for case 2

5.4.5 Hydraulic Fracture Length

This represents the length of the hydraulic fractures, the value in the control file is 400 ft, and simulations results obtained are shown in **Fig. 5.37 – 5.40**.

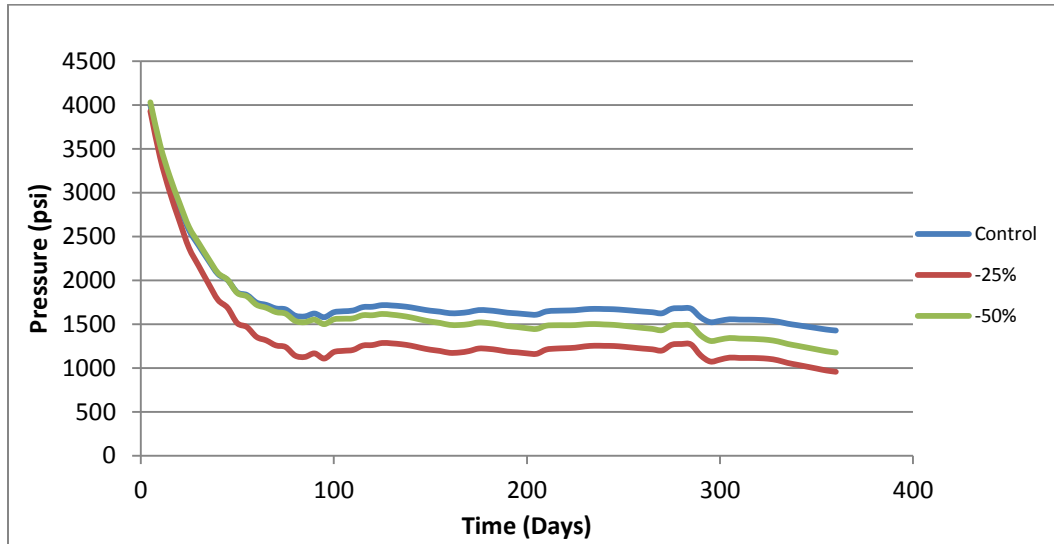


Figure 5.37: Change in pressure due to decrease in hydraulic fracture length for case 2

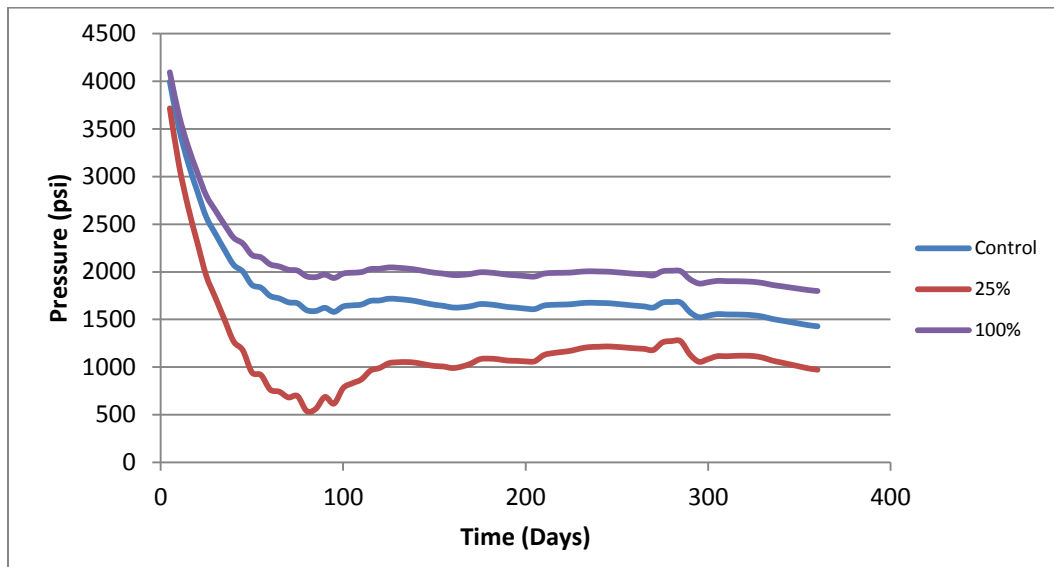


Figure 5.38: Change in pressure due to increase in hydraulic fracture length for case 2

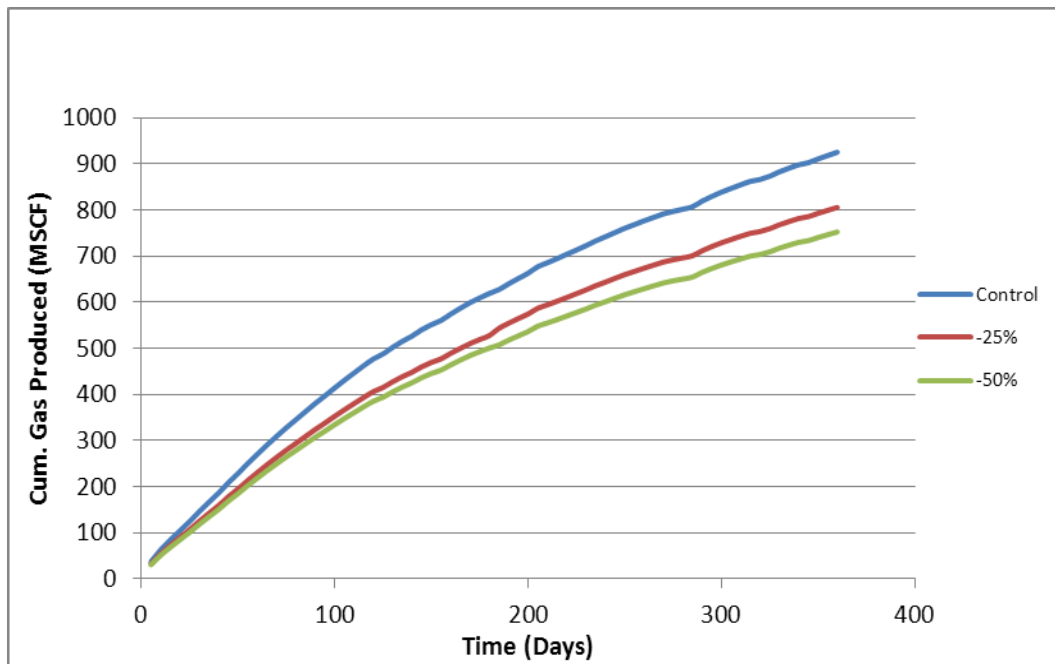


Figure 5.39: Change in cum. gas produced due to decrease in hydraulic fracture length for case 2

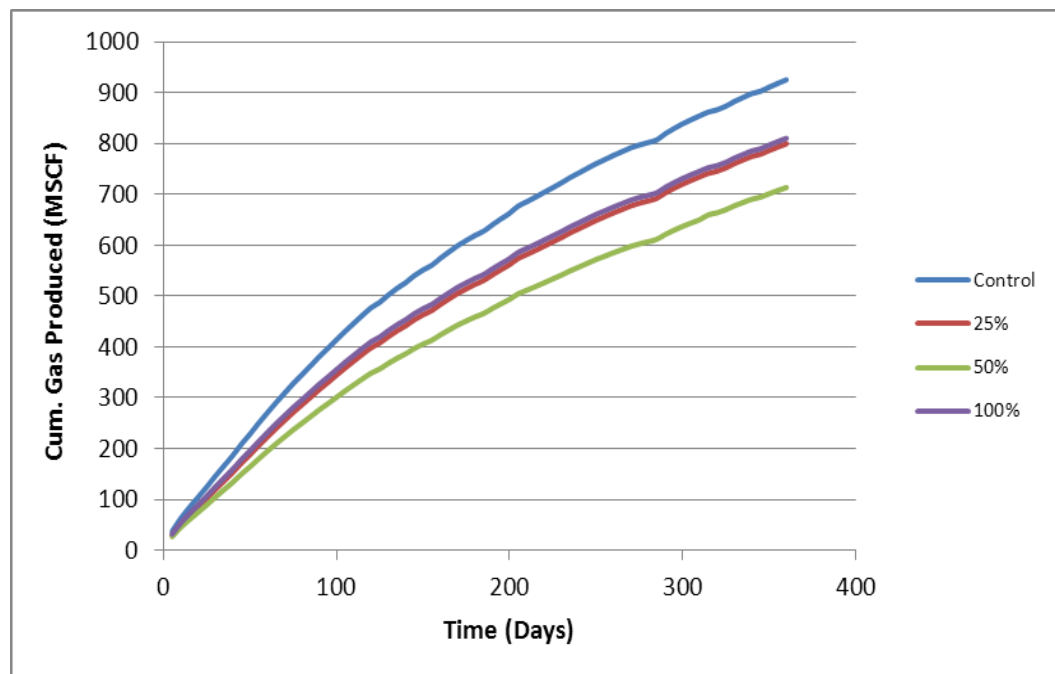


Figure 5.40: Change in cum. gas produced due to increase in hydraulic fracture length for case 2

5.4.6 Number of Hydraulic Fracture Stages

This represents the number of hydraulic fracture stages, the value in the control file is 10 stages, it is varied in steps and the simulation results are shown in, **Fig. 5.41 & 5.42.**

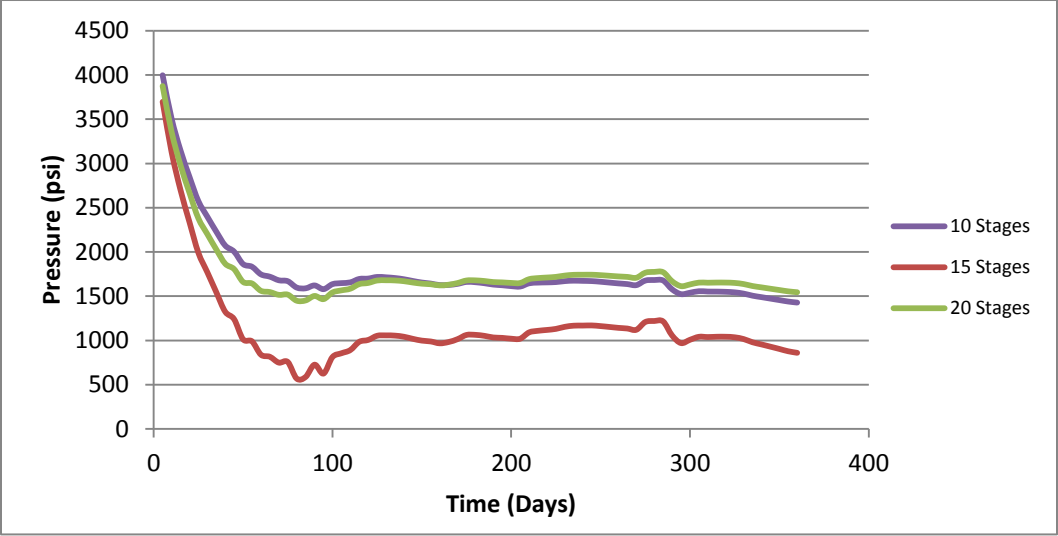


Figure 5.41: Change in pressure response due to change in hydraulic fracture stages for case 2

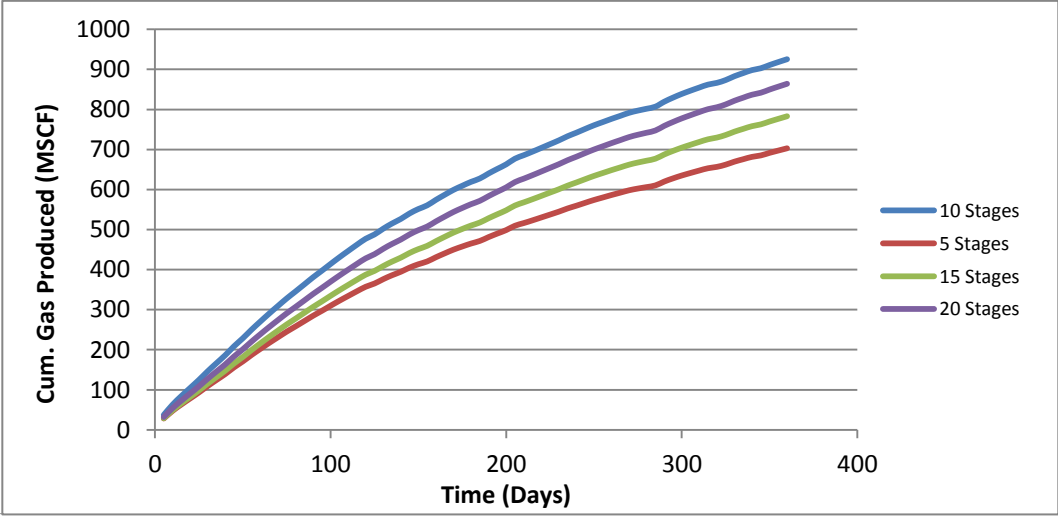


Figure 5.42: Change in cum. gas production due to change in hydraulic fracture stages for case 2

5.5 Case 3: Uniformly Distributed Fracture Pattern of Two Fracture Sets

We will consider the reservoir having 2 fracture sets which are uniformly distributed; one will be made the primary fracture set while the other is the secondary fracture set. Properties of the primary fracture set will be varied while the secondary is kept constant.

Table 5.9 shows the reservoir parameters for the Eagle Ford shale gas.

Table 5.9: Reservoir parameters for an Eagle Ford shale gas well for case 3

Reservoir and Fracture Properties for Well A	
Parameter	Value
Wellbore Radius (ft)	0.33
Wellbore Lateral Length (ft)	3710
Number of Fracture Stages	10
Depth (ft)	10875
Pay Zones Thickness (ft)	283
Reservoir Pressure	7000
Specific Gravity	0.621
Temperature (F)	285
BHFP (psi)	3600
Drainage Area (Acres)	80
Reservoir Size (ft)	(933.38 , 3733.52)
Reservoir Permeability (nd)	55
Reservoir Porosity (%)	4

Table 5.10: Control data fed into FracGen for case 3

Fracture Property	Primary	Secondary	Source
Fracture Aperture (ft)	2.E-04	2.E-04	Assumed
Fracture Length (mean)	280	280	Assumed
Fracture Orientation (degree)	N 45° E	N 120° E	Assumed
Fracture Density (ft/ft ²)	0.042	0.014	From Case1
Hydraulic Fracture Aperture (ft)	2.E-04		Assumed
Hydraulic Fracture Length (ft)	400		Well Data
Hydraulic Fracture Orientation	E-W		Assumed
Hydraulic Fracture Stages	10		Well Data

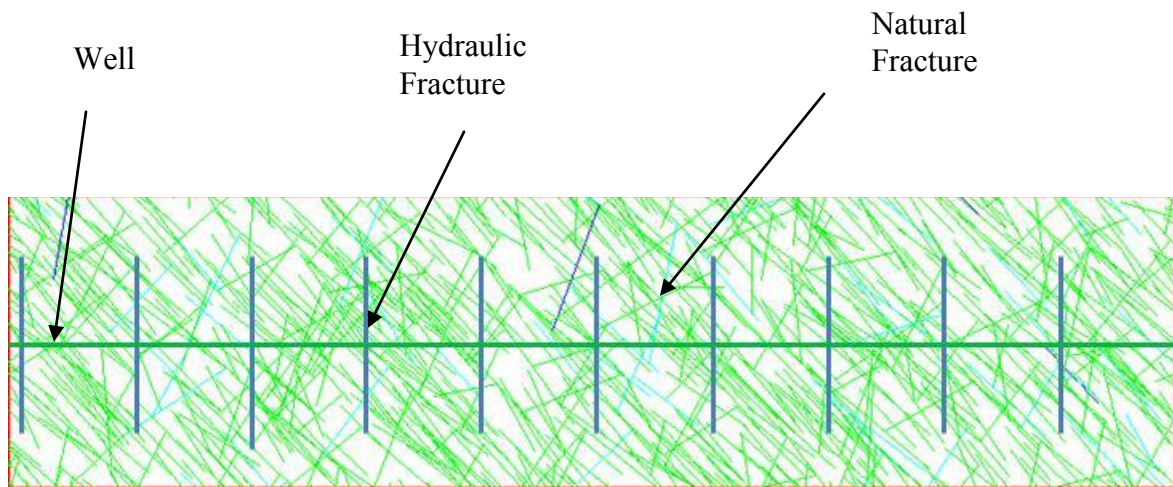


Figure 5.43: FracGen fracture map showing the well profile for case 3

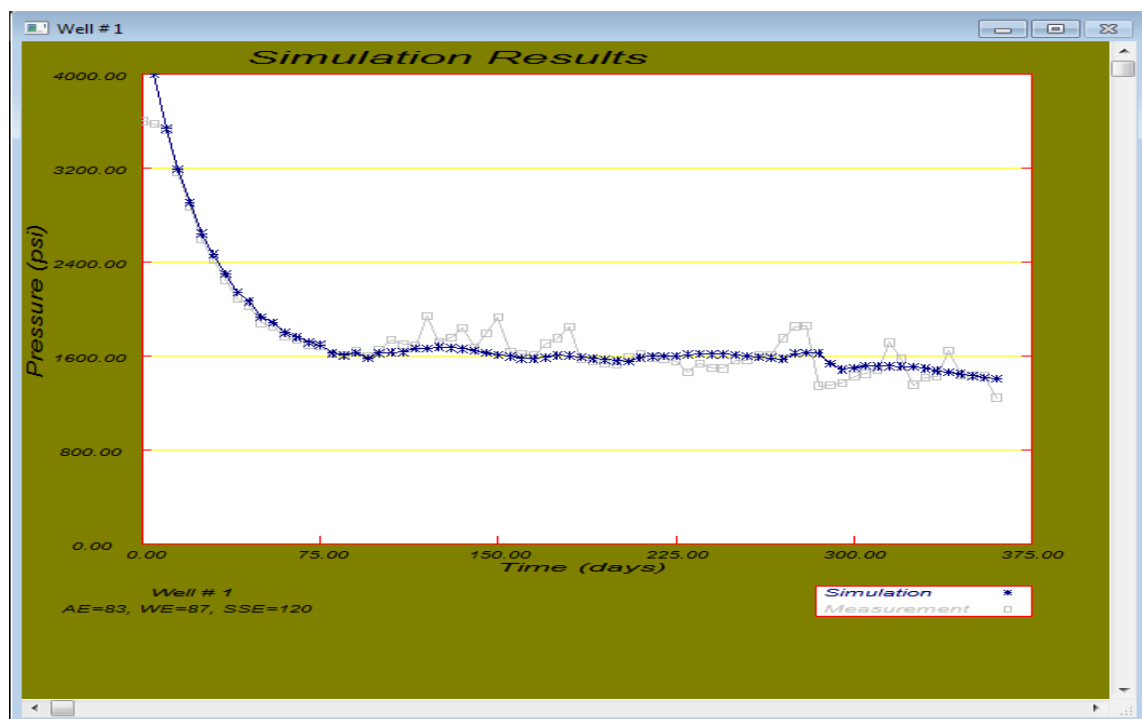


Figure 5.44: NFlow output showing the simulation result for case 3

from the input parameters that created the fracture map **Fig. 5.43**.

From the input parameters that created the fracture map **Fig. 5.43**, using the same procedure described in case 1 the simulation output is obtained, and shown in **Fig. 5.44**.

Fig. 5.44 shows the simulation result for the case run above and is taken to be the control case. From the control fracture/well properties stated in **Table 5.10**, the next step is to vary the parameters stated to obtain **Table 5.11** and then observe the changes in the reservoir response due to change in fracture/well properties, The values in **Table 5.11** are used as input parameters for FracGen.

Table 5.11: Data variation fed into FracGen for the primary fracture set for case 3

Fracture/Well Prop.	-50%	-25%	Control	+25%	+50%
Fracture Aperture (ft)	0.00001	0.00015	0.00002	0.000025	0.00003
Fracture Density (pts/ft ²)	0.00005	0.0001	0.00015	0.0002	0.00025
Fracture Length (ft)	140	210	280	350	420
Hydraulic Fracture Aperture (ft)	0.00001	0.000015	0.00002	0.000025	0.00003
Hydraulic Fracture Length(ft)	200	300	400	500	600

Some preliminary calculations were carried out shown in **Appendix 2**, this is to ensure that the 2d fracture density is either kept constant or varied when altering fracture properties by using the relationship relating 2d fracture density with the other properties.

5.5.1 Fracture Aperture

This represents the width of the fracture opening; the value in the control file is 0.00002 ft. and standard deviation of 0.00002, this value is varied and the results obtained were used to run flow simulation and **Fig. 5.45 & 5.46** shows the response observed.

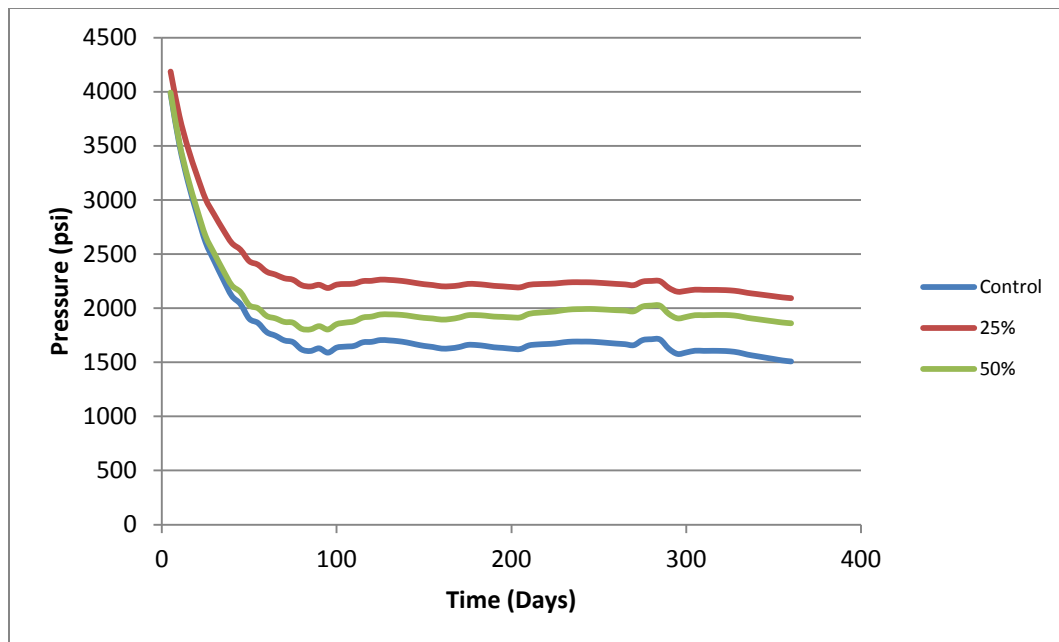


Figure 5.45: Change in pressure response due to increase in fracture aperture for case 3

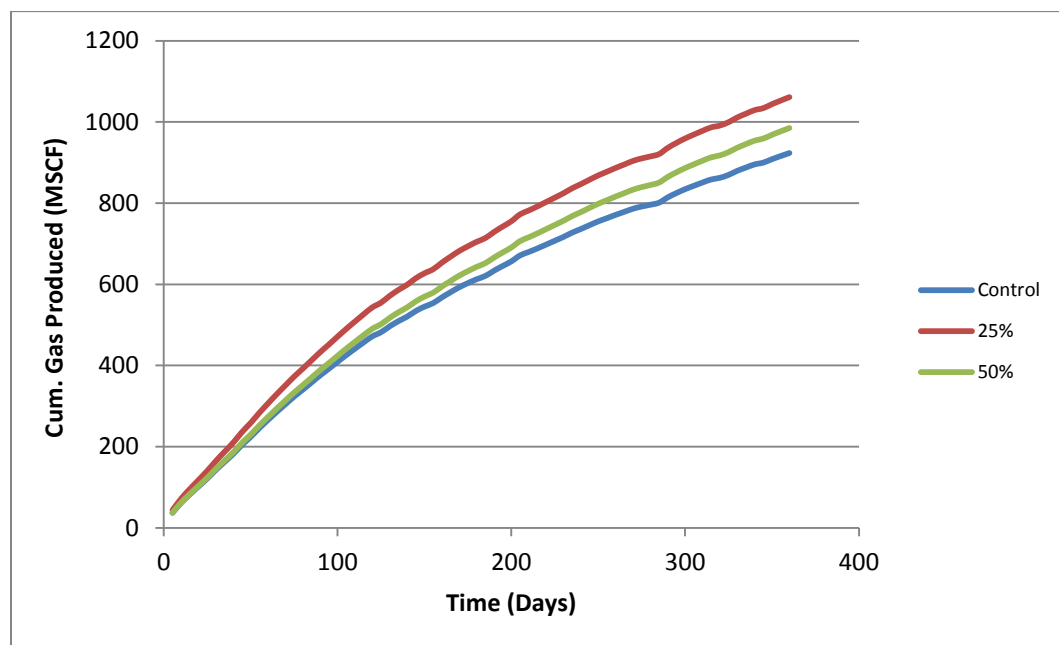


Figure 5.46: Change in cum. gas production due to increase in fracture aperture for case 3

5.5.2 Fracture Density

The fracture density represents the number of fractures per unit area/volume, the value in the control file is 0.00015 pts/ft and it is varied in steps from the control and the values obtained were used to run simulations and results are shown in **Fig. 5.47 & 5.48**.

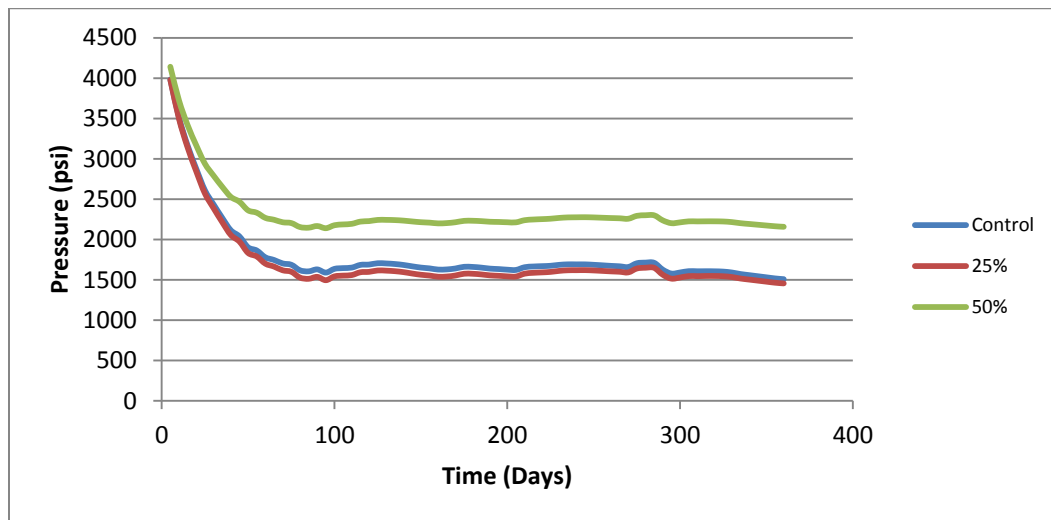


Figure 5.47: Change in pressure response due to increase in fracture density for case 3

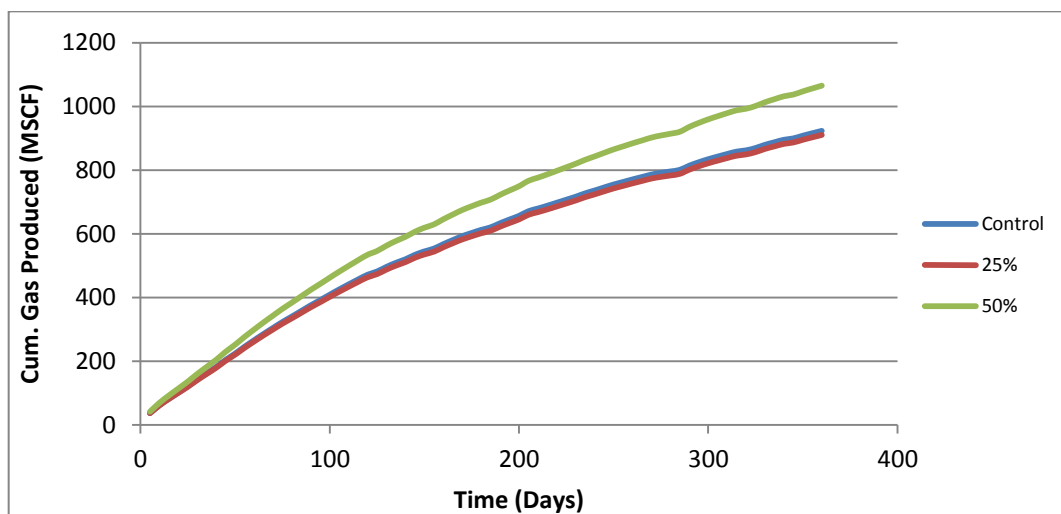


Figure 5.48: Change in cum. gas production due to increase in fracture density for case 3

5.5.3 Fracture Length

This represents the mean length of the fracture with a fracture set, the value in the control file is 280 ft, and the simulations results obtained are shown in **Fig. 5.49 & 5.50**.

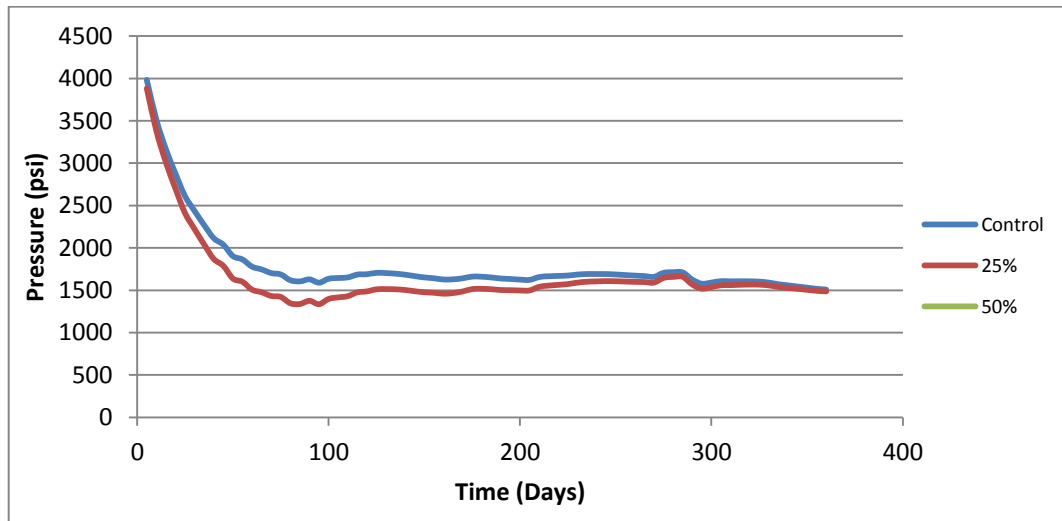


Figure 5.49: Change in pressure response due to increase in fracture length for case 3

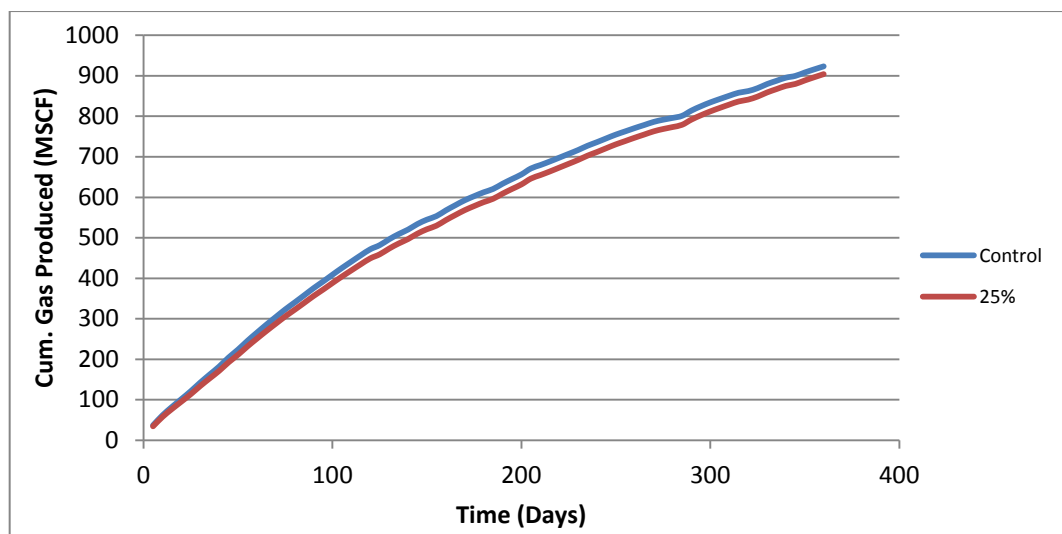


Figure 5.50: Change in cum. gas production due to increase in fracture length for case 3

5.5.4 Number of Hydraulic Fracture Stages

This represents the number of fracture stages; the number of stages is 10 in the control file. The simulation results are shown in **Fig. 5.51 & 5.52**.

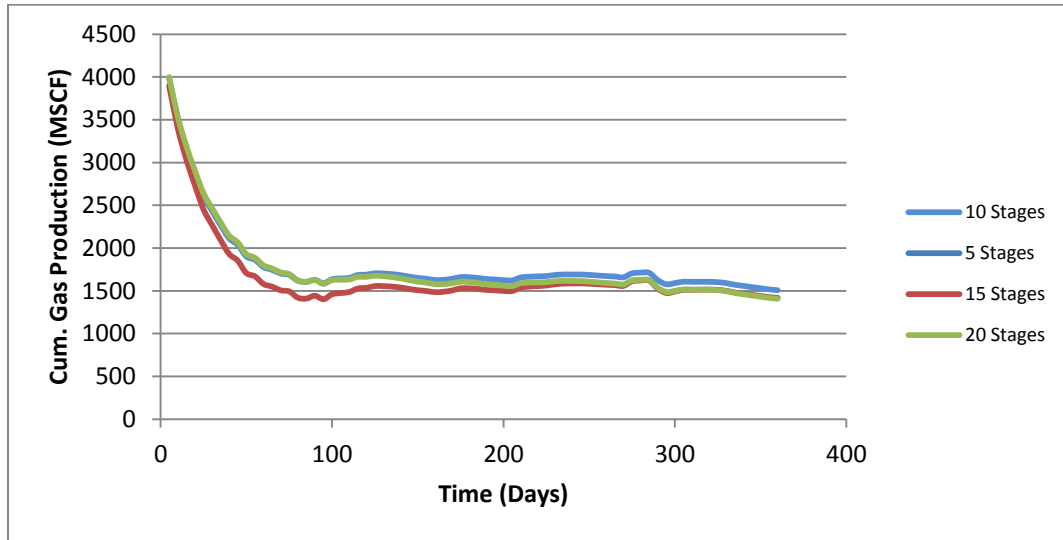


Figure 5.51: Change in pressure for different hydraulic fracture stages for case 3

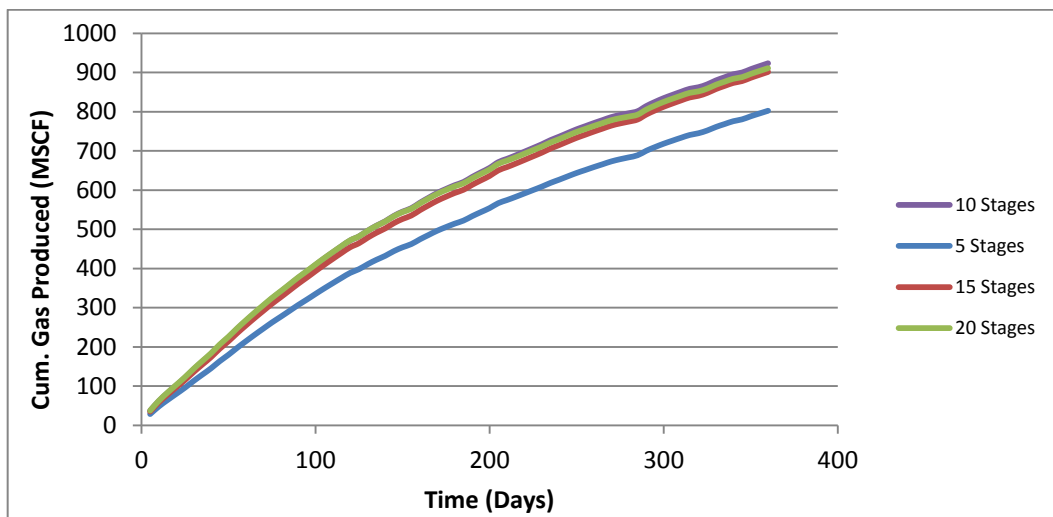


Figure 5.52: Change in cum. gas production for change in hydraulic fracture stages for case 3

5.5.5 Hydraulic Fracture Aperture

This represents the aperture of the hydraulic fractures, the value in the control file is 0.00002 ft and simulations results obtained are shown in **Fig. 5.53 – 5.56**.

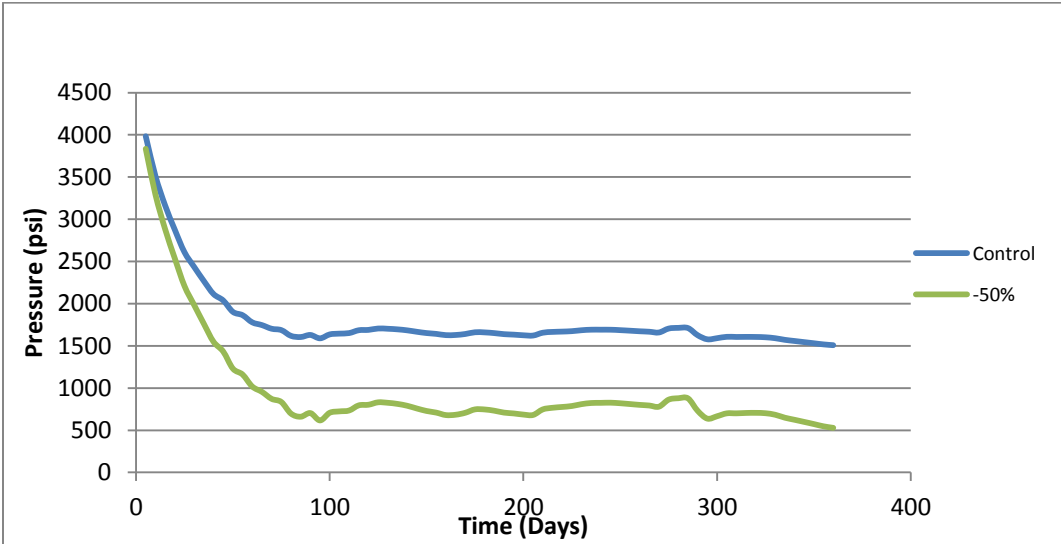


Figure 5.53: Change in pressure due to decrease in hydraulic fracture aperture for case 3

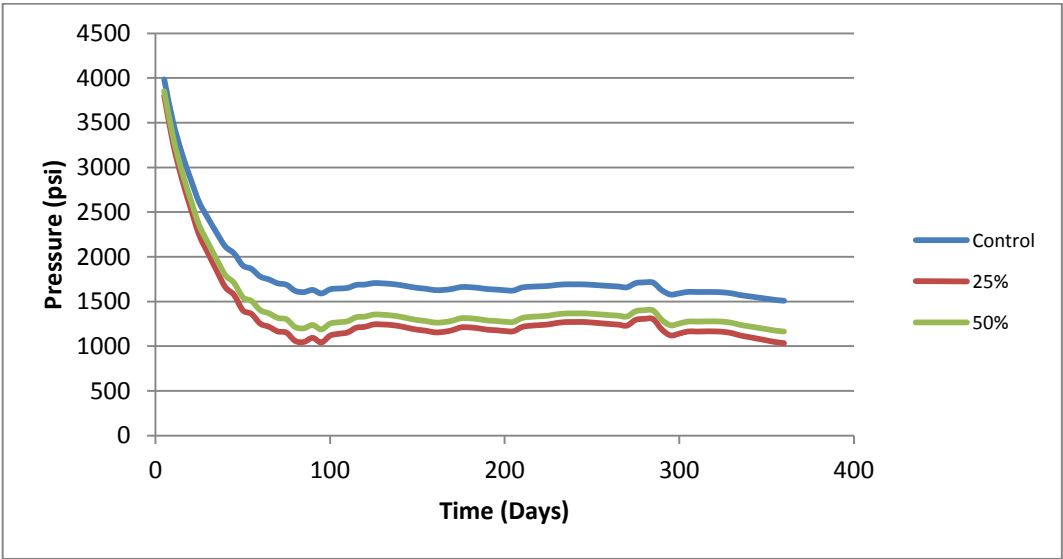


Figure 5.54: Change in pressure due to increase in hydraulic fracture aperture for case 3

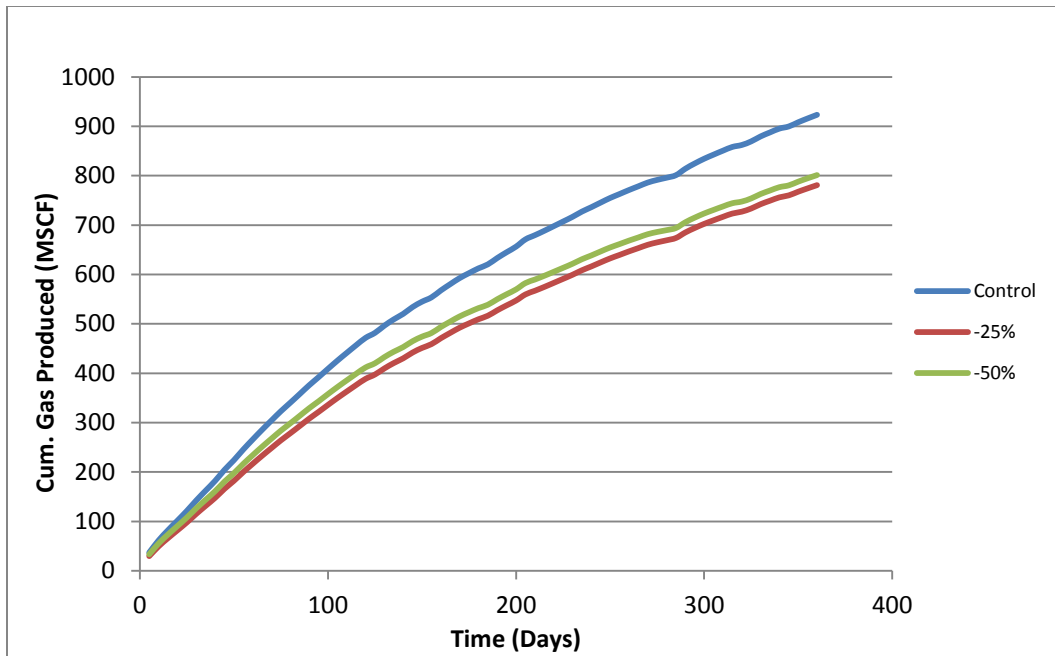


Figure 5.55: Change in cum. gas produced due to decrease in hydraulic fracture aperture for case 3

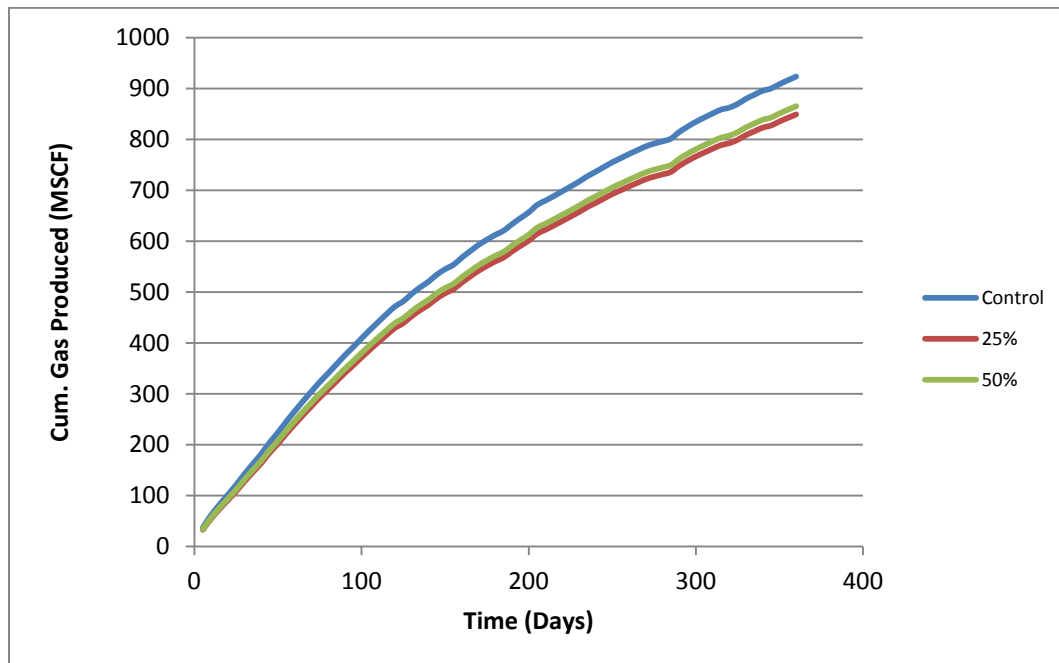


Figure 5.56: Change in cum. gas produced due to increase in hydraulic fracture aperture for case 3

5.5.6 Hydraulic Fracture Length

This represents the aperture of the hydraulic fractures, the value in the control file is 400 ft and simulations results obtained are shown in **Fig. 5.57 & 5.58**.

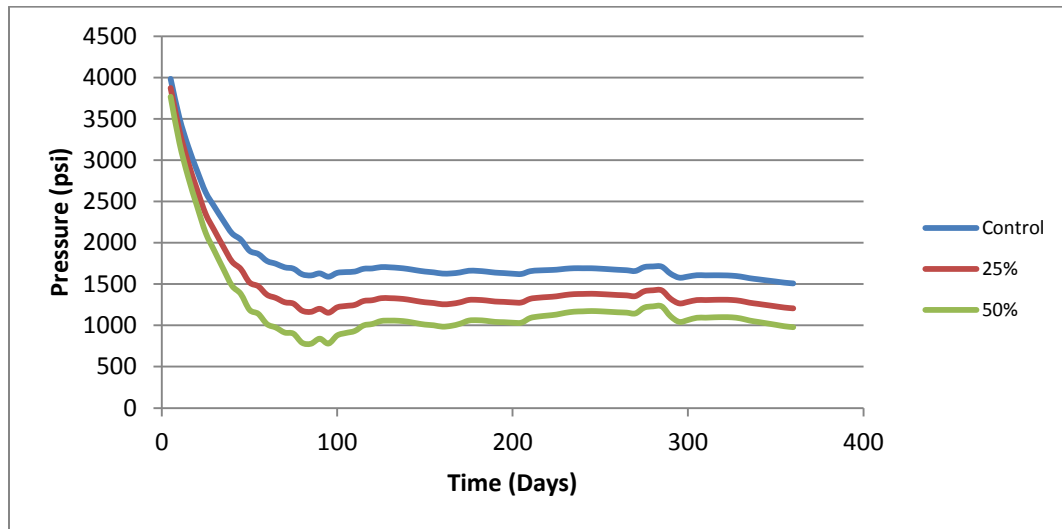


Figure 5.57: Change in pressure due to increase in hydraulic fracture length for case 3

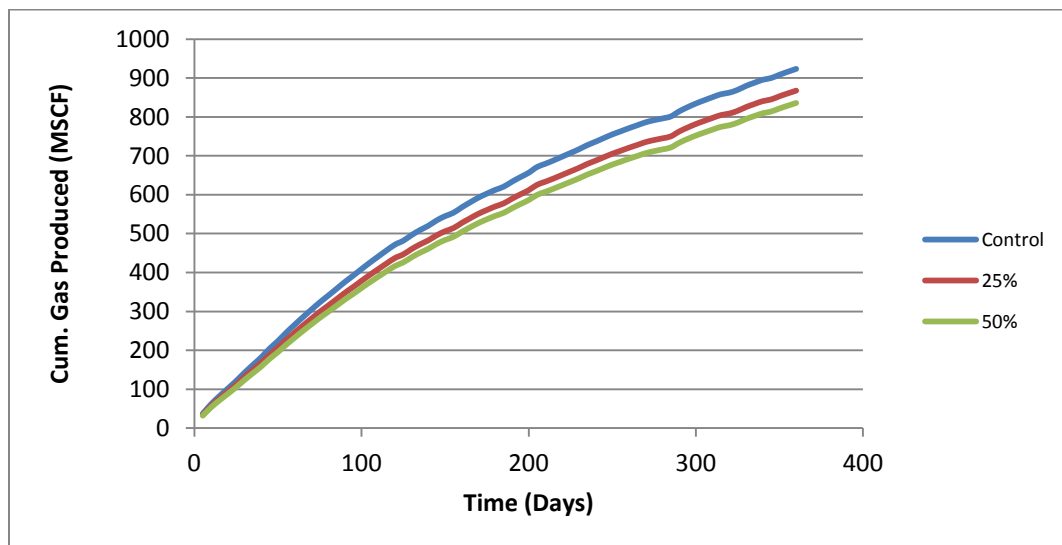


Figure 5.58: Change in cum. gas produced due to increase in hydraulic fracture length for case 3

5.6 Case 4: Two Fracture Sets with One Clustered and the Other Uniformly Distributed

We will consider the reservoir having 2 fracture sets where one is clustered and the other is uniformly distributed, the clustered fracture network is the primary fracture set while the uniformly distributed network is the secondary fracture set, the properties of the primary fracture set will be varied while that of the secondary is kept constant.

Table 5.12 shows the reservoir parameters for the Eagle Ford shale gas. To obtain some parameters in **Table 5.13** preliminary calculations were carried out shown in **Appendix 2**, this is to ensure that the 2d- fracture density is either kept constant or varied when altering fracture properties by using the relationship relating 2d-fracture density with the other properties.

Table 5.12: Reservoir parameters for an Eagle Ford shale gas well for case 4

Reservoir and Fracture Properties for Well A	
Parameter	Value
Wellbore Radius (ft)	0.33
Wellbore Lateral Length (ft)	3710
Number of Fracture Stages	10
Depth (ft)	10875
Pay Zones Thickness (ft)	283
Reservoir Pressure	7000
Specific Gravity	0.621
Temperature (F)	285
BHFP (psi)	3600
Drainage Area (Acres)	80
Reservoir Size (ft)	(933.38 , 3733.52)
Reservoir Permeability (nd)	60
Reservoir Porosity (%)	5.5

Table 5.13: Control data fed into FracGen for case 4

Fracture Property	Primary	Secondary	Source
Fracture Aperture (ft)	0.0002	0.0002	Assumed
Mean Fracture Length (ft)	280	280	Assumed
Fracture Orientation (deg.) (Mean, St. dev.)	N 45° E, 8.0	N 120° E	Assumed
2D- Fracture density (ft/ft ²)	0.042	0.014	From Case 1
Hydraulic Fracture Aperture (ft)	2.E-04		Assumed
Hydraulic Fracture Length (ft)	400		Well Data
Hydraulic Fracture Orientation	E-S		Assumed
Number of Hydraulic Fracture Stages	10		Well Data
Cluster Orientation (deg.) (Mean, St. dev.)	N 40° E, 10.0	-	Assumed
Mean cluster Length (ft)	1500	-	Assumed
Mean Intra-cluster Fracture spacing (ft)	40	-	Assumed
Mean Intra-cluster Fracture density (ft)	0.00006	-	Assumed
Density of cluster center-point (pts/ft ²)	0.000004307		Assumed

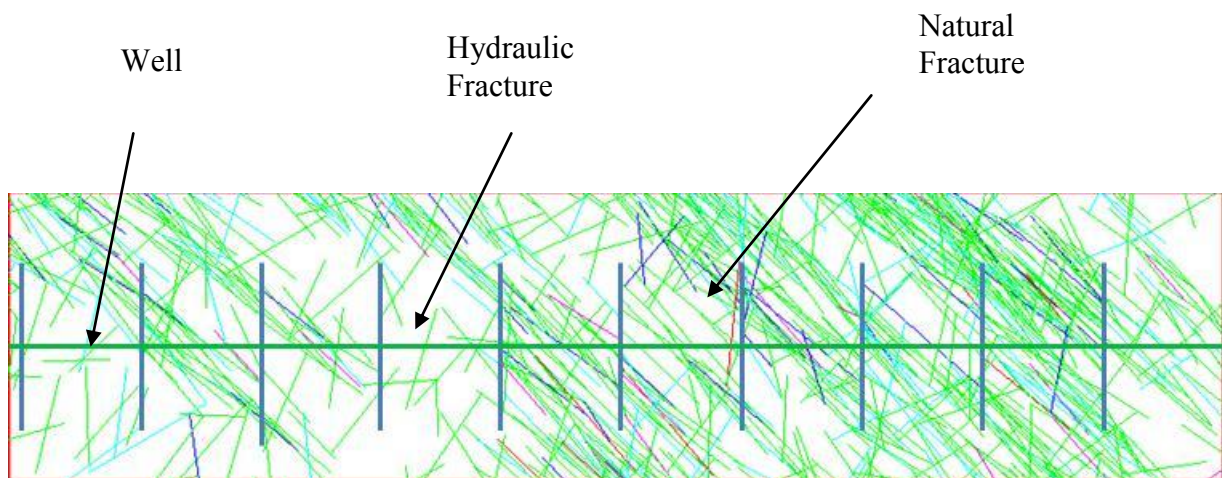


Figure 5.59: FracGen fracture map showing the well profile for case 4

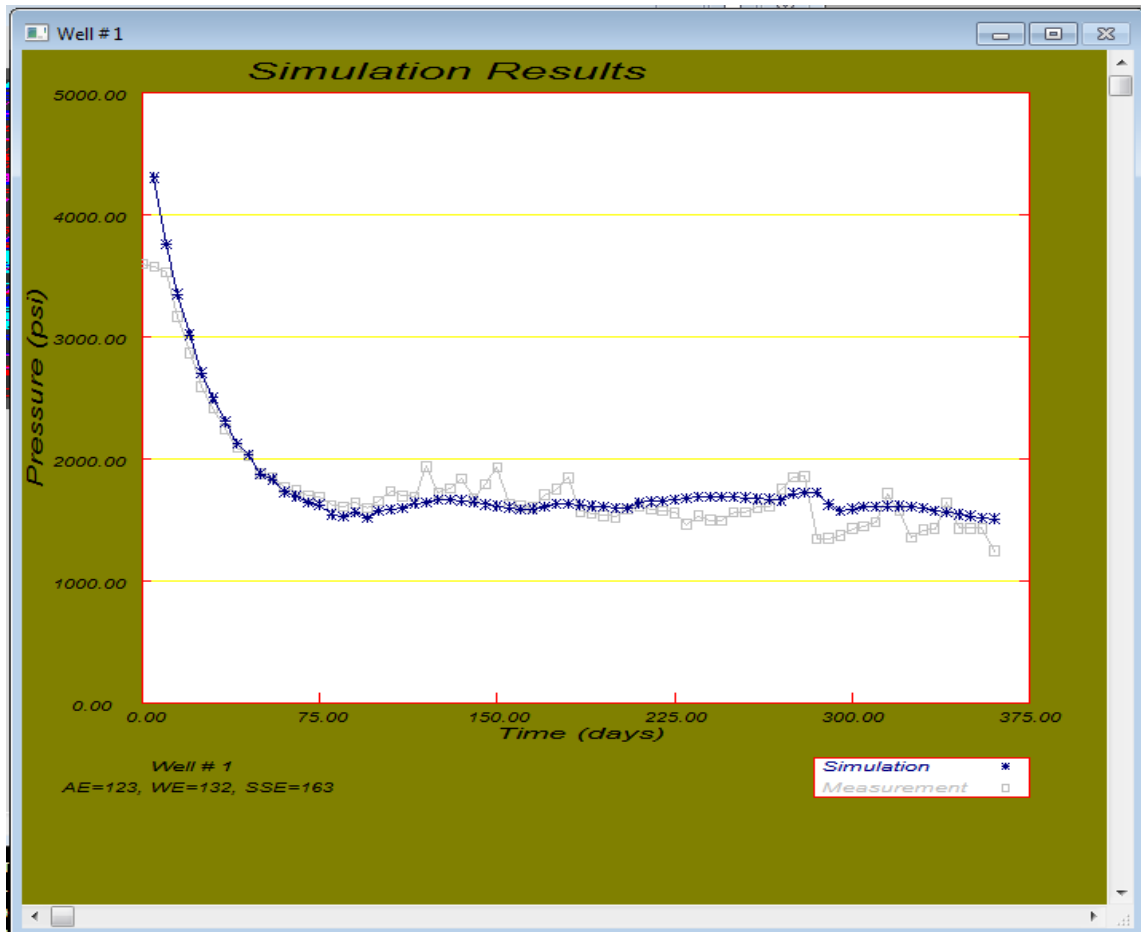


Figure 5.60: NFlow output showing the simulation result for case 4

Using the same procedure described in case 1, the fracture map **Fig. 5.59** and the simulation output is obtained shown in **Fig. 5.60**, from the input parameters that was used to create the fracture map.

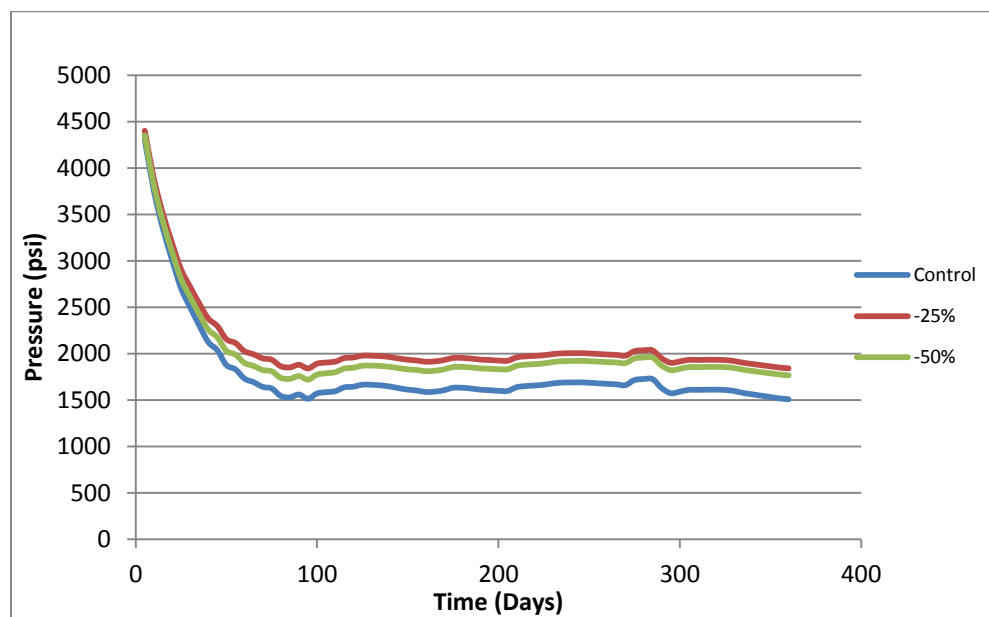
Fig. 5.60 shows the simulation result for the case run above and is taken to be as the control case. The next step is to vary the fracture/well properties **Table 5.13** and observe the changes in the reservoir response. The values in **Table 5.14** are input parameters for FracGen.

Table 5.14: Data fed into FracGen for the different fracture properties for case 4

Fracture/Well Prop.	-50%	-25%	Control	25%	50%	100%
Fracture Aperture (ft)	0.000010	0.000015	0.000020	0.000025	0.000030	-
Fracture Density (ft/ft ²)	0.021	0.032	0.042	0.053	0.063	0.084
Fracture Length (ft)	140	210	280	350	420	560
Hydraulic Fracture Aperture (ft)	0.00001	0.000015	0.00002	0.000025	0.00003	0.00004
Hydraulic Fracture Length(ft)	200	300	400	500	600	800
Density of cluster center point (pts/ft ²)	7.727E-06	5.431E-06	4.307E-06	3.655E-06	3.243E-06	2.795E-06

5.6.1 Fracture Aperture

This represents the width of the fracture opening; the value in the control file is 0.00002 ft, this value is varied in steps and the results obtained were used to run flow simulation and the response observed is shown in **Fig. 5.61 - 5.64**.

**Figure 5.61: Change in pressure response due to decrease in fracture aperture for case 4**

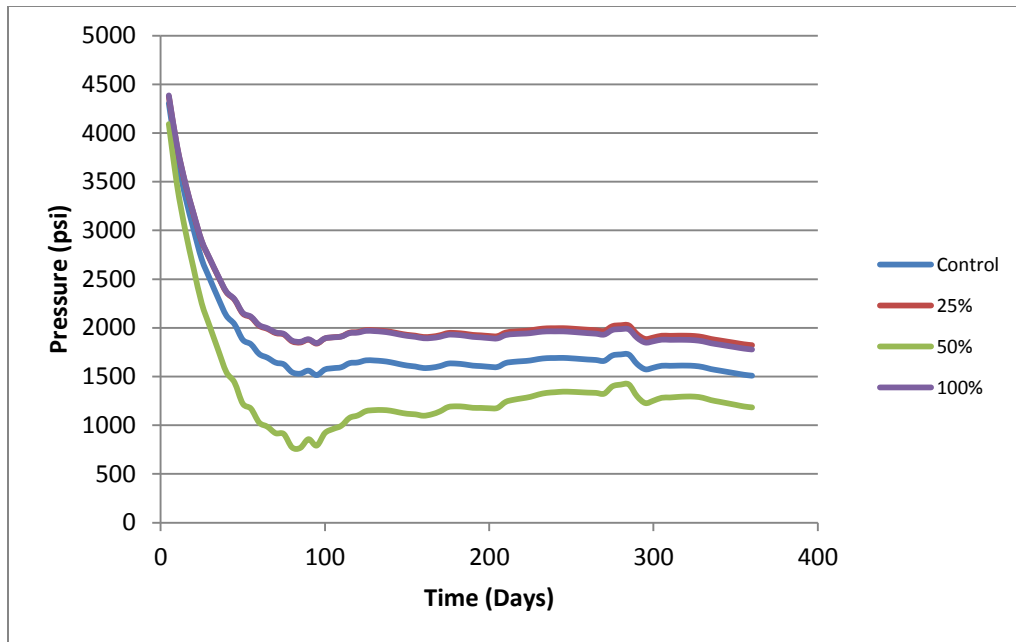


Figure 5.62: Change in pressure response due to increase in fracture aperture for case 4

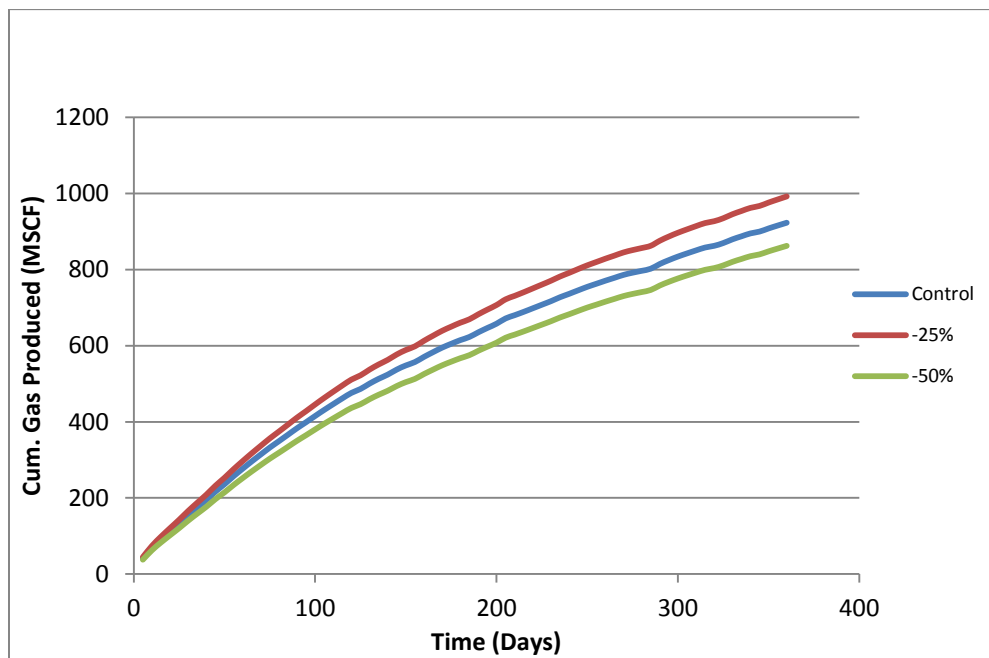


Figure 5.63: Change in cum. gas production due to decrease in fracture aperture for case 4

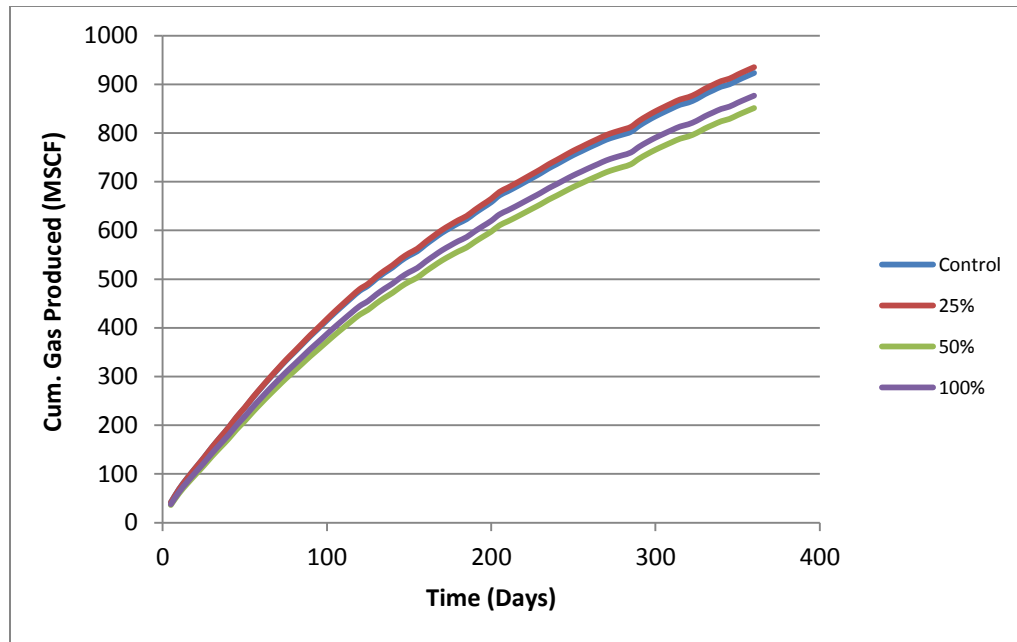


Figure 5.64: Change in cum. gas production due to increase in fracture aperture for case 4

5.6.2 Fracture Density

This represents the number of fractures per unit area/ volume, the value in the control file is 0.000004307 pts/ft. This value varied in steps from the control and the values obtained were used to run simulations and results are shown in **Fig. 5.65 - 5.68**.

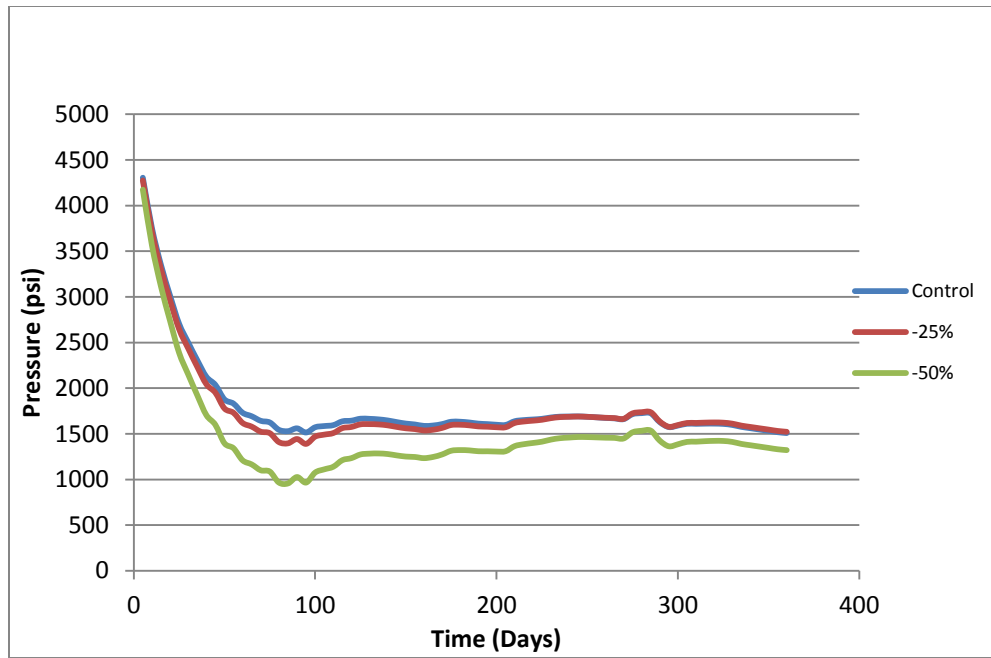


Figure 5.65: Change in pressure response due to decrease in fracture density for case 4

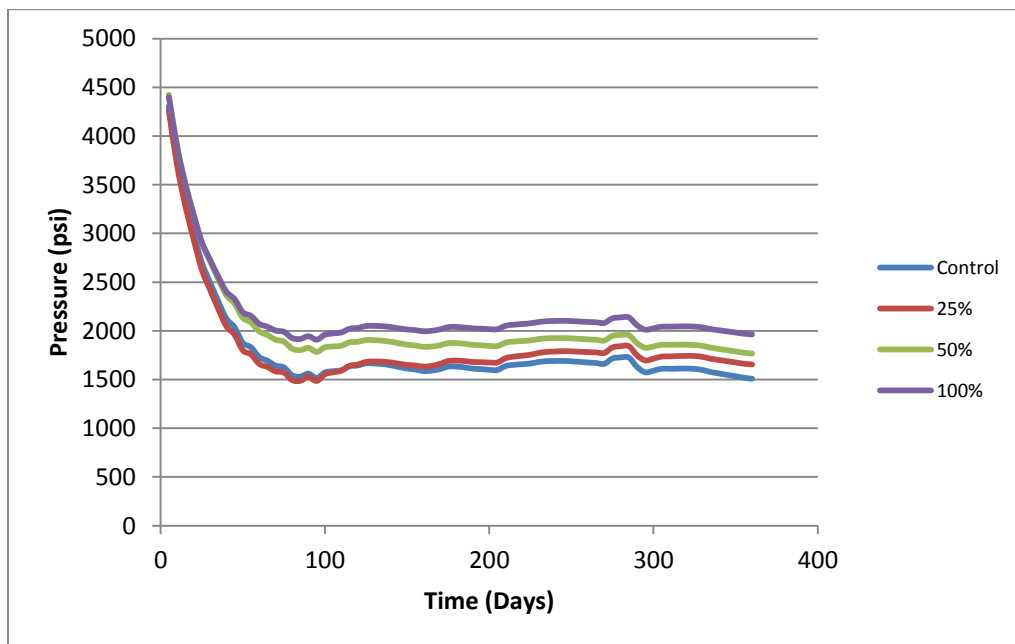


Figure 5.66: Change in pressure response due to increase in fracture density for case 4

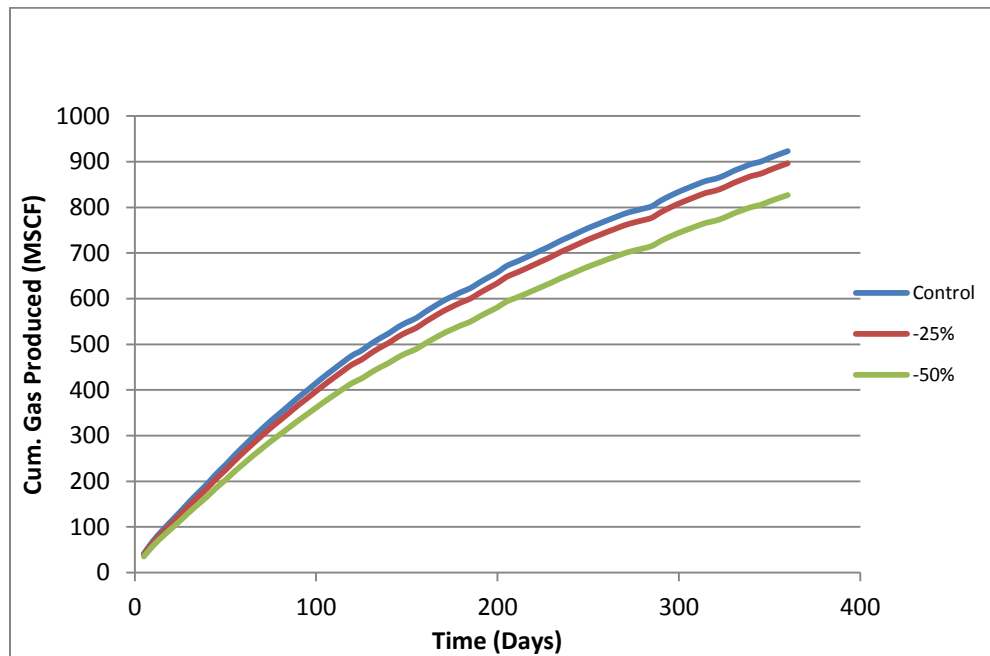


Figure 5.67: Change in cum. gas production due to decrease in fracture density for case 4

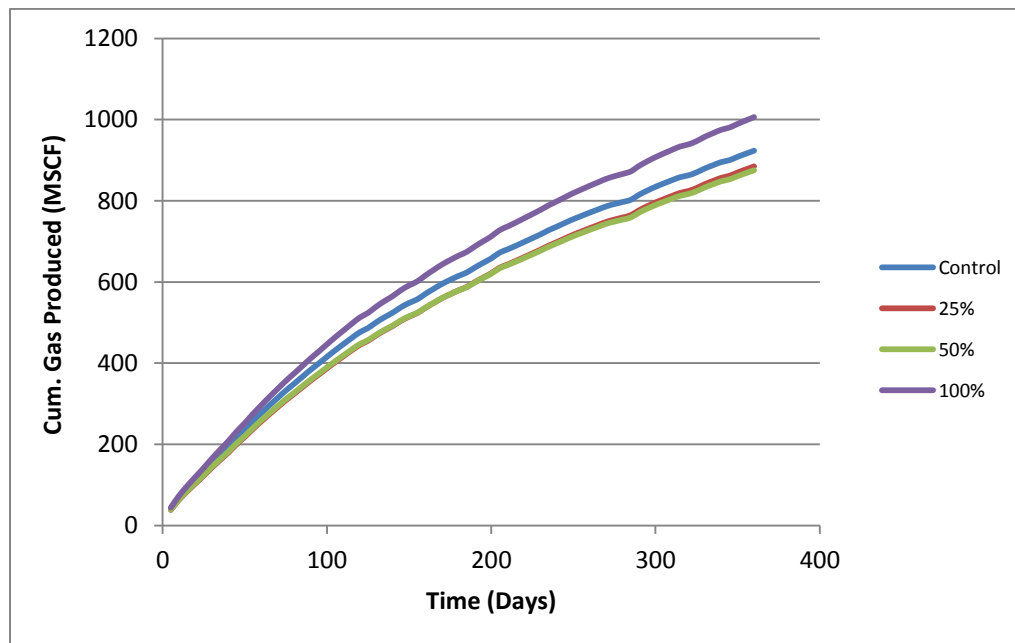


Figure 5.68: Change in cum. gas production due to increase in fracture density for case 4

5.6.3 Fracture Length

This represents the mean length of the fracture with a fracture set. The mean fracture length is 280 ft. The simulation results obtained are shown in **Fig. 5.69 - 5.72**.

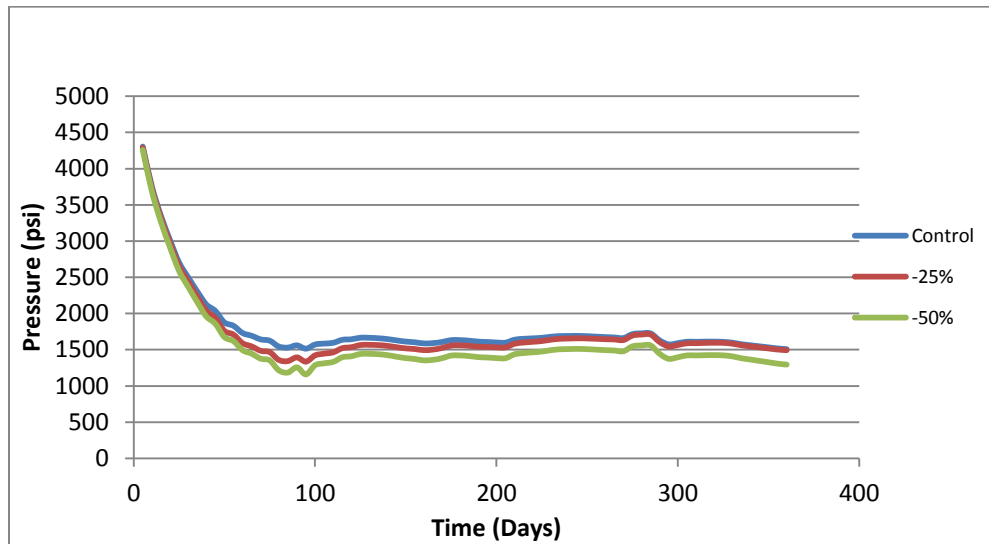


Figure 5.69: Change in pressure response due to decrease in fracture length for case 4

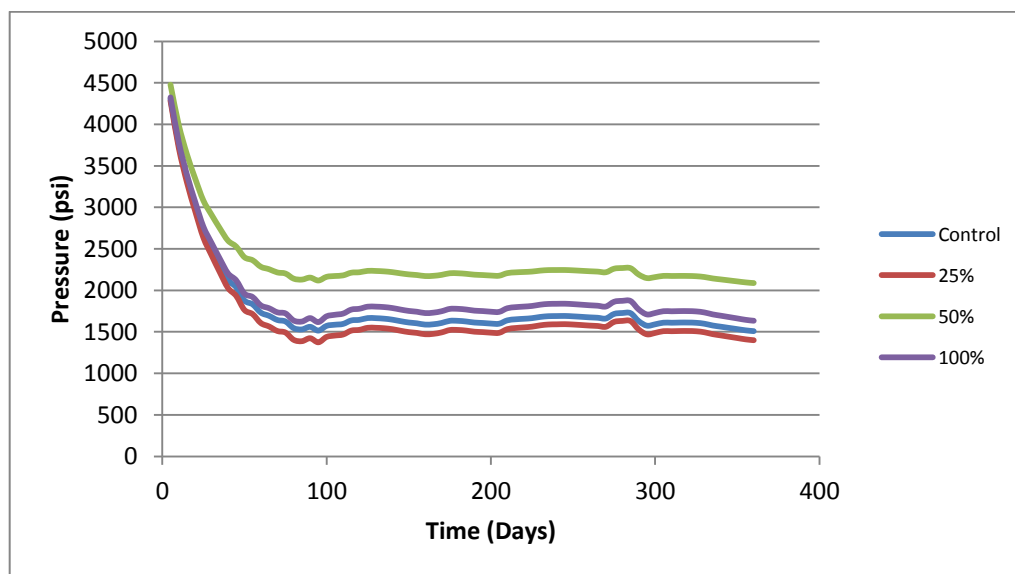


Figure 5.70: Change in pressure response due to increase in fracture length for case 4

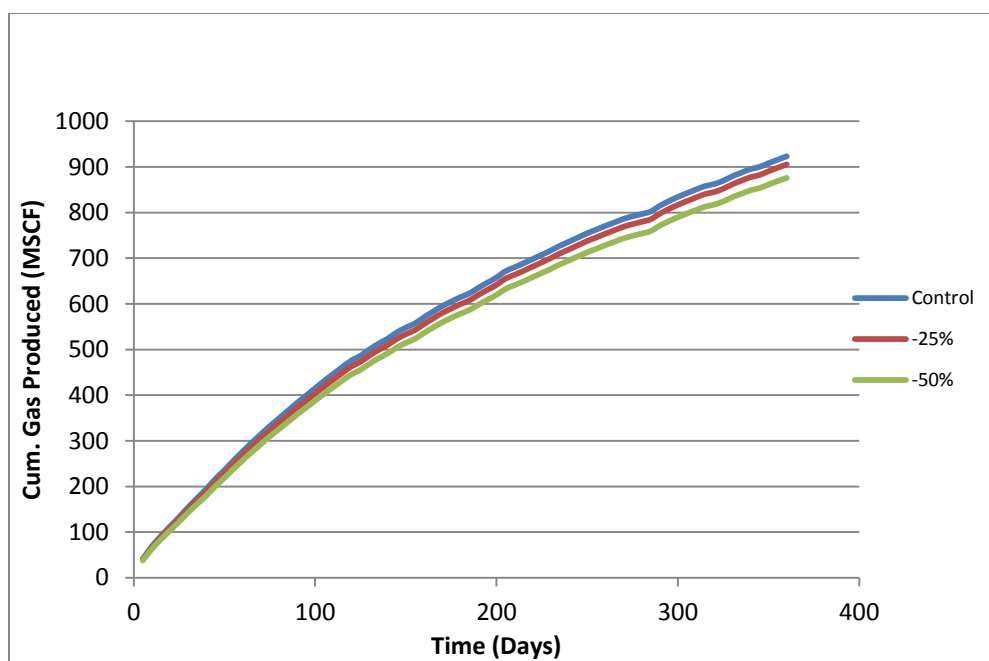


Figure 5.71: Change in cum. gas production due to decrease in fracture length for case 4

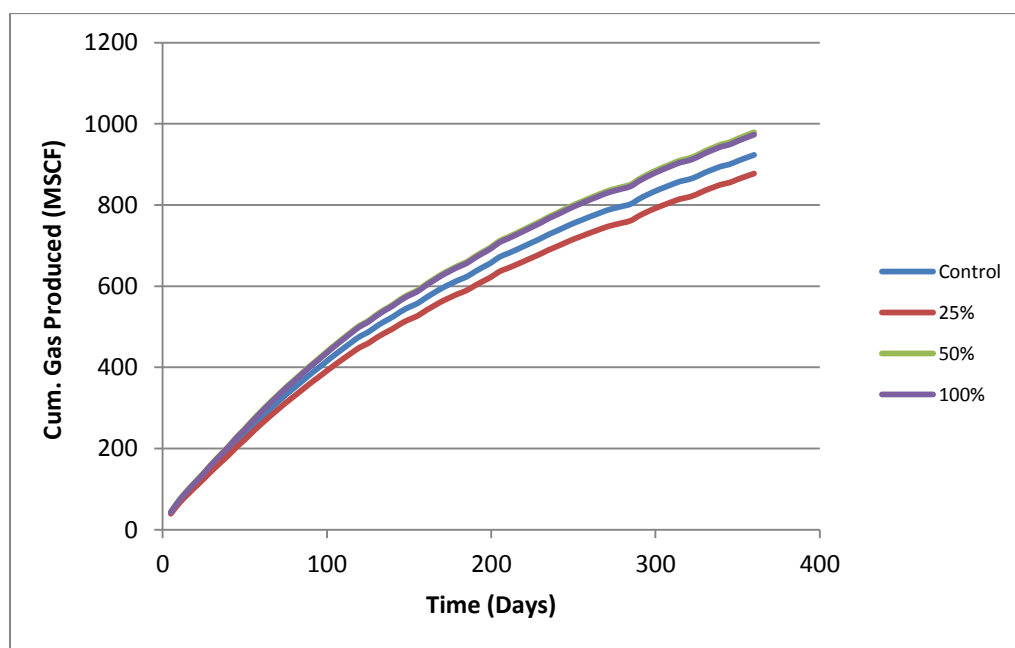


Figure 5.72: Change in cum. gas production due to increase in fracture length for case 4

5.6.4 Number of Hydraulic Fracture Stages

This represents the number of fracture stages; the number of stages is 10 in the control file. The simulation and results are shown in **Fig. 5.73 & 5.74**.

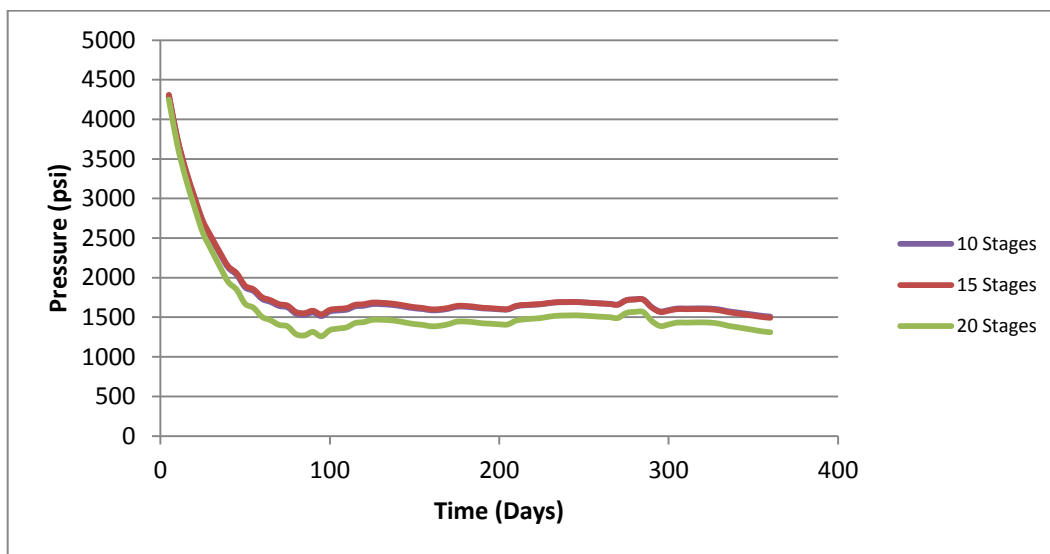


Figure 5.73: Change in pressure due to increase in hydraulic fracture stages for case 4

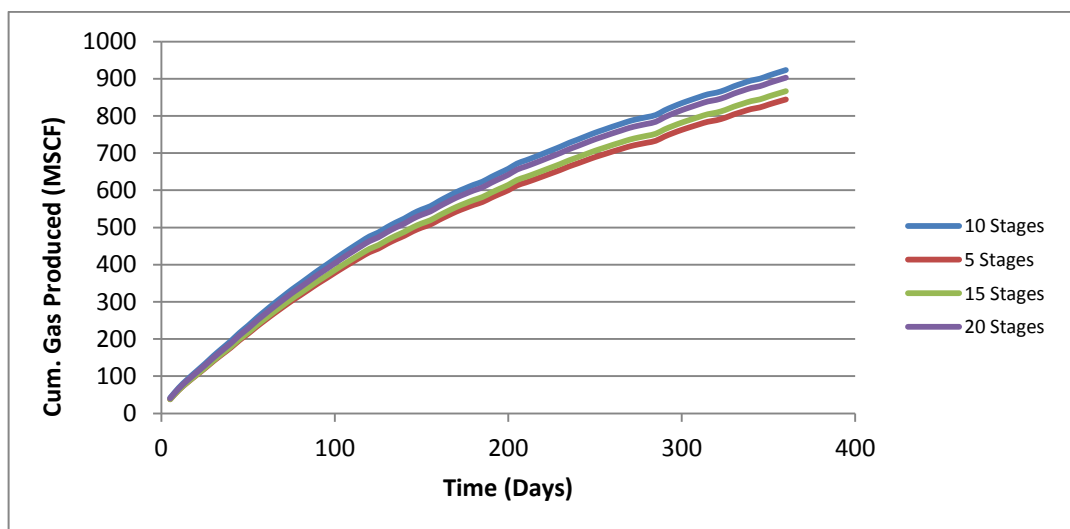


Figure 5.74: Change in cum. gas production due to change in hydraulic fracture stages for case 4

5.6.5 Hydraulic Fracture Aperture

This represents the aperture of the hydraulic fractures, the value in the control file is 0.00002 ft and simulations results obtained are shown in **Fig. 5.75 – 5.78**.

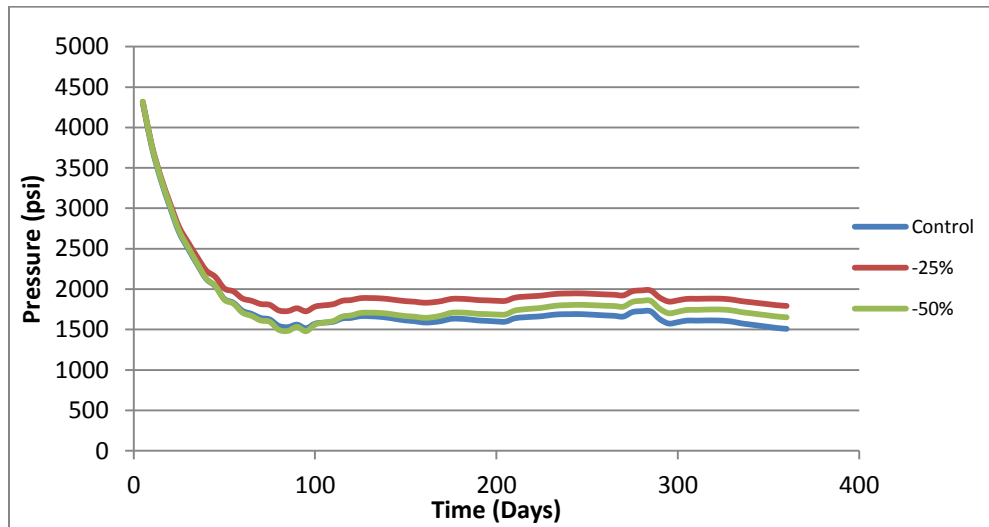


Figure 5.75: Change in pressure due to decrease in hydraulic fracture aperture for case 4

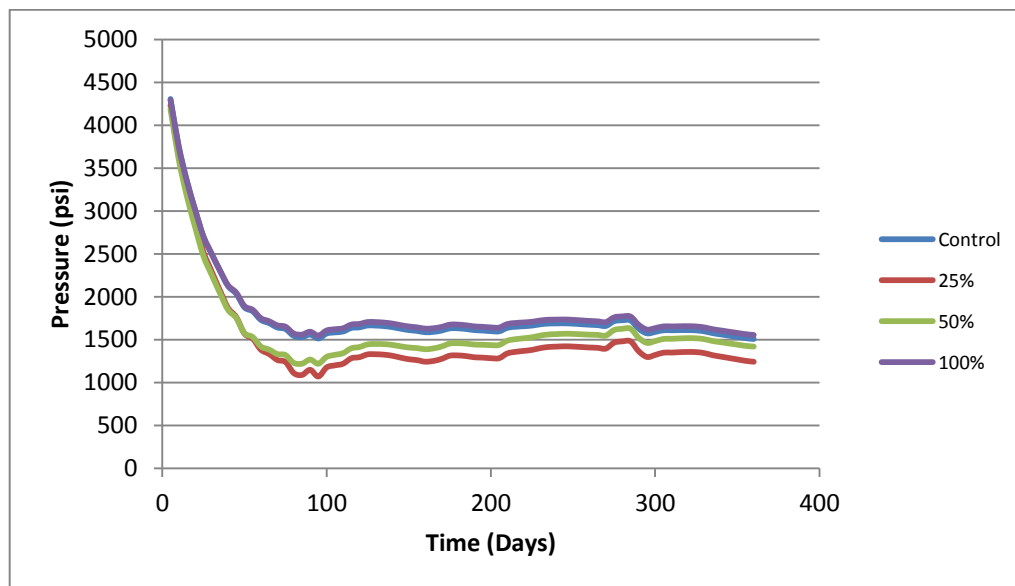


Figure 5.76: Change in pressure due to increase in hydraulic fracture aperture for case 4

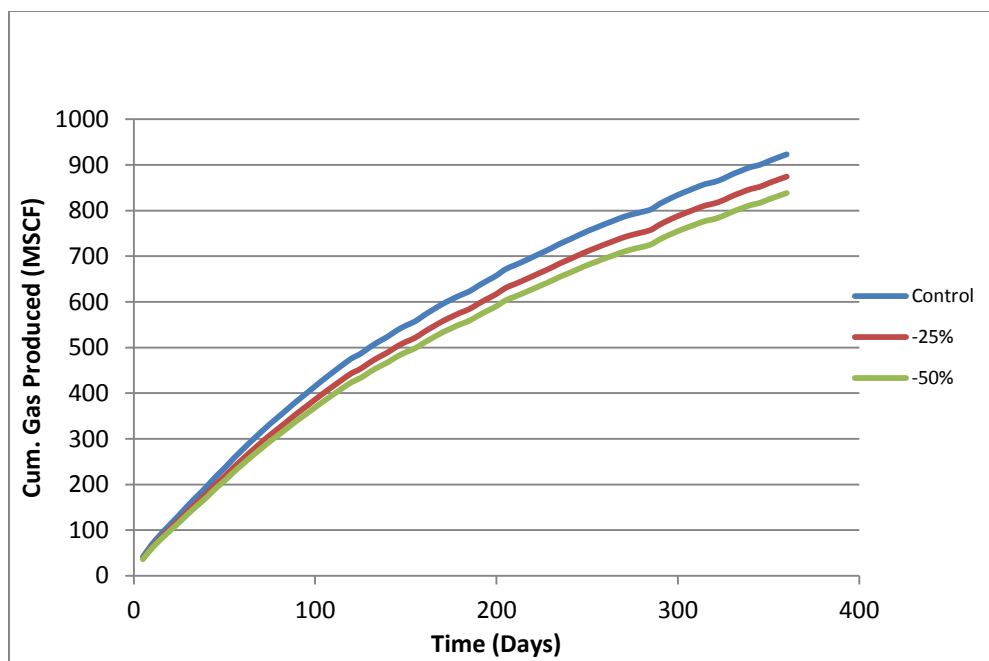


Figure 5.77: Change in cum. gas produced due to decrease in hydraulic fracture aperture for case 4

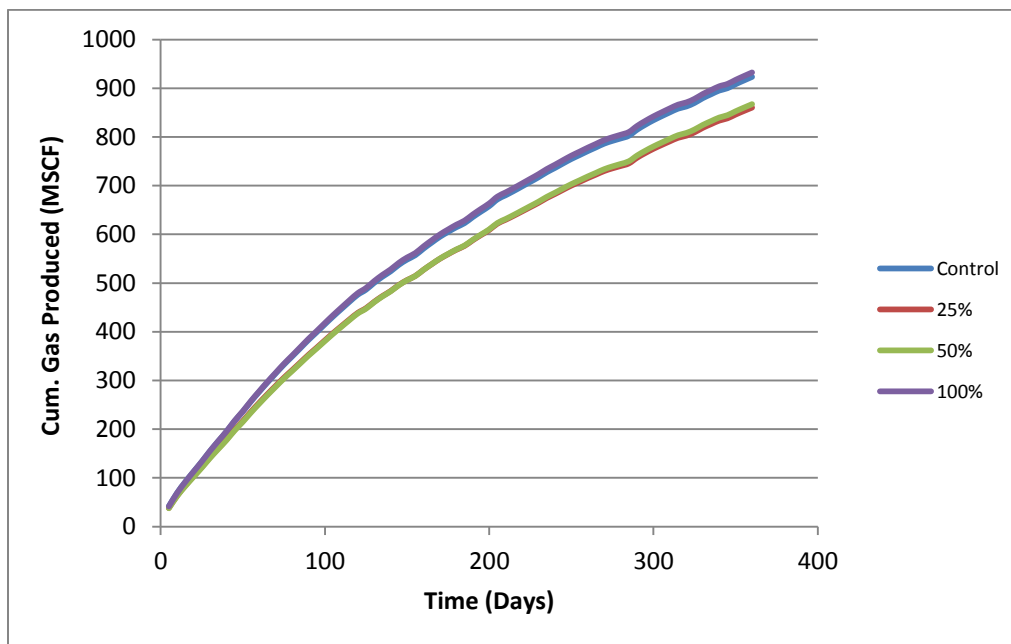


Figure 5.78: Change in cum. gas produced due to increase in hydraulic fracture aperture for case 4

5.6.6 Hydraulic Fracture Length

This represents the aperture of the hydraulic fractures, the value in the control file is 400 ft and simulation results obtained are shown in **Fig. 5.79 – 5.82**.

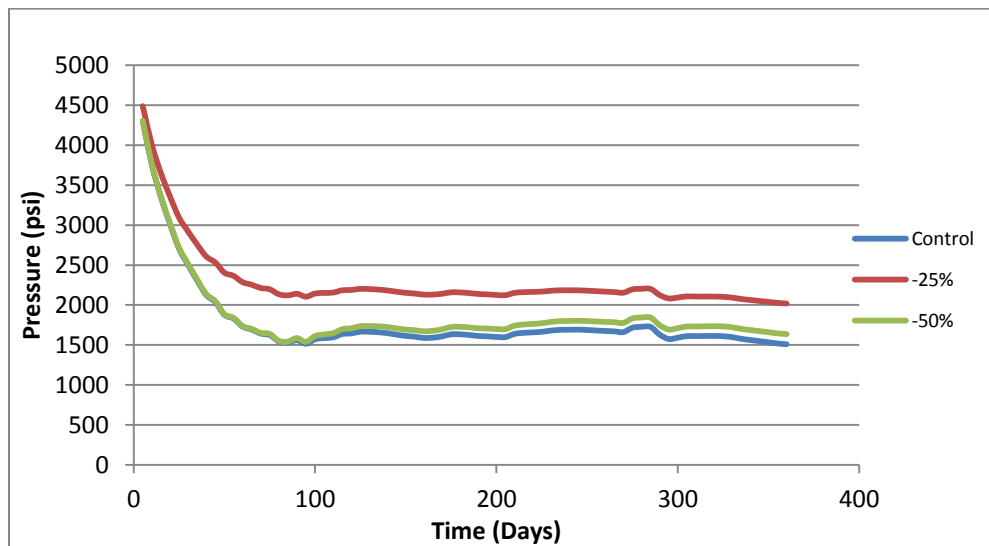


Figure 5.79: Change in pressure due to decrease in hydraulic fracture length for case 4

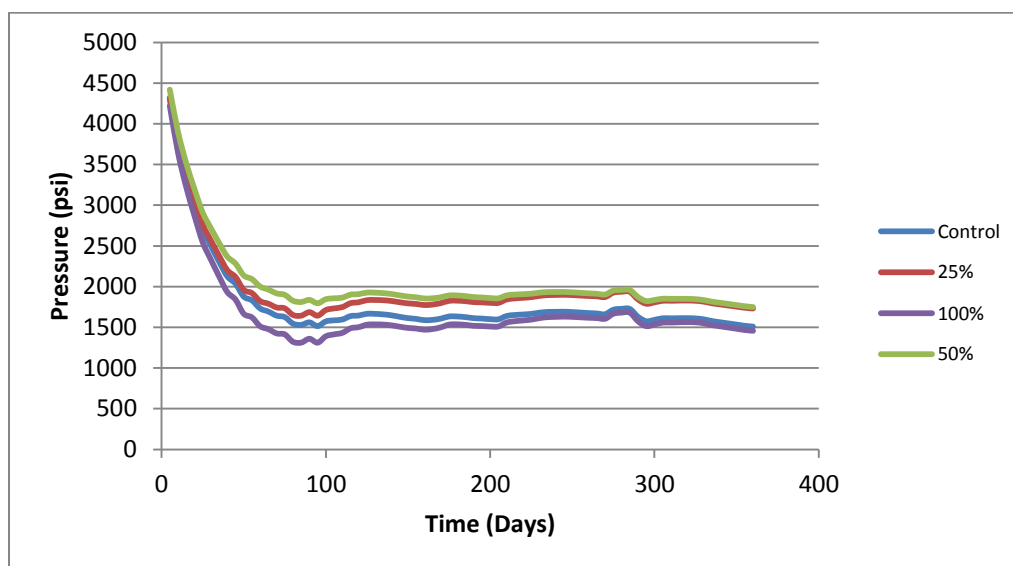


Figure 5.80: Change in pressure due to increase in hydraulic fracture length for case 4

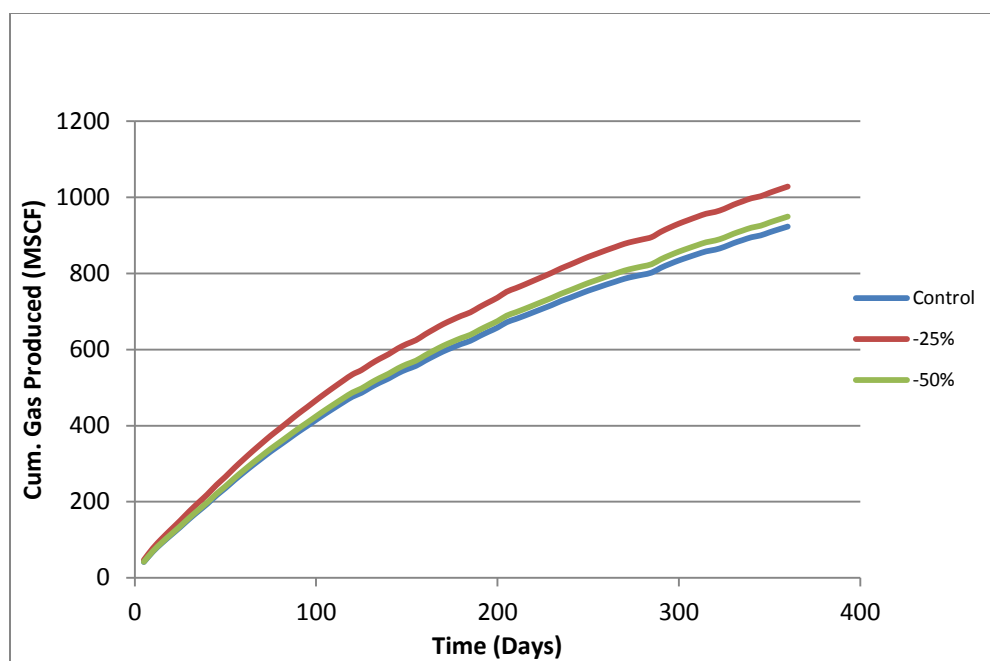


Figure 5.81: Change in cum. gas produced due to decrease in hydraulic fracture length for case 4

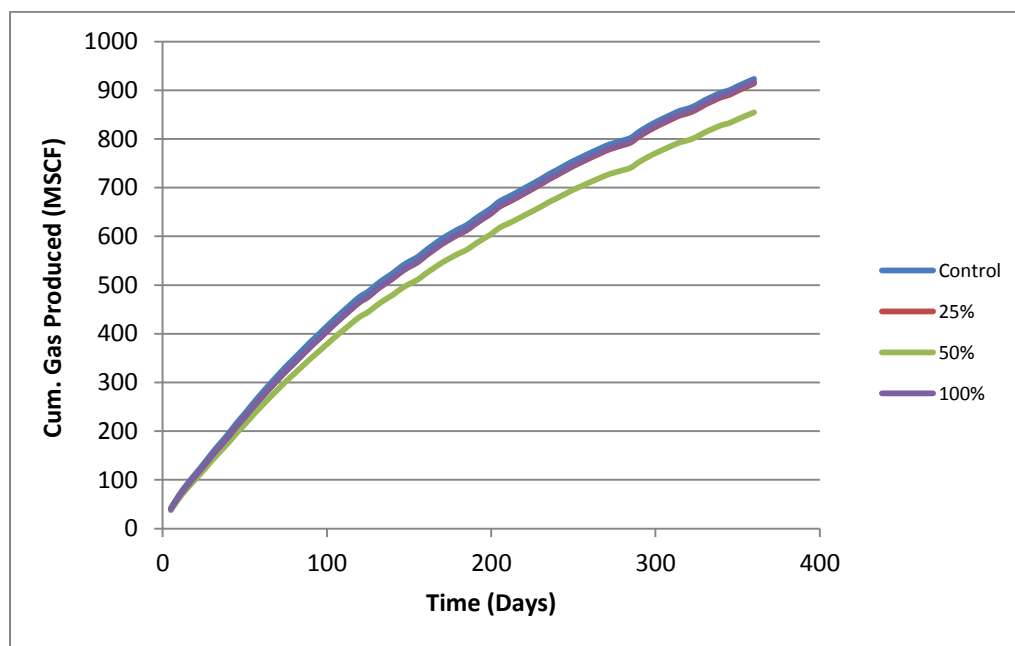


Figure 5.82: Change in cum. gas produced due to increase in hydraulic fracture length for case 4

5.7 Fracture/Well Properties Comparison Plots

5.7.1 Fracture Networks

For the fracture distribution comparison, **Fig. 5.83** shows that case 1 which represents the uniformly distributed fracture network has the highest cumulative gas production while case 3 which represents the uniformly distributed network of 2 fracture sets is next and the clustered fracture network with a passive uniform network is next also though very close to the single clustered network.

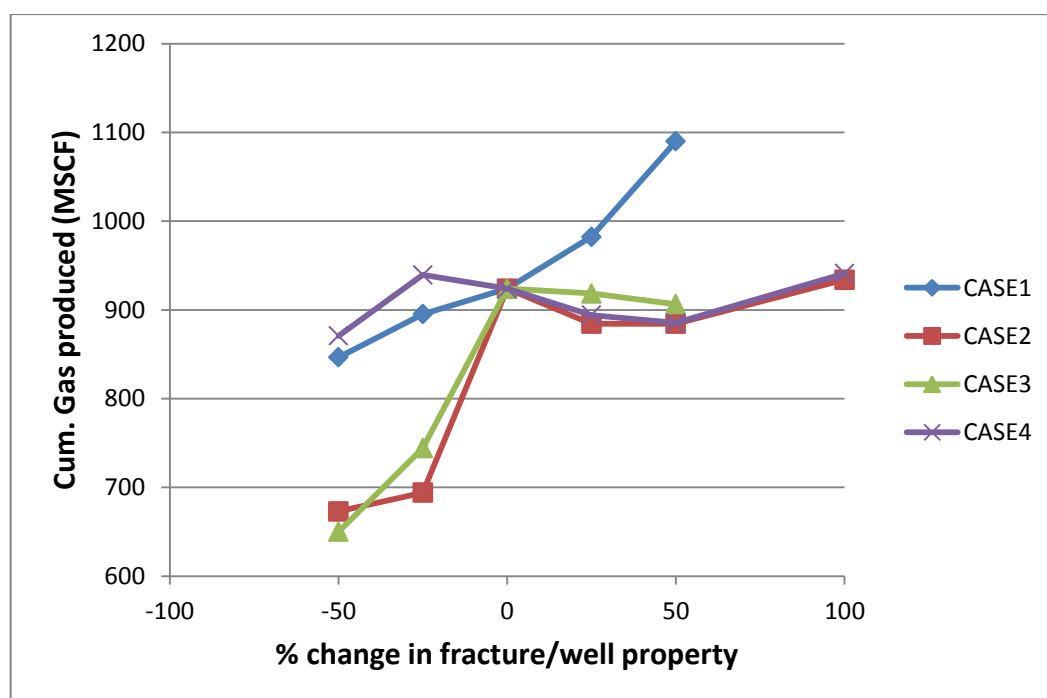


Figure 5.83: Change in cum. gas production for different fracture networks

5.7.2 Fracture/Well Property

For the Fracture/well properties comparison, **Fig. 5.84** shows the comparison plot for the different fracture and well properties studied, from the graph we can see that the fracture property that produced the highest change in cumulative gas production due to change in the fracture property is the fracture aperture, a similar trend is also seen when comparing the well properties, the hydraulic fracture aperture shows a slightly higher value to the hydraulic fracture length. Also the plot shows that the fracture/well properties usually reach a maximum value such that further increase will not result in increase in cumulative gas production.

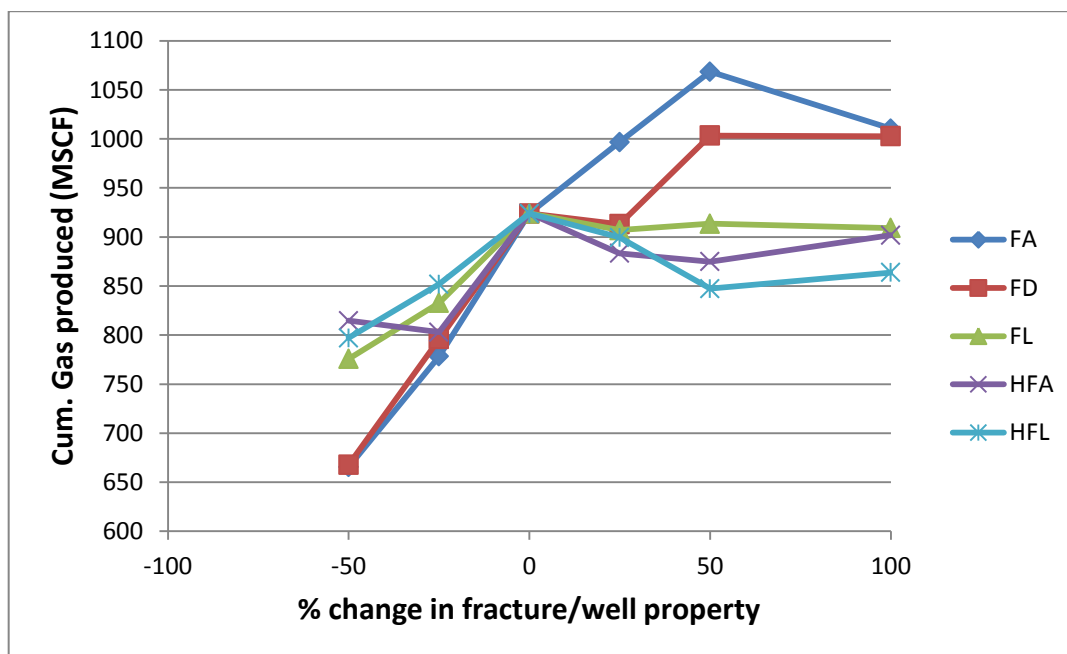


Figure 5.84: Change in cum. gas production for different fracture /well property

5.7.3 Hydraulic Fracture Stages

From the plot in **Fig. 5.85**, we can see that the maximum number of hydraulic fracture stages is 10 for most of the fracture networks except for case 1 where it is 15 and after the maximum value is reached the increase in the cumulative gas production is not appreciable to justify the investment.

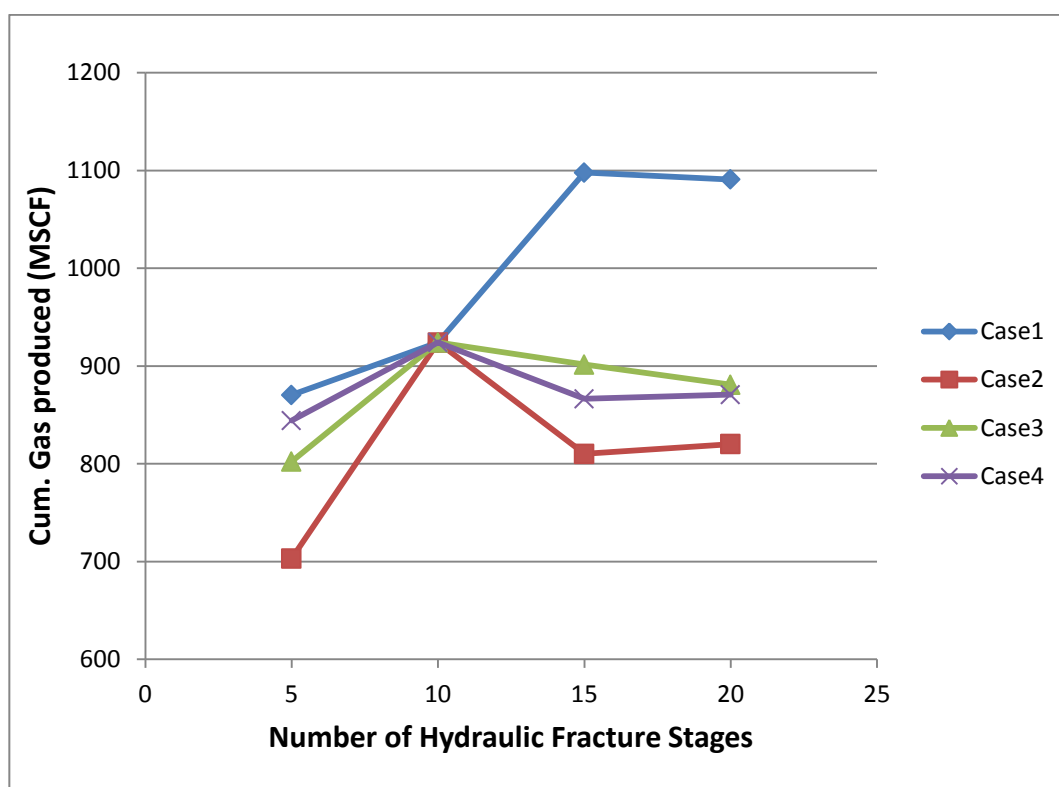


Figure 5.85: Change in cum. gas production for different hydraulic fracture stages

CHAPTER VI

CONCLUSIONS AND RECOMMENDATIONS

6.1 Conclusion

Based on the work done in this thesis, the following conclusions were drawn.

- 1) Uniform fracture network distribution produced the highest cumulative gas production of all the fracture networks studied.
- 2) 10 fracture stages is a suitable number of fracture stages as increasing the number of fracture stages does not necessarily increase productivity of the well significantly to justify the extra investment for the period studied except for case 1 where the optimal value is 15, and this may be due to the larger reservoir volume.
- 3) In order of their impact on cumulative production of the well, we have the following fracture/well properties arranged as follows: fracture aperture, fracture density, fracture length, hydraulic fracture aperture and hydraulic fracture length.
- 4) For the same 2d- fracture density having more than one fracture set did not produce a higher cumulative gas production.

The study shows that for this reservoir having a fracture with wider aperture gives a better reservoir performance than having longer fractures.

An observation made in the course of this project which is important to note.

- 1) Productivity in clustered fracture network depends solely on well placement, thus if the well placement is such that it intersects properly with the clustered fracture networks the productivity will be maximized but if not the productivity could be

very poor thus fracture analysis of the reservoir could be an important factor that could affect productivity by influencing the well /hydraulic fracture placement.

6.2 Recommendations

The following are recommendations of the work that can be done to further test and confirm some observation obtained from this work.

- 1) Other fractured shale gas reservoir should be modeled using FracGen & NFflow to confirm some of the observations made.
- 2) A methodology to quantify the fracture connectivity using a parameter can also be investigated.

REFERENCES

- Adler, P.M., Thovert, J., and Mourzenko, V.V. 2009. Percolation, and Faults and Fractures in Rock. In *Encyclopedia of Complexity and Systems Science*, ed. R.A. Meyers, 717-730. Heidelberg, Germany: Springer.
- Aziz, K. and Settari, A. 1985. *Petroleum Reservoir Simulation*. London: Elsevier Applied Science Publishers Co.
- Barton, C.A. and Zoback, M.D. 1992. Self-Similar Distribution and Properties of Macroscopic Fractures at Depth in Crystalline Rock in the Cajon Pass Scientific Drill Hole. *Journal of Geophysical Research* **97** (4): 5181-5200.
- Bonnet, E. 1997. La Localisation de la De'Formation Dans Les Milieu Fragiles-Ductiles: Approche Expe'rim mentale et Application a'la Lithosphe're Continentale. PhD dissertation, University of Rennes, Rennes, France.
- Bonnet, E., Bour, O., Odling, N.E., Davy, P., Main, P.I. and Berkowitz, B. 2001. Scaling of Fracture Systems in Geological Media. *Reviews of Geophysics* **39** (3): 347-383.
- Boyle, E.J., McKoy, M.L., Sams, N.W., Hatzignatiou, D.G., Dean, J.H., Seth, J.K. and Nicoletti, P. 2010. *Fracgen & NFflow Naturally-Fractured Natural Gas Reservoir Simulator Users Guide*. Morgantown, West Virginia: National Energy Technology Laboratory (NETL).
- Carbotte, S.M. and McDonald, K.C. 1994. Comparison of Seafloor Tectonic Fabric at Intermediate, Fast, and Super Fast Spreading Ridges: Influence of Spreading Rate, Plate Motions, and Ridge Segmentation on Fault Patterns. *Journal of Geophysical Research* **99** (7): 13609 -13631.
- Cowie, P., Scholz, C.H., Edwards, M. and Malinverno, A. 1993. Fault Strain and Seismic Coupling on Mid-Ocean Ridges. *Journal of Geophysical Research* **98** (10): 17911-17920.
- Cowie, P.A. 1998. Normal Fault Growth in Three Dimensions in Continental and Oceanic Crust. In *Faulting and Magmatism at Mid-Ocean Ridges*, ed. W.R. Buck, P.T. Delaney, J.A. Karson and Y. Lagabrielle, 325-348. Washington, D.C.: American Geophysical Union.
- Cowie, P.A., Sornette, D. and Vanneste, C. 1995. Multifractal Scaling Properties of a Growing Fault Population. *Geophysical Journal International* **122** (2): 457-469.

- Cox, D.R. and Lewis, P.A.W. 1966. *The Statistical Analysis of Series of Events*. London: Chapman and Hall.
- Cruden, D.M. 1977. Describing the Size of Discontinuities. *International Journal of Rock Mechanics and Mining Sciences & Geomechanics Abstracts* **14** (2): 133-137.
- Davis, J.C.E. 1986. *Statistics and Data Analysis in Geology*. New York: John Wiley.
- Davy, P. 1993. On the Frequency-Length Distribution of the San Andreas Fault System, *Journal of Geophysical Research* **98** (7): 12141-12151.
- Davy, P., Sornette, A. and Sornette, D. 1990. Some Consequences of a Proposed Fractal Nature of Continental Faulting. *Nature* **348** (2): 56-58.
- Dershowitz, W., Eiben, T. and La Pointe, P. 1998. The Application of Discrete Fracture Network Models to Fractured Reservoir Engineering: Analytical Approach, Data Sets and Early Results in Yates Field, West Texas. *Proc.*, Rocky Mountain Association of Geologists Symposium, Denver, Colorado.
- Dershowitz, W.S. and Einstein, H.H. 1988. Characterizing Rock Joint Geometry with Joint System Models. *Rock Mechanics and Rock Engineering* **21** (1): 21-51.
- Dershowitz, W.S., La Pointe, P.R. and Doe, T.W. 2004. Advances in Discrete Fracture Network Modeling. *Proc.*, US EPA/NGWA Fractured Rock Conference, Portland, Maine.
- Ghosh, K. and Mitra, S. 2009. Structural Controls of Fracture Orientations, Intensity and Connectivity, Teton Anticline, Sawtooth Range, Montana. *AAPG Bulletin* **93** (8): 95–1014.
- Gilman, J.R. 2003. Practical Aspects of Simulation of Fractured Reservoirs. *Proc.*, International Forum on Reservoir Simulation, Bühl, Germany.
- Golf-Racht, T.D.V. 1982. *Fundamentals of Fractured Reservoir Engineering*. Amsterdam, Netherlands: Elsevier Publishing Co.
- Guohai, J. Pashin, J.C. 2008. Discrete Fracture Network Models of the Secarb Carbon Sequestration Test Site, Deerlick Creek Field, Black Warrior Basin, Alabama. *Proc.*, International Coalbed & Shale Gas Symposium, Tuscaloosa, Alabama.
- Hatzignatiou, D.G. 1999. Reservoir Engineering Aspects of Horizontal Wells in Stochastic Naturally Fractured Gas Reservoirs. Paper SPE 54626 presented at the SPE Western Regional Meeting, Anchorage, Alaska, USA, 26-28 May. doi: 10.2118/54626-MS.

Hatzignatiou, D.G. and McKoy, M.L. 2000. Probabilistic Evaluation of Horizontal Wells in Stochastic Naturally Fractured Gas Reservoirs. Paper SPE 65459 presented at the SPE/PS-CIM International Conference on Horizontal Well Technology, Calgary, Alberta, Canada, 6-8 November. doi: 10.2118/65459-MS.

Herbert, A.W. 1996. Modeling Approaches for Discrete Fracture Network Flow Analysis. *Developments in Geotechnical Engineering* **79** (2): 213-229.

Hudson, J.A. and Priest, S.D. 1979. Discontinuities and Rock Mass Geometry. *International Journal of Rock Mechanics and Mining Sciences & Geomechanics Abstracts* **16** (6): 339-362.

Hunt, A. and Ewing, R. 2005. *Percolation Theory for Flow in Porous Media*, second edition. Berlin, Germany: Springer.

Jing, L. and Stephansson, O. 2007. *Fundamentals of Discrete Element Methods for Rock Engineering: Theory and Applications*. Amsterdam, Netherlands: Elsevier Publishing Co.

Kagan, Y.Y. 1997. Seismic Moment-Frequency Relation for Shallow Earthquakes: Regional Comparison. *Journal of Geophysical Research* **102** (2): 2835-2852.

Kazemi, H., Merrill, L., Porterfield, L.S. and Zeman, P. 1976. Numerical Simulation of Water-Oil Flow in Naturally Fractured Reservoirs. *SPE Journal*. **16** (6): 317-326; *Trans., AIME*, **261**. SPE-5719-PA. doi: 10.2118/5719-PA.

King, P.R., Buldyrev, S.V. and Dokholyan, N.V. 2002. Flow between Two Sites in Percolation Systems. *Physical Review E* **62** (6): 8270-8281.

Main, I.G. 1996. Statistical Physics, Seismogenesis, and Seismic Hazard, *Reviews of Geophysics* **34** (4): 433-462.

Main, I.G. and Burton, P.W. 1984. Information Theory and the Earthquake Frequency Magnitude Distribution. *Bulletin of the Seismological Society of America* **74** (4): 1409-1426.

McKoy, M.L. and Sams, N.W. 1997. Tight Gas Reservoir Simulation: Modeling Discrete Irregular Strata-Bound Fracture Networks and Network Flow, Including Dynamic Recharge from the Matrix. Contract No. DE-AC21-95MC31346, National Energy Technology Laboratory, US DOE, Morgantown, West Virginia.

Nelson, R. 2001. *Geological Analysis of Naturally Fractured Reservoirs*. Houston, Texas: Gulf Publishing Company.

- Nur, A. 1982. The Origin of Tensile Fracture Lineaments. *Journal of Structural Geology* **4** (1): 31-40.
- Odling, N.E., Gillespie, P., Bourguine, B., Castaing, J. P., Chiles, N. P., Christensen, E., Fillion, A. et al. 1999. Variations in Fracture System Geometry and Their Implications for Fluid Flow in Fractured Hydrocarbon Reservoirs. *Petroleum Geoscience* **5** (4): 373-384.
- Parsons, R.W. 1966. Permeability of Idealized Fractured Rock. *SPE Journal* **6** (2): 126-136; *Trans., AIME*, **237**. SPE-1289-PA. doi: 10.2118/1289-PA.
- Petrel Fractural Modeling Course Manual, Version 2010 User Guide. 2010. Houston, Texas: Schlumberger.
- Priest, S.D. and Hudson, J.A. 1981. Estimation of Discontinuity Spacing and Trace Length Using Scanline Surveys. *International Journal of Rock Mechanics and Mining Sciences & Geomechanics Abstracts* **18** (3): 183-197.
- Reiss, L. 1980. *The Reservoir Engineering Aspects of Fractured Formations*, trans. M. Creusot. Paris, France: Technip.
- Renshaw, C.E. 1999. Computationally Efficient Models for the Growth of Large Fracture Systems. In *Fracture of Rock*, ed. M. H. Aliabadi, Chap. 3, 83-124. Boston: WIT Press.
- Sams, N.W. 1995. Technical Report on NFlow, a Novel Dry Gas Flow Simulator for Irregular, Discontinuous, Strata-Bound Fracture Networks. Contract No. DE-AC21-95MC31346, National Energy Technology Laboratory, US DOE, Morgantown, West Virginia.
- Sornette, D. and Sornette, A. 1999. General Theory of the Modified Gutenberg-Richter Law for Large Seismic Moments. *Bulletin of the Seismological Society of America* **89** (4): 1121-1130.
- Stauffer, D. and Aharony, A. 1994. *Introduction to Percolation Theory*, second edition. Philadelphia, Pennsylvania: Taylor and Francis.
- Warren, J.E. and Root, P.J. 1963. The Behavior of Naturally Fractured Reservoirs. *SPE Journal* **3** (3): 245 – 255. SPE-426-PA. doi: 10.2118/426-PA.
- Xu, C., Dowd, P.A., Mardia, K. and Fowell, R.J. 2006. A Connectivity Index for Discrete Fracture Networks. *Mathematical Geology* **38** (5): 611-634.

APPENDIX 1

A1.1 FracGen Input File

```

FILE IDENTIFICATION (<= 80 CHARACTERS)          FRACGEN 6th EDITION
Well GU#3, Single-Layer Model
X & Y DIMENSIONS OF FLOW REGION
933.38 3733.58
EFFECTIVE DEPTH OF MID-LAYER; EFFECTIVE THICKNESS OF FRACTURED LAYER
10875 283.0
NUMBER OF SETS (including LEVEL 0 sample trace set)
3
MODEL ----- SET 0
0
NUMBER OF SAMPLE TRACES (OR BOREHOLES)
0
SAMPLE TRACES: X-LEFT, Y-LEFT, X-RIGHT, Y-RIGHT, WIDTH, SHIFT(%)

NAME OF DATA FILE FOR INTERSECTED FRACTURES

MODEL ----- SET 1
1
SET IDENTIFICATION (<= 80 CHARACTERS)
Seismically-resolved faults, interpretation of May 1999
MEAN AND SDEV OF FRACTURE ORIENTATION (360.0 = UNI)
0.0 0.0
MIN/MEAN AND MAX/DEV FRACTURE LENGTH, DIST. (0=UNI,1=EXP,2=LOG,3=INT)
0.0 0.0 0
MEAN AND SDEV OF FRACTURE APERTURE
0.0 0.0
DENSITY OF FRACTURE CENTER POINTS
0.0
CORRELATIONS (len=F(order), ori=F(len), wid=F(len))
0.0 0.0 0.0
MAXIMUM PERCENT FRACTURE SHIFT: MODE I, II, III
0.0 0.0 0.0
SYNTHETIC ANNEALING CONTROLS (pstart,nswaps,swapl,ifreq)
100.0 0 0 0
RELATIVE FREQUENCIES OF T-TERMINATIONS (T2,T1)
0.0 0.0
FRACTURE INTERSECTION FREQUENCIES (%): ZERO TO 10+ INTERSECTIONS
0.0 0.0 0.0 0.0 0.0 0.0 0.0 0.0 0.0 0.0
PERCENT FRACS PENETRATING OVERLYING LAYER; CORRELATION TO FRAC LENGTH
0.0 0.0
NUMBER OF USER-SUPPLIED FRACTURES
10
FRACTURES: X-LEFT, Y-LEFT, X-RIGHT, Y-RIGHT, WIDTH, SHIFT(%), PERCENT
266.0 370.0 666.0 370.0 0.000020 0.0 0.0
266.0 740.0 666.0 740.0 0.000020 0.0 0.0
266.0 1110.0 666.0 1110.0 0.000020 0.0 0.0
266.0 1480.0 666.0 1480.0 0.000020 0.0 0.0
266.0 1850.0 666.0 1850.0 0.000020 0.0 0.0

```

266.0 2220.0 666.0 2220.0 0.000020 0.0 0.0
 266.0 2590.0 666.0 2590.0 0.000020 0.0 0.0
 266.0 2960.0 666.0 2960.0 0.000020 0.0 0.0
 266.0 3330.0 666.0 3330.0 0.000020 0.0 0.0
 266.0 3700.0 666.0 3700.0 0.000020 0.0 0.0
 MODEL ----- SET 3
 1
 SET IDENTIFICATION (<= 80 CHARACTERS)
 Set 1a, Regional Extension (Master) Fractures
 MEAN AND SDEV OF FRACTURE ORIENTATION (360.0=UNI)
 45.0 8.0
 MIN/MEAN AND MAX/DEV FRACTURE LENGTH, DIST. (0=UNI,1=EXP,2=LOG,3=INT)
 260.00 300.00 0
 MEAN AND SDEV OF FRACTURE APERTURE
 0.00002 0.00002
 DENSITY OF FRACTURE CENTER POINTS
 0.0002
 CORRELATIONS (len=F(order), ori=F(len), wid=F(len))
 1.0 0.8 0.7
 MAXIMUM PERCENT FRACTURE SHIFT: MODE I, II, III
 20.0 0.0 0.0
 SYNTHETIC ANNEALING CONTROLS (pstart,nswaps,swapl,ifreq)
 80.0 10 20 3
 RELATIVE FREQUENCIES OF T-TERMINATIONS (T2,T1)
 15.0 52.0
 FRACTURE INTERSECTION FREQUENCIES (%): ZERO TO 10+ INTERSECTIONS
 0.0 0.0 0.0 0.0 0.0 0.0 0.0 0.0 0.0
 PERCENT FRACS PENETRATING OVERLYING LAYER; CORRELATION TO FRAC LENGTH
 0.0 0.0
 NUMBER OF USER-SUPPLIED FRACTURES
 0
 FRACTURES: X-LEFT, Y-LEFT, X-RIGHT, Y-RIGHT, WIDTH, SHIFT(%), PERCENT

A1.2 FLO File

Well GU#3, Single-Layer Model

933.380 3733.580 283.000 0.000

X-left	Y-left	X-right	Y-right	Aperture	Layer	Number
266.000	370.000	666.000	370.000	.200E-04	1	1
266.000	740.000	666.000	740.000	.200E-04	1	2
266.000	1110.000	666.000	1110.000	.200E-04	1	3
266.000	1480.000	666.000	1480.000	.200E-04	1	4
266.000	1850.000	666.000	1850.000	.200E-04	1	5
266.000	2220.000	666.000	2220.000	.200E-04	1	6
266.000	2590.000	666.000	2590.000	.200E-04	1	7
266.000	2960.000	666.000	2960.000	.200E-04	1	8
266.000	3330.000	666.000	3330.000	.200E-04	1	9
266.000	3700.000	666.000	3700.000	.200E-04	1	10
807.005	3190.070	933.380	3315.425	.103E-03	1	11
820.397	1677.381	933.380	1787.950	.444E-05	1	12

361.059	1332.330	578.829	1480.000	.317E-04	1	13
903.218	354.667	933.380	383.479	.278E-04	1	14
426.521	1585.075	649.820	1784.974	.170E-04	1	15
0.000	58.186	173.333	275.515	.924E-05	1	16
623.141	2590.000	809.822	2787.288	.561E-04	1	17
732.898	3083.480	933.380	3275.663	.156E-04	1	18
0.000	560.417	34.100	596.925	.389E-04	1	19
745.606	379.182	933.380	577.947	.481E-04	1	20
597.202	2052.917	826.928	2245.070	.231E-04	1	21
0.000	1228.278	120.086	1345.137	.289E-04	1	22
754.501	2900.282	933.380	3063.390	.108E-04	1	23
265.817	2903.026	449.903	3139.066	.113E-04	1	24
589.638	1850.000	774.366	2069.748	.353E-04	1	25
326.471	3582.048	480.262	3733.580	.730E-04	1	26
84.584	2481.117	252.288	2728.984	.251E-04	1	27
633.447	370.000	933.380	580.097	.438E-04	1	28
69.169	2334.258	291.583	2534.320	.313E-04	1	29
0.000	632.563	144.781	799.539	.244E-04	1	30
275.816	2960.000	463.303	3196.891	.269E-04	1	31
667.704	617.959	849.650	855.358	.267E-04	1	32
0.000	2180.131	191.325	2389.389	.367E-04	1	33
0.000	2130.540	72.652	2186.433	.134E-04	1	34
439.717	215.758	648.743	429.561	.176E-04	1	35
543.144	740.000	757.861	920.068	.203E-04	1	36
457.060	3515.232	635.628	3733.580	.346E-04	1	37
0.000	25.674	30.150	58.854	.648E-05	1	38
557.443	3151.158	767.390	3363.917	.170E-04	1	39
328.535	154.909	554.645	370.000	.124E-04	1	40
94.318	721.667	296.364	941.830	.144E-04	1	41
253.686	1376.614	469.192	1583.596	.236E-04	1	42
0.000	1638.473	161.068	1787.674	.276E-04	1	43
286.733	1652.724	445.626	1850.000	.297E-04	1	44
127.203	561.254	288.669	740.000	.586E-04	1	45
725.351	1814.746	933.380	2009.851	.199E-04	1	46
661.686	2220.000	879.034	2378.741	.518E-04	1	47
0.000	2830.763	4.813	2835.119	.481E-04	1	48
97.010	797.768	325.384	989.989	.183E-04	1	49
0.000	3504.193	72.020	3561.666	.273E-04	1	50
554.798	3426.769	720.775	3674.730	.318E-04	1	51
0.000	1711.003	220.671	1910.843	.186E-04	1	52
886.586	0.000	933.380	55.398	.317E-04	1	53
360.571	1480.000	610.536	1718.094	.328E-04	1	54
821.376	370.290	933.380	452.282	.417E-04	1	55
489.004	796.906	679.721	1026.071	.889E-05	1	56
161.725	2417.512	341.595	2649.375	.261E-04	1	57
420.667	0.000	523.822	77.072	.258E-04	1	58
843.401	2099.394	933.380	2193.011	.943E-05	1	59
191.253	3527.636	390.016	3700.000	.128E-04	1	60
707.739	2226.344	916.384	2439.123	.289E-04	1	61
480.514	1027.319	657.416	1266.922	.219E-04	1	62
0.000	1664.443	180.869	1847.965	.547E-04	1	63
0.000	1478.139	110.525	1578.240	.482E-04	1	64
331.184	1110.000	528.242	1353.448	.830E-05	1	65

0.000	2986.288	65.196	3024.010	.498E-04	1	66
131.151	3024.132	341.841	3234.318	.251E-04	1	67
602.757	2483.124	811.003	2695.707	.404E-04	1	68
0.000	3250.045	148.480	3388.410	.304E-04	1	69
266.018	2092.297	470.898	2308.054	.121E-03	1	70
779.632	3308.693	933.380	3427.263	.533E-04	1	71
107.006	2342.510	331.816	2590.000	.361E-04	1	72
0.000	958.997	74.198	1025.298	.157E-04	1	73
305.229	1850.000	554.934	2098.474	.208E-04	1	74
130.851	2461.509	333.455	2679.116	.321E-04	1	75
31.270	649.200	233.542	867.068	.101E-04	1	76
441.372	1995.220	683.699	2236.078	.323E-04	1	77
719.035	28.277	921.503	245.890	.536E-05	1	78
877.593	2874.499	933.380	2947.053	.161E-04	1	79
318.675	127.251	516.842	294.646	.126E-04	1	80
130.124	0.000	192.925	78.202	.116E-04	1	81
804.457	298.971	933.380	431.187	.113E-04	1	82
922.142	1026.538	933.380	1036.329	.511E-04	1	83
122.704	3551.440	289.987	3733.580	.586E-05	1	84
0.000	1737.641	177.772	1882.181	.232E-04	1	85
185.160	2682.979	393.467	2894.562	.205E-04	1	86
0.000	6.861	54.600	73.114	.141E-04	1	87
526.843	2220.000	756.375	2439.162	.205E-04	1	88
0.000	3156.249	80.098	3215.022	.172E-04	1	89
0.000	3244.188	42.046	3281.005	.705E-05	1	90
0.000	3429.894	111.830	3530.814	.399E-04	1	91
0.000	3628.897	85.333	3733.580	.473E-04	1	92
790.301	2156.999	933.380	2314.338	.152E-04	1	93
742.412	2143.742	923.713	2303.708	.175E-04	1	94
0.000	2787.496	139.639	2943.379	.285E-04	1	95
234.829	3100.030	430.705	3330.000	.172E-04	1	96
0.000	424.046	196.666	583.404	.828E-05	1	97
550.870	1286.790	747.904	1508.124	.620E-04	1	98
759.573	2103.634	933.380	2285.911	.107E-03	1	99
300.247	1596.167	512.614	1802.784	.294E-04	1	100
143.467	663.395	341.304	883.892	.890E-05	1	101
739.455	492.029	933.380	672.593	.179E-04	1	102
370.589	370.000	554.456	568.700	.281E-04	1	103
127.529	1481.533	329.326	1698.241	.622E-04	1	104
183.997	1681.781	351.622	1850.000	.104E-04	1	105
292.234	274.279	542.076	433.125	.227E-04	1	106
329.015	3262.740	529.020	3480.959	.246E-04	1	107
606.671	71.778	815.019	282.021	.115E-04	1	108
0.000	3546.488	101.336	3662.354	.111E-04	1	109
323.842	1072.208	552.435	1260.015	.852E-05	1	110
0.000	602.166	27.247	630.874	.256E-04	1	111
624.159	3035.379	787.195	3282.123	.109E-04	1	112
515.106	1737.365	744.785	1923.645	.214E-04	1	113
702.367	3688.932	733.897	3733.580	.221E-04	1	114
871.756	2285.220	933.380	2341.486	.136E-04	1	115
695.087	2078.454	911.221	2280.032	.411E-04	1	116
84.679	1073.746	309.400	1265.678	.139E-04	1	117
19.814	355.500	216.154	576.261	.305E-04	1	118

722.370	2681.846	901.303	2916.914	.196E-04	1	119
857.657	2553.384	933.380	2626.888	.177E-04	1	120
272.527	2046.201	433.551	2220.000	.247E-04	1	121
398.508	687.601	631.297	869.142	.263E-04	1	122
107.113	1808.005	272.157	2022.192	.203E-04	1	123
0.000	2917.450	38.633	2961.174	.119E-04	1	124
0.000	2561.289	80.524	2622.524	.195E-04	1	125
540.610	87.754	763.760	280.832	.124E-04	1	126
390.147	1480.000	589.038	1674.587	.205E-04	1	127
541.566	3087.708	745.161	3301.232	.151E-04	1	128
95.270	573.900	280.076	803.856	.208E-04	1	129
596.963	2411.111	802.637	2622.583	.706E-05	1	130
931.954	53.711	933.380	55.593	.201E-04	1	131
257.643	960.111	439.586	1192.227	.315E-04	1	132
51.186	206.652	244.419	429.409	.791E-05	1	133
542.153	66.868	782.751	249.459	.171E-04	1	134
600.492	1850.000	802.780	2087.968	.134E-04	1	135
519.366	1163.536	727.663	1372.175	.237E-04	1	136
812.778	1936.233	933.380	2064.147	.116E-04	1	137
254.039	3272.093	454.247	3488.409	.183E-04	1	138
598.483	1022.185	826.482	1208.925	.900E-05	1	139
0.000	3069.422	130.581	3206.295	.363E-04	1	140
615.793	0.000	786.905	220.610	.247E-04	1	141
884.323	3100.407	933.380	3144.968	.857E-05	1	142
654.125	3575.157	887.600	3726.126	.413E-04	1	143
865.080	2664.337	933.380	2717.279	.262E-04	1	144
775.481	10.652	933.380	201.925	.278E-04	1	145
894.450	2861.328	933.380	2893.028	.196E-04	1	146
736.833	1192.196	933.380	1401.839	.101E-04	1	147
599.454	66.640	841.680	233.798	.195E-04	1	148
637.267	3463.107	806.428	3673.640	.214E-04	1	149
750.323	3578.122	906.984	3733.580	.726E-05	1	150
889.713	1462.190	933.380	1507.167	.996E-05	1	151
507.993	112.314	694.131	340.120	.117E-04	1	152
379.684	851.230	594.857	1051.733	.234E-04	1	153
643.344	3238.209	830.887	3477.358	.190E-04	1	154
115.510	765.780	342.520	922.601	.412E-05	1	155
0.000	1375.415	8.539	1384.952	.156E-04	1	156
0.000	2022.546	79.491	2091.889	.181E-04	1	157
92.125	1176.463	311.285	1372.336	.838E-05	1	158
580.863	36.348	796.326	236.254	.137E-04	1	159
291.393	2450.163	513.453	2642.661	.908E-05	1	160
758.394	1732.242	933.380	1910.331	.263E-04	1	161
782.493	1303.515	933.380	1430.695	.251E-04	1	162
603.966	3330.000	783.448	3507.788	.213E-04	1	163
675.385	59.762	873.478	276.391	.210E-04	1	164
853.035	3543.332	933.380	3630.582	.174E-04	1	165
414.431	3330.000	625.682	3532.666	.113E-04	1	166
168.526	3707.168	192.781	3733.580	.142E-04	1	167
657.957	1975.791	856.543	2191.682	.202E-04	1	168
803.632	2683.771	933.380	2805.282	.143E-04	1	169
568.806	2886.837	774.946	3095.353	.270E-04	1	170
252.286	365.234	457.334	574.800	.136E-04	1	171

214.505	175.665	438.229	370.000	.399E-04	1	172
685.069	931.977	875.942	1154.415	.980E-05	1	173
281.020	1962.490	493.805	2164.017	.218E-04	1	174
611.150	2308.897	805.219	2528.482	.177E-04	1	175
270.101	1424.108	461.325	1646.105	.124E-04	1	176
663.799	3589.611	845.764	3733.580	.264E-04	1	177
198.875	3324.308	405.142	3532.279	.837E-05	1	178
662.355	915.083	855.002	1135.566	.380E-04	1	179
731.755	1332.302	918.131	1558.088	.157E-04	1	180
521.963	2075.322	725.625	2266.698	.119E-04	1	181
630.756	1780.781	838.850	1986.649	.301E-04	1	182
599.048	2361.001	812.036	2561.750	.388E-04	1	183
558.295	895.475	738.766	1137.083	.158E-04	1	184
344.191	1850.000	511.555	2022.047	.618E-05	1	185
162.409	1725.936	366.681	1935.425	.582E-04	1	186
602.982	3643.837	691.681	3733.580	.488E-04	1	187
286.203	2539.785	502.405	2728.956	.311E-04	1	188
57.023	2637.677	273.391	2834.465	.119E-04	1	189
715.983	3112.240	933.380	3292.109	.158E-04	1	190
491.304	1041.934	708.265	1217.253	.797E-05	1	191
704.245	3724.167	713.586	3733.580	.657E-04	1	192
573.873	192.942	808.920	377.038	.255E-04	1	193
335.853	2386.108	547.132	2590.000	.121E-04	1	194
376.076	1850.000	550.049	2014.042	.280E-04	1	195
283.272	3028.848	487.194	3238.140	.554E-04	1	196
759.777	1857.890	933.380	1987.153	.125E-04	1	197
0.000	1156.830	132.229	1274.515	.153E-04	1	198
851.600	3296.486	933.380	3377.348	.938E-05	1	199
879.742	2604.484	933.380	2661.686	.228E-04	1	200
0.000	1431.486	159.075	1582.328	.215E-04	1	201
722.696	3277.672	902.727	3495.062	.772E-05	1	202
174.435	2655.029	400.342	2839.849	.212E-04	1	203
0.000	2841.242	48.857	2895.742	.158E-04	1	204
575.108	3457.111	781.984	3657.834	.128E-04	1	205
0.000	2499.222	134.722	2593.550	.194E-04	1	206
58.575	2647.538	292.719	2821.658	.889E-05	1	207
686.282	19.869	907.276	210.375	.325E-04	1	208
0.000	996.205	86.494	1091.294	.217E-04	1	209
0.000	2350.995	183.837	2555.719	.724E-05	1	210
22.446	3282.412	210.297	3505.553	.948E-05	1	211
0.000	3489.210	33.735	3531.114	.293E-04	1	212
490.653	3277.651	679.474	3499.765	.723E-05	1	213
270.064	3375.269	512.115	3582.551	.690E-05	1	214
669.869	2784.841	834.520	2973.246	.208E-04	1	215
434.549	3433.517	630.397	3649.342	.141E-04	1	216
0.000	628.646	215.060	799.443	.974E-05	1	217
0.000	3168.924	194.517	3358.256	.386E-04	1	218
433.821	2590.000	554.080	2799.716	.247E-04	1	219
41.346	894.924	239.913	1108.108	.171E-04	1	220
0.000	683.503	159.294	861.953	.386E-04	1	221
97.605	2052.495	300.728	2261.146	.158E-04	1	222
754.989	2154.839	907.687	2346.777	.197E-04	1	223
799.400	3710.830	821.705	3733.580	.819E-05	1	224

0.000	2264.865	159.029	2408.496	.121E-04	1	225
788.523	2608.071	933.380	2769.404	.291E-04	1	226
531.323	3135.318	736.286	3341.669	.622E-05	1	227
534.639	2220.000	768.235	2416.742	.880E-05	1	228
551.952	3444.693	761.967	3667.280	.390E-04	1	229
241.972	2084.384	441.243	2295.949	.102E-04	1	230
583.228	2426.835	751.419	2634.882	.113E-04	1	231
185.662	1134.823	402.993	1327.736	.257E-04	1	232
794.821	1752.246	933.380	1877.437	.112E-04	1	233
0.000	3529.121	32.693	3562.304	.122E-04	1	234
0.000	1692.384	211.379	1889.340	.130E-04	1	235
915.705	341.046	933.380	356.455	.888E-05	1	236
138.955	2957.781	321.630	3201.941	.254E-04	1	237
403.952	3216.231	586.606	3442.049	.418E-04	1	238
202.314	2889.575	400.328	3102.006	.425E-04	1	239
0.000	1954.104	137.467	2113.914	.268E-04	1	240
865.409	2761.191	933.380	2824.043	.197E-04	1	241
0.000	236.019	129.858	368.798	.181E-04	1	242
538.659	3330.000	717.593	3532.289	.261E-04	1	243
560.472	3592.219	735.816	3733.580	.131E-04	1	244
542.850	2758.208	724.428	2984.535	.155E-04	1	245
57.730	1501.258	282.523	1684.704	.114E-04	1	246
774.862	2220.430	933.380	2339.063	.178E-04	1	247
481.705	3008.467	656.772	3239.692	.122E-04	1	248
703.542	1940.843	907.332	2147.126	.118E-04	1	249
664.858	565.651	890.470	747.644	.682E-05	1	250
458.298	2294.785	660.749	2476.695	.108E-04	1	251
864.794	1894.829	933.380	1954.791	.955E-05	1	252
515.709	3330.000	724.321	3498.791	.143E-04	1	253
261.765	2282.288	482.918	2469.375	.244E-04	1	254
104.139	0.000	164.957	63.447	.209E-04	1	255
871.454	1474.586	933.380	1545.001	.146E-04	1	256
173.280	2732.838	396.917	2960.000	.121E-04	1	257
512.821	740.000	676.469	918.107	.184E-04	1	258
0.000	3650.640	70.374	3733.580	.867E-05	1	259
601.650	1936.259	796.444	2150.419	.154E-04	1	260
498.630	2168.513	726.423	2347.118	.261E-04	1	261
65.649	2884.360	272.599	3086.722	.309E-04	1	262
0.000	894.898	14.978	909.811	.475E-05	1	263
0.000	1994.897	121.068	2103.991	.102E-04	1	264
640.627	3607.510	766.210	3733.580	.218E-04	1	265
0.000	1057.710	162.394	1176.476	.107E-04	1	266
64.992	1616.119	282.636	1806.455	.965E-05	1	267
476.130	214.132	661.267	436.169	.139E-04	1	268
105.727	509.716	288.010	740.000	.816E-05	1	269
438.955	1166.782	642.416	1394.162	.106E-04	1	270
663.711	370.000	836.203	582.111	.215E-04	1	271
512.477	2524.283	697.638	2746.118	.199E-04	1	272
699.621	0.000	783.274	97.320	.156E-04	1	273
0.000	3077.463	92.785	3169.347	.103E-04	1	274
807.193	123.029	933.380	224.778	.119E-04	1	275
690.706	2669.294	891.191	2903.630	.413E-04	1	276
919.954	1274.320	933.380	1288.954	.171E-04	1	277

590.152	3657.541	669.481	3733.580	.634E-05	1	278
195.731	698.905	458.235	912.869	.504E-05	1	279
0.000	2266.479	145.336	2384.707	.288E-04	1	280
206.364	3535.912	401.417	3700.000	.101E-04	1	281
730.334	1461.477	930.451	1669.291	.704E-05	1	282
616.884	139.768	823.925	340.533	.209E-04	1	283
666.324	2846.651	880.551	3039.703	.298E-04	1	284
247.225	1424.901	453.468	1626.411	.770E-05	1	285
420.484	889.248	591.900	1110.000	.113E-04	1	286
0.000	2998.474	62.107	3069.560	.201E-04	1	287
210.629	3053.578	411.963	3267.799	.110E-04	1	288
0.000	221.234	35.607	261.787	.161E-04	1	289
655.066	2643.200	835.535	2830.514	.747E-05	1	290
551.020	1637.392	721.943	1840.876	.271E-04	1	291
687.688	2168.628	887.497	2376.129	.275E-04	1	292
195.706	2479.376	412.542	2668.989	.209E-04	1	293
0.000	3316.446	13.671	3330.909	.271E-04	1	294
623.886	1780.538	807.483	2002.399	.257E-04	1	295
846.056	2736.805	933.380	2813.995	.138E-04	1	296
791.315	2720.383	933.380	2869.481	.339E-04	1	297
0.000	2310.692	19.805	2325.704	.172E-04	1	298
443.106	3130.350	697.536	3338.561	.827E-05	1	299
570.471	911.776	768.370	1096.217	.864E-05	1	300
399.310	2590.000	575.059	2766.904	.398E-04	1	301
711.533	2353.341	903.392	2567.698	.982E-05	1	302
0.000	1317.585	154.847	1499.466	.147E-04	1	303
529.158	3330.000	780.025	3529.844	.125E-04	1	304
231.525	1306.339	404.547	1480.000	.418E-04	1	305
423.882	1553.111	665.974	1774.245	.223E-04	1	306
267.924	2960.000	478.046	3145.232	.408E-04	1	307
374.028	1191.991	580.160	1392.386	.103E-04	1	308
870.527	406.271	933.380	469.961	.118E-04	1	309
452.874	1289.226	668.551	1479.125	.147E-04	1	310
0.000	1229.781	71.575	1303.356	.167E-04	1	311
0.000	703.702	171.236	930.350	.136E-04	1	312
652.041	2719.724	865.013	2912.364	.111E-04	1	313
438.216	0.000	609.993	170.131	.268E-04	1	314
482.612	180.309	707.572	358.691	.260E-04	1	315
0.000	1161.356	156.691	1335.976	.186E-04	1	316
0.000	2189.919	194.827	2350.706	.242E-04	1	317
41.538	3274.579	218.024	3500.941	.790E-05	1	318
530.435	2590.000	735.814	2763.935	.277E-04	1	319
460.597	3560.504	633.087	3733.580	.316E-04	1	320
0.000	613.098	132.782	748.776	.135E-04	1	321
383.085	2384.920	566.108	2590.000	.446E-05	1	322
926.501	2476.640	933.380	2481.522	.164E-04	1	323
596.799	1389.269	814.728	1575.556	.680E-05	1	324
438.790	2762.608	651.162	2960.000	.129E-04	1	325
73.223	415.552	279.950	600.216	.883E-05	1	326
0.000	300.366	80.634	422.172	.305E-04	1	327
0.000	1811.976	142.333	1957.736	.162E-04	1	328
103.977	3261.366	300.048	3470.248	.670E-05	1	329
684.279	255.263	889.055	455.592	.931E-05	1	330

0.000 2832.793 150.788 2990.287 .242E-04 1 331
 852.707 3404.638 933.380 3467.840 .305E-04 1 332
 596.165 2921.447 809.510 3112.520 .178E-04 1 333
 105.368 3212.396 329.193 3391.050 .980E-05 1 334
 0.000 3398.684 20.755 3414.580 .241E-04 1 335
 380.973 1110.000 534.106 1282.698 .135E-04 1 336
 170.105 1190.812 379.793 1385.711 .170E-04 1 337
 314.601 2498.111 462.580 2743.094 .758E-05 1 338
 411.606 2822.287 606.287 3032.034 .405E-04 1 339
 394.751 2528.307 622.550 2701.460 .427E-04 1 340
 0.000 2292.307 75.567 2376.487 .634E-05 1 341
 0.000 2904.864 135.380 3070.394 .252E-04 1 342
 788.194 2683.681 933.380 2855.978 .134E-04 1 343
 0.000 1794.164 40.231 1839.971 .427E-04 1 344
 19.925 2796.370 218.424 3002.094 .102E-04 1 345
 797.164 580.349 933.380 709.211 .196E-04 1 346
 642.457 0.000 699.106 57.279 .168E-04 1 347
 192.658 1367.849 411.204 1551.999 .221E-04 1 348
 0.000 303.344 118.238 418.038 .165E-04 1 349
 255.109 1426.829 463.528 1622.084 .216E-04 1 350
 587.916 1045.265 781.881 1269.465 .503E-04 1 351
 1.018 3436.285 210.978 3629.728 .104E-04 1 352
 733.278 1491.695 914.579 1642.181 .224E-04 1 353
 530.733 1174.921 746.498 1478.263 .716E-05 1 354
 422.307 3434.877 607.534 3652.028 .443E-05 1 355
 0.000 3579.138 113.349 3733.580 .108E-04 1 356
 642.312 1850.000 891.357 2071.766 .124E-04 1 357
 174.851 1966.445 373.034 2171.620 .183E-04 1 358
 157.972 8.953 360.590 209.674 .146E-04 1 359
 860.564 3680.014 920.415 3733.580 .667E-05 1 360
 221.254 203.122 425.719 370.000 .120E-04 1 361
 383.595 2590.000 521.618 2743.107 .271E-04 1 362
 905.304 663.476 933.380 687.025 .547E-05 1 363
 316.254 3700.000 346.438 3733.580 .802E-05 1 364
 649.285 226.543 848.097 430.521 .178E-04 1 365
 483.147 2220.000 626.059 2386.460 .380E-04 1 366
 76.125 2298.569 282.734 2494.568 .852E-05 1 367
 637.386 2559.195 841.625 2757.611 .224E-04 1 368
 412.107 3287.791 611.794 3490.690 .121E-04 1 369
 31.748 1721.965 217.000 1926.913 .142E-04 1 370
 842.618 2380.475 933.380 2495.498 .234E-04 1 371
 203.684 20.826 443.414 219.539 .319E-04 1 372
 99.042 326.485 306.838 520.660 .165E-04 1 373
 140.502 2902.551 381.330 3093.317 .333E-04 1 374
 382.436 994.103 549.748 1257.807 .514E-05 1 375
 30.893 2558.200 232.454 2776.842 .477E-05 1 376
 0.000 3161.837 182.913 3305.403 .496E-04 1 377
 122.692 3325.693 320.484 3529.535 .255E-04 1 378
 163.580 1689.084 344.674 1912.856 .825E-05 1 379
 596.449 494.903 799.211 693.675 .246E-04 1 380
 636.686 269.816 830.730 463.868 .125E-04 1 381
 851.738 2294.533 933.380 2384.817 .335E-04 1 382
 118.559 0.000 210.446 124.453 .372E-04 1 383

314.160 3524.116 500.570 3700.000 .301E-04 1 384
142.893 2333.547 364.963 2581.487 .153E-04 1 385
329.424 828.144 518.271 1039.381 .148E-04 1 386
0.000 313.969 56.391 396.626 .208E-04 1 387
383.764 1264.717 612.485 1480.000 .110E-04 1 388
877.570 0.000 878.241 1.058 .124E-04 1 389
408.242 278.362 613.945 512.054 .118E-04 1 390
558.340 210.238 742.247 425.512 .410E-04 1 391
522.742 0.000 686.831 176.665 .188E-04 1 392
234.875 983.268 431.102 1181.403 .114E-04 1 393
222.006 1088.883 398.214 1254.075 .167E-04 1 394
206.200 2855.919 404.728 3057.591 .133E-04 1 395
392.287 2269.054 628.208 2425.278 .432E-04 1 396
66.019 2144.278 261.583 2348.728 .830E-05 1 397
0.000 1765.516 177.781 1944.675 .272E-04 1 398
50.037 2310.058 199.309 2535.037 .254E-04 1 399
152.466 2558.551 345.706 2765.054 .915E-05 1 400
435.115 3700.000 464.377 3733.580 .123E-04 1 401
0.000 2385.620 51.573 2428.954 .184E-04 1 402
711.734 753.807 909.369 955.936 .102E-04 1 403
9.913 3317.853 199.183 3492.351 .571E-05 1 404
697.954 3307.846 918.861 3532.930 .178E-04 1 405
0.000 2283.582 117.575 2411.848 .114E-04 1 406
436.954 2220.000 620.664 2411.421 .563E-05 1 407
593.998 327.612 809.556 510.209 .264E-04 1 408
90.781 1191.094 298.993 1381.971 .347E-04 1 409
898.964 160.235 933.380 191.971 .283E-04 1 410
929.690 2692.957 933.380 2697.178 .784E-05 1 411
851.501 2758.809 933.380 2831.598 .183E-04 1 412
447.628 165.303 654.403 357.530 .111E-04 1 413
0.000 471.293 8.119 480.488 .124E-04 1 414
333.798 2403.729 488.928 2590.000 .102E-04 1 415
0.000 1314.497 130.855 1474.956 .185E-04 1 416
669.382 1239.089 867.751 1439.783 .456E-04 1 417
14.075 772.620 197.756 986.791 .195E-04 1 418
178.549 2066.530 357.246 2220.000 .664E-05 1 419
0.000 234.065 81.401 315.181 .166E-04 1 420
0.000 3358.485 77.220 3421.334 .942E-05 1 421
540.531 687.401 751.254 874.499 .403E-04 1 422
0.000 2165.669 183.001 2378.326 .146E-04 1 423
339.768 1480.000 607.709 1670.697 .807E-05 1 424
431.669 1030.265 637.618 1222.451 .222E-04 1 425
279.223 2322.557 471.785 2590.000 .174E-04 1 426
362.780 865.455 633.636 1110.000 .740E-05 1 427
586.813 1272.341 767.579 1535.252 .168E-04 1 428
0.000 3511.637 50.897 3557.559 .856E-05 1 429
526.293 2468.444 734.064 2658.319 .568E-05 1 430
318.496 1480.000 520.769 1689.952 .149E-04 1 431
52.268 3664.388 113.561 3733.580 .138E-04 1 432
864.042 0.000 933.380 73.448 .337E-04 1 433
809.633 2739.607 933.380 2899.995 .239E-04 1 434
0.000 2210.149 54.720 2263.922 .167E-04 1 435
892.447 2405.272 933.380 2449.488 .406E-04 1 436

352.647	3222.713	498.239	3447.375	.625E-05	1	437
428.291	2686.329	593.439	2821.264	.430E-05	1	438
19.042	1951.083	207.421	2159.739	.133E-04	1	439
0.000	3622.019	56.609	3678.927	.213E-04	1	440
0.000	3096.116	4.140	3099.463	.114E-04	1	441
408.441	2261.123	618.644	2470.644	.159E-04	1	442
31.381	3592.527	164.237	3733.580	.227E-04	1	443
0.000	2049.570	27.567	2079.948	.184E-04	1	444
157.797	34.459	372.992	260.079	.133E-04	1	445
804.237	848.413	933.380	942.313	.871E-05	1	446
436.361	2699.689	690.195	2941.865	.167E-04	1	447
538.107	816.191	737.506	993.086	.185E-04	1	448
715.833	0.000	883.274	166.769	.706E-05	1	449
913.943	1972.681	933.380	1989.355	.145E-04	1	450
734.724	2217.475	921.549	2383.174	.192E-04	1	451
68.553	3414.281	247.051	3649.802	.790E-05	1	452
0.000	3574.714	99.120	3684.797	.379E-05	1	453
0.000	3460.720	130.223	3555.326	.142E-04	1	454
106.785	3711.001	123.507	3733.580	.857E-05	1	455
0.000	1613.287	131.867	1738.720	.118E-04	1	456
0.000	215.786	78.911	290.821	.264E-04	1	457
719.845	610.007	933.380	799.327	.179E-04	1	458
598.788	566.204	792.633	768.941	.120E-04	1	459
881.578	3544.057	933.380	3589.625	.917E-05	1	460
710.289	3001.966	858.321	3203.711	.136E-04	1	461
760.390	3241.557	933.380	3418.212	.130E-04	1	462
260.582	1745.704	453.688	1948.999	.248E-04	1	463
260.067	3218.022	462.283	3408.145	.185E-04	1	464
821.256	1385.515	933.380	1483.912	.102E-04	1	465
118.759	1614.071	353.773	1850.000	.144E-04	1	466
0.000	1215.116	90.938	1353.418	.221E-04	1	467
176.816	367.138	371.179	569.037	.405E-04	1	468
146.659	1906.248	344.327	2104.887	.902E-05	1	469
282.864	2260.982	468.605	2470.723	.115E-04	1	470
447.375	1782.474	639.493	1909.307	.281E-04	1	471
0.000	375.730	86.423	462.410	.148E-03	1	472
621.722	3700.000	649.663	3733.580	.117E-04	1	473
0.000	2174.389	29.396	2212.282	.251E-04	1	474
572.992	310.163	782.414	532.028	.353E-04	1	475
51.360	1058.011	248.694	1256.586	.176E-04	1	476
108.940	2398.834	324.733	2590.000	.124E-04	1	477
886.225	3138.054	933.380	3178.911	.247E-04	1	478
323.084	1065.119	504.912	1240.493	.914E-05	1	479
191.050	2274.990	392.408	2474.105	.822E-05	1	480
221.858	1171.936	444.881	1389.170	.173E-04	1	481
172.765	2553.037	380.935	2739.853	.106E-04	1	482
527.437	2220.000	705.068	2372.669	.231E-04	1	483
178.813	2056.971	354.238	2220.000	.137E-04	1	484
640.284	3330.000	892.888	3547.311	.209E-04	1	485
300.443	1850.000	479.596	2107.248	.829E-05	1	486
0.000	863.498	186.742	1022.077	.584E-05	1	487
532.959	562.691	696.641	789.263	.957E-05	1	488
146.958	1859.713	404.485	2065.622	.108E-04	1	489

427.421	1065.005	580.359	1252.121	.518E-05	1	490
286.068	2526.795	519.646	2760.971	.167E-04	1	491
547.377	2112.146	719.055	2261.900	.161E-04	1	492
914.271	1585.594	933.380	1600.044	.125E-04	1	493
451.765	2497.967	622.475	2696.852	.137E-04	1	494
318.389	3013.791	513.589	3177.910	.140E-04	1	495
0.000	2166.536	5.038	2171.524	.153E-04	1	496
442.913	3700.000	497.445	3733.580	.279E-04	1	497
591.905	222.234	782.044	474.089	.581E-05	1	498
290.919	3473.982	501.242	3700.000	.271E-04	1	499
125.593	2148.915	355.608	2306.575	.228E-04	1	500
0.000	1801.545	190.054	1974.487	.395E-04	1	501
21.594	441.544	190.899	650.142	.196E-04	1	502
364.583	211.595	510.182	449.347	.656E-05	1	503
746.697	2199.772	933.380	2404.218	.661E-05	1	504
236.639	455.063	417.586	740.000	.353E-04	1	505
0.000	652.095	210.180	798.594	.659E-05	1	506
0.000	3262.930	186.716	3435.096	.121E-04	1	507
734.082	1078.356	933.380	1264.166	.459E-04	1	508
217.610	0.000	343.402	169.052	.261E-04	1	509
422.193	1671.615	646.875	1850.000	.122E-04	1	510
657.286	1850.000	822.008	2075.407	.114E-04	1	511
853.057	938.713	933.380	1017.987	.206E-04	1	512
151.774	3524.087	368.835	3651.954	.101E-04	1	513
203.996	2136.582	422.974	2308.421	.719E-05	1	514
0.000	2631.675	41.872	2668.963	.703E-05	1	515
894.019	1957.846	933.380	1994.717	.747E-05	1	516
63.203	1456.721	270.172	1634.716	.260E-04	1	517
445.750	3228.247	630.677	3436.150	.202E-04	1	518
142.249	2579.845	323.690	2790.774	.134E-04	1	519
688.602	1233.322	903.536	1409.918	.134E-04	1	520
814.670	3335.714	933.380	3453.214	.931E-05	1	521
0.000	3509.240	187.434	3714.517	.131E-04	1	522
15.106	1260.483	184.400	1481.126	.188E-04	1	523
307.715	1318.717	471.545	1559.636	.283E-04	1	524
113.152	1918.096	299.338	2124.588	.235E-04	1	525
468.909	185.087	699.360	375.310	.162E-04	1	526
203.181	1441.475	413.862	1622.826	.267E-04	1	527
253.144	770.344	452.809	986.575	.110E-04	1	528
470.771	2782.046	633.079	2960.000	.957E-05	1	529
270.674	2043.956	480.086	2220.000	.857E-05	1	530
769.474	1673.302	933.380	1836.053	.956E-05	1	531
871.566	3555.584	933.380	3611.802	.157E-04	1	532
342.008	167.726	528.247	370.000	.242E-04	1	533
99.807	1535.596	308.711	1737.296	.323E-04	1	534
0.000	36.245	193.807	170.038	.184E-04	1	535
0.000	3406.773	36.728	3463.038	.483E-05	1	536
26.364	528.400	214.411	714.131	.557E-05	1	537
337.511	3252.024	508.714	3470.409	.106E-04	1	538
647.817	1698.542	849.715	1888.832	.113E-04	1	539
636.286	1480.000	844.373	1747.673	.185E-04	1	540
82.025	2269.845	300.607	2402.300	.903E-05	1	541
874.601	617.864	933.380	677.790	.133E-04	1	542

192.401 2996.540 400.389 3179.941 .133E-04 1 543
0.000 1357.469 91.333 1446.743 .566E-05 1 544
927.861 3611.458 933.380 3616.808 .769E-05 1 545
0.000 3023.403 96.153 3129.032 .112E-04 1 546
190.498 2147.916 407.335 2315.879 .170E-04 1 547
809.172 0.000 836.699 30.921 .200E-04 1 548
35.840 582.443 226.037 842.133 .106E-04 1 549
185.107 3349.097 346.267 3530.725 .733E-05 1 550
840.438 2079.414 933.380 2136.394 .336E-04 1 551
266.505 756.592 431.776 984.431 .686E-05 1 552
38.375 315.194 215.733 527.835 .122E-04 1 553
0.000 1751.878 174.343 1895.253 .131E-04 1 554
833.066 483.698 933.380 595.630 .933E-05 1 555
165.687 585.466 390.512 795.804 .129E-04 1 556
0.000 3006.915 172.066 3159.355 .673E-05 1 557
45.890 1910.280 253.325 2093.460 .178E-04 1 558
371.936 418.404 572.935 618.028 .128E-04 1 559
93.536 2315.086 315.029 2581.403 .433E-04 1 560
696.963 1663.051 888.265 1862.803 .403E-04 1 561
92.915 1099.828 330.095 1326.390 .128E-04 1 562
695.639 1430.621 904.778 1629.104 .139E-04 1 563
238.333 2226.191 442.899 2429.214 .210E-04 1 564
0.000 1701.288 134.318 1800.731 .144E-04 1 565
829.941 652.499 933.380 748.171 .122E-04 1 566
224.195 3450.869 437.806 3700.000 .358E-04 1 567
654.034 3168.225 838.949 3373.478 .957E-05 1 568
74.024 131.830 296.125 370.000 .246E-04 1 569
759.913 2138.914 933.380 2257.033 .182E-04 1 570
0.000 3444.552 140.251 3570.545 .122E-04 1 571
0.000 1075.064 118.937 1216.906 .118E-04 1 572
178.112 2570.578 354.382 2782.892 .970E-05 1 573
427.882 0.000 532.017 102.565 .145E-04 1 574
583.695 1349.149 783.763 1516.962 .443E-04 1 575
74.763 2667.129 274.183 2857.637 .264E-04 1 576
415.692 2284.553 594.551 2480.769 .956E-05 1 577
903.317 3697.377 933.380 3731.966 .383E-04 1 578
436.013 440.702 677.587 630.854 .256E-05 1 579
841.197 599.159 933.380 676.298 .737E-05 1 580
126.585 2278.015 326.756 2467.452 .114E-04 1 581
515.478 3569.819 631.668 3733.580 .959E-05 1 582
0.000 1306.604 147.548 1470.356 .999E-05 1 583
100.600 1906.952 288.596 2108.382 .295E-04 1 584
835.785 581.722 933.380 693.549 .212E-04 1 585
244.403 1355.266 443.953 1554.150 .883E-05 1 586
18.626 2875.313 199.694 3038.963 .136E-04 1 587
319.952 2097.388 538.619 2220.000 .121E-04 1 588
511.938 1355.174 713.953 1542.181 .389E-05 1 589
807.628 1763.817 933.380 1945.727 .259E-04 1 590
167.810 172.672 323.919 370.000 .958E-05 1 591
92.465 174.120 271.591 303.856 .247E-04 1 592
693.822 3600.827 790.765 3733.580 .288E-04 1 593
691.482 3137.268 910.820 3395.174 .109E-04 1 594
724.358 2624.768 917.320 2751.518 .750E-04 1 595

0.000	1279.928	0.159	1280.055	.481E-04	1	596
0.000	1827.320	57.307	1870.663	.119E-04	1	597
453.855	555.881	601.378	740.000	.107E-04	1	598
0.000	1526.313	83.413	1632.229	.271E-04	1	599
333.470	3578.314	537.100	3733.580	.249E-04	1	600
0.000	1126.246	46.326	1168.945	.222E-04	1	601
614.820	3564.792	747.597	3733.580	.175E-04	1	602
618.053	1297.684	782.623	1466.242	.134E-04	1	603
578.058	2752.391	761.386	2956.975	.107E-04	1	604
760.659	2751.058	920.780	2883.664	.226E-04	1	605
157.423	192.129	330.913	370.000	.134E-04	1	606
429.260	1179.053	670.610	1371.573	.558E-05	1	607
714.117	1405.055	906.211	1601.186	.618E-05	1	608
682.474	2861.205	821.510	3045.417	.255E-04	1	609
430.487	1678.200	648.673	1810.491	.137E-04	1	610
0.000	1267.553	95.151	1412.204	.838E-05	1	611
51.527	3356.218	199.080	3551.955	.122E-04	1	612
0.000	736.335	254.842	896.585	.558E-05	1	613
837.845	2663.003	933.380	2749.935	.646E-05	1	614
571.004	3330.000	719.062	3444.009	.118E-04	1	615
163.387	3379.094	360.178	3570.087	.246E-04	1	616
506.712	2804.967	705.691	2993.652	.948E-05	1	617
708.537	2190.279	903.903	2381.934	.922E-05	1	618
645.736	0.000	834.677	145.190	.211E-04	1	619
513.770	51.631	698.989	253.509	.168E-04	1	620
813.666	2528.265	933.380	2691.174	.130E-04	1	621
81.259	356.794	261.785	562.763	.111E-04	1	622
240.407	1308.988	427.258	1585.735	.165E-04	1	623
457.553	1480.000	639.328	1698.768	.138E-04	1	624
714.039	0.000	767.851	53.972	.175E-04	1	625
0.000	611.182	3.268	614.499	.388E-05	1	626
159.188	2722.358	314.084	2906.887	.152E-04	1	627
652.379	2355.548	891.066	2553.926	.272E-04	1	628
890.702	203.565	933.380	241.436	.137E-04	1	629
268.849	1294.911	451.663	1480.000	.125E-04	1	630
77.360	0.000	94.395	12.171	.111E-04	1	631
462.982	1339.280	621.353	1534.596	.975E-05	1	632
359.347	2590.000	506.481	2750.214	.130E-04	1	633
452.023	1713.382	622.622	1926.593	.227E-04	1	634
867.092	3111.374	933.380	3172.616	.196E-04	1	635
167.170	2239.527	344.374	2447.189	.297E-04	1	636
832.371	877.187	933.380	999.508	.337E-04	1	637
0.000	1110.527	18.554	1126.184	.183E-04	1	638
536.578	1742.526	733.772	1954.665	.126E-04	1	639
271.380	1179.519	445.300	1389.454	.275E-05	1	640
818.596	2889.083	933.380	3020.875	.954E-05	1	641
0.000	1870.320	31.849	1898.893	.128E-04	1	642
596.479	1716.927	811.268	1884.995	.208E-04	1	643
196.373	374.022	384.479	500.339	.866E-05	1	644
0.000	3499.593	16.699	3509.953	.116E-04	1	645
623.460	2003.071	780.873	2237.200	.891E-05	1	646
64.078	1587.734	244.035	1772.697	.283E-04	1	647
0.000	2916.357	127.039	3071.791	.867E-05	1	648

0.000 3684.670 38.018 3733.580 .341E-04 1 649
 264.033 70.850 440.697 274.912 .149E-04 1 650
 664.803 994.172 863.322 1180.386 .160E-04 1 651
 560.676 2287.976 767.187 2485.450 .839E-05 1 652
 0.000 3346.773 174.729 3494.468 .311E-04 1 653
 263.716 0.000 355.834 77.443 .848E-05 1 654
 153.652 1039.081 335.300 1241.245 .113E-04 1 655
 440.204 2416.983 600.112 2590.000 .451E-05 1 656
 779.864 2813.256 933.380 3001.828 .667E-05 1 657
 690.132 384.746 891.751 566.792 .325E-04 1 658
 81.193 1583.178 272.829 1775.604 .842E-05 1 659
 670.458 3149.749 852.918 3365.211 .905E-05 1 660
 772.423 80.457 933.380 274.763 .473E-04 1 661
 799.597 2688.001 933.380 2824.260 .730E-05 1 662
 286.879 1480.000 517.370 1666.405 .888E-05 1 663
 536.872 1593.237 717.340 1795.940 .357E-04 1 664
 30.399 421.293 195.254 582.260 .293E-04 1 665
 0.000 437.600 125.889 570.044 .845E-05 1 666
 606.366 2396.523 833.832 2555.707 .436E-04 1 667
 594.174 3330.000 806.964 3538.633 .782E-05 1 668
 431.907 1611.953 618.155 1766.676 .224E-04 1 669
 97.169 2286.408 261.168 2438.870 .136E-04 1 670
 739.660 1164.220 933.380 1313.121 .126E-04 1 671
 0.000 1658.456 32.001 1696.913 .367E-04 1 672
 428.384 2517.302 625.002 2659.095 .189E-04 1 673
 864.304 2030.571 933.380 2101.465 .134E-04 1 674
 13.810 2752.321 194.996 2977.814 .296E-04 1 675
 852.881 2201.490 933.380 2260.621 .387E-05 1 676
 531.483 2129.304 722.345 2321.290 .964E-05 1 677
 510.425 413.001 712.618 652.003 .108E-04 1 678
 0.000 1385.462 81.187 1458.123 .307E-05 1 679
 545.333 2825.724 722.054 3018.001 .185E-04 1 680
 517.149 0.000 585.873 67.969 .136E-04 1 681
 0.000 1539.191 37.958 1574.511 .150E-04 1 682
 362.318 3330.000 588.046 3476.439 .145E-04 1 683
 205.268 161.574 427.741 370.000 .213E-04 1 684
 255.065 2793.657 406.904 3007.899 .109E-04 1 685
 0.000 2530.386 75.503 2606.591 .691E-05 1 686
 132.897 2455.978 306.148 2672.738 .108E-04 1 687
 0.000 464.057 137.283 584.083 .119E-04 1 688
 611.437 3700.000 635.817 3733.580 .962E-05 1 689
 888.536 250.544 933.380 315.257 .175E-04 1 690
 262.125 3296.693 474.806 3463.047 .853E-05 1 691
 500.255 3557.825 644.174 3733.580 .377E-04 1 692
 843.790 47.388 933.380 152.064 .138E-04 1 693
 795.045 2605.660 933.380 2760.949 .760E-05 1 694
 463.533 1893.075 680.215 2054.006 .119E-04 1 695
 727.120 2246.108 877.565 2365.814 .127E-04 1 696
 385.458 137.811 574.293 331.861 .761E-05 1 697
 240.308 3116.877 416.957 3330.000 .577E-05 1 698
 426.592 205.595 654.002 435.475 .522E-05 1 699
 0.000 2322.040 65.310 2386.289 .953E-05 1 700
 0.000 1012.444 7.450 1018.512 .695E-05 1 701

0.000	2490.278	191.968	2639.829	.183E-04	1	702
588.970	370.000	750.174	523.683	.134E-04	1	703
18.763	1870.138	200.847	2068.802	.231E-04	1	704
890.062	2386.875	933.380	2426.271	.149E-04	1	705
665.998	3592.896	817.039	3733.580	.130E-04	1	706
193.547	1550.488	378.867	1745.896	.220E-04	1	707
389.251	370.000	566.509	578.385	.196E-04	1	708
475.156	3700.000	511.924	3733.580	.489E-05	1	709
118.638	3128.107	308.033	3330.000	.329E-04	1	710
235.890	277.998	434.026	492.957	.163E-04	1	711
0.000	2607.359	26.922	2655.650	.135E-04	1	712
73.042	2103.748	279.336	2297.153	.117E-04	1	713
0.000	1772.746	113.071	1897.133	.272E-04	1	714
472.793	841.530	651.280	1065.428	.864E-05	1	715
2.153	2611.220	173.296	2809.805	.173E-04	1	716
119.625	3715.202	136.231	3733.580	.132E-04	1	717
851.749	3520.369	933.380	3592.203	.531E-05	1	718
145.277	2491.589	351.524	2663.969	.209E-04	1	719
279.142	740.000	500.427	918.029	.677E-05	1	720
510.094	3561.453	634.696	3733.580	.133E-04	1	721
907.815	351.401	933.380	370.614	.744E-05	1	722
248.067	3710.186	268.949	3733.580	.838E-05	1	723
350.847	2440.214	575.361	2665.591	.290E-04	1	724
644.790	504.213	874.617	693.820	.131E-04	1	725
333.287	438.100	509.574	640.667	.990E-05	1	726
726.999	2665.501	878.011	2848.244	.157E-04	1	727
200.176	537.164	444.341	740.000	.360E-04	1	728
733.729	332.073	930.107	514.919	.118E-04	1	729
180.893	2288.383	333.131	2509.294	.686E-05	1	730
610.206	2431.280	774.535	2593.689	.549E-05	1	731
704.645	2959.876	913.432	3126.849	.981E-05	1	732
870.489	955.918	933.380	1054.742	.164E-04	1	733
93.900	2966.818	266.208	3172.343	.108E-04	1	734
731.117	0.000	901.785	205.641	.363E-04	1	735
212.260	1944.460	417.163	2167.103	.154E-04	1	736
233.307	1690.227	428.575	1850.000	.949E-05	1	737
277.278	291.508	445.512	450.967	.148E-04	1	738
930.273	2686.945	933.380	2689.236	.775E-05	1	739
286.943	3730.265	289.239	3733.580	.793E-05	1	740
762.690	0.000	899.116	197.150	.287E-04	1	741
482.057	1414.379	633.329	1577.303	.833E-05	1	742
514.328	1903.609	690.182	2130.690	.651E-05	1	743
214.381	2824.056	371.082	3050.938	.210E-04	1	744
83.977	1716.263	336.815	1904.796	.998E-05	1	745
0.000	457.701	157.965	575.710	.238E-04	1	746
309.891	285.505	468.729	536.960	.187E-04	1	747
839.435	2638.383	933.380	2775.144	.276E-04	1	748
737.507	3206.924	933.380	3362.593	.423E-04	1	749
587.364	209.453	742.419	350.001	.728E-05	1	750
336.047	1360.380	514.186	1537.300	.434E-05	1	751
463.243	665.582	599.656	870.793	.111E-04	1	752
0.000	2834.700	71.541	2907.515	.805E-05	1	753
12.372	1120.968	167.052	1308.615	.133E-04	1	754

772.954	1977.793	933.380	2126.892	.122E-04	1	755
451.277	2220.000	598.176	2364.265	.136E-04	1	756
528.951	1480.000	750.710	1665.026	.138E-04	1	757
294.637	740.000	477.786	969.289	.671E-05	1	758
818.744	3338.856	933.380	3507.077	.197E-04	1	759
704.975	3316.799	924.634	3543.128	.613E-05	1	760
770.758	2762.863	921.402	2884.471	.700E-05	1	761
0.000	378.975	175.776	530.860	.206E-04	1	762
881.678	335.099	933.380	378.772	.104E-04	1	763
589.119	1657.467	758.031	1906.694	.141E-04	1	764
0.000	2869.320	43.067	2932.752	.903E-05	1	765
542.214	819.834	718.154	1079.405	.353E-04	1	766
811.281	0.000	933.380	82.745	.537E-05	1	767
642.097	2220.000	815.290	2424.150	.236E-04	1	768
238.639	1106.740	365.904	1294.814	.160E-04	1	769
0.000	159.690	136.327	361.326	.586E-05	1	770
726.427	1743.458	933.380	1883.348	.764E-05	1	771
474.986	573.979	638.221	740.000	.140E-04	1	772
0.000	2728.429	106.380	2885.972	.157E-04	1	773
660.586	3447.222	838.429	3630.836	.132E-04	1	774
29.937	490.231	171.047	694.133	.825E-05	1	775
769.763	1305.972	933.380	1435.726	.889E-05	1	776
129.079	0.000	226.581	144.766	.499E-05	1	777
0.000	3164.682	168.229	3355.726	.868E-05	1	778
315.777	1688.784	549.349	1850.000	.907E-05	1	779
0.000	1599.249	6.757	1606.085	.278E-04	1	780
320.706	2960.000	450.028	3082.508	.146E-04	1	781
298.087	3506.453	492.646	3636.635	.225E-04	1	782
383.359	401.811	626.624	640.952	.901E-05	1	783
395.135	740.000	541.829	960.024	.449E-05	1	784
550.614	676.643	624.873	740.000	.258E-05	1	785
0.000	810.060	161.675	917.695	.138E-04	1	786
743.577	786.374	918.103	902.510	.622E-05	1	787
626.557	2590.000	863.139	2835.929	.296E-04	1	788
588.031	740.000	830.813	993.598	.897E-05	1	789
561.656	2704.712	837.927	2887.863	.184E-04	1	790
311.751	3520.534	582.591	3700.000	.204E-04	1	791
721.895	0.000	733.620	17.715	.130E-04	1	792
433.588	3627.297	481.682	3700.000	.689E-05	1	793
0.000	323.085	26.078	362.543	.239E-04	1	794
449.431	370.000	635.682	652.614	.851E-05	1	795
505.689	816.954	720.325	1030.825	.133E-04	1	796
877.511	198.608	933.380	235.323	.809E-05	1	797
547.390	0.000	640.075	141.182	.933E-05	1	798
704.838	1568.182	928.268	1730.247	.791E-05	1	799
397.136	2022.651	565.796	2220.000	.632E-05	1	800
399.102	2590.000	630.750	2838.880	.645E-05	1	801
903.186	3494.808	933.380	3541.167	.663E-05	1	802
569.069	140.699	753.521	333.647	.952E-05	1	803
461.139	3145.108	581.256	3330.000	.250E-04	1	804
276.155	2235.904	412.009	2343.957	.801E-05	1	805
291.313	3589.772	461.287	3700.000	.127E-04	1	806
728.225	38.154	933.380	170.913	.553E-05	1	807

311.391	3330.000	626.013	3533.161	.710E-05	1	808
241.586	1563.116	426.611	1850.000	.153E-04	1	809
345.208	1615.099	648.350	1810.101	.143E-04	1	810
0.000	698.896	20.803	731.238	.937E-05	1	811
592.428	2050.730	736.121	2274.364	.461E-05	1	812
674.265	2360.761	777.222	2426.733	.158E-04	1	813
871.354	1727.249	933.380	1766.971	.174E-04	1	814
398.794	0.000	553.751	99.124	.194E-04	1	815
343.196	0.000	485.314	127.870	.124E-04	1	816
70.904	1585.831	347.259	1850.000	.185E-04	1	817
312.249	3700.000	365.046	3733.580	.181E-04	1	818
915.778	978.191	933.380	989.374	.832E-05	1	819
247.219	1906.217	348.292	2026.203	.118E-04	1	820
8.747	1236.790	165.470	1483.562	.654E-05	1	821
678.554	1269.730	857.131	1551.074	.677E-05	1	822
0.000	3015.410	33.059	3036.313	.359E-04	1	823
384.226	2590.000	581.659	2714.758	.206E-04	1	824
68.743	1382.896	333.335	1613.934	.150E-04	1	825
593.544	1237.836	922.324	1445.341	.841E-05	1	826
922.990	1688.692	933.380	1695.242	.466E-05	1	827
40.944	554.338	219.681	837.743	.314E-04	1	828
85.493	1751.190	223.320	1837.860	.195E-04	1	829
702.314	663.117	933.380	808.329	.644E-05	1	830
491.251	1245.235	619.784	1364.203	.110E-04	1	831
143.274	1084.588	300.001	1214.066	.773E-05	1	832
165.595	3120.418	500.762	3330.000	.770E-05	1	833
332.754	1850.000	453.945	2043.554	.187E-04	1	834
346.961	1616.227	521.698	1725.352	.649E-05	1	835
471.721	370.000	671.176	494.243	.116E-04	1	836
268.631	0.000	449.636	112.604	.113E-04	1	837
20.481	1072.689	217.323	1388.632	.133E-04	1	838
654.916	186.656	831.208	469.794	.206E-04	1	839
464.120	73.233	672.383	201.769	.538E-05	1	840
451.973	3074.215	610.007	3330.000	.133E-04	1	841
744.345	2916.960	835.295	3064.360	.818E-05	1	842
424.832	126.428	615.068	243.359	.823E-05	1	843
305.014	2220.000	719.688	2474.709	.845E-05	1	844
570.843	1850.000	670.520	2011.976	.767E-05	1	845
286.977	638.086	420.235	740.000	.505E-05	1	846
170.314	0.000	203.527	54.081	.816E-05	1	847
886.572	2436.178	933.380	2512.817	.385E-05	1	848
265.728	0.000	563.805	180.620	.124E-04	1	849
688.804	2129.537	889.447	2459.918	.134E-04	1	850
815.976	3114.092	933.380	3307.551	.107E-04	1	851
467.160	2803.594	587.782	2960.000	.638E-05	1	852
909.190	3291.430	933.380	3331.646	.156E-04	1	853
932.800	672.053	933.380	673.019	.142E-04	1	854
498.115	2590.000	785.881	2761.986	.103E-04	1	855
163.172	3056.077	431.780	3216.486	.795E-05	1	856
728.132	2382.965	933.380	2608.012	.941E-05	1	857
0.000	2109.064	23.700	2148.773	.217E-04	1	858
194.234	1201.785	396.568	1322.033	.887E-05	1	859
662.404	1110.000	781.291	1247.914	.553E-05	1	860

840.330	2497.241	895.490	2590.109	.116E-04	1	861
788.823	1401.437	910.829	1607.014	.164E-04	1	862
593.187	827.466	878.907	1075.663	.260E-04	1	863
916.564	1771.493	933.380	1781.413	.622E-05	1	864
634.028	2341.498	892.395	2635.401	.601E-05	1	865
212.061	189.274	318.694	370.000	.174E-04	1	866
573.982	370.000	776.167	551.955	.470E-05	1	867
699.474	733.834	826.367	841.466	.608E-04	1	868
0.000	3615.647	181.910	3721.743	.102E-04	1	869
739.796	712.023	933.380	824.723	.464E-05	1	870
739.757	2277.020	933.380	2608.951	.457E-05	1	871
82.158	3189.807	323.850	3330.000	.789E-05	1	872
414.793	618.340	542.040	740.000	.303E-05	1	873
0.000	1878.367	203.199	1995.793	.943E-05	1	874
83.149	3013.813	170.687	3123.602	.187E-04	1	875
66.030	0.000	173.511	74.427	.631E-05	1	876
545.482	2220.000	676.461	2315.915	.300E-05	1	877
36.300	2828.018	171.576	3064.460	.102E-04	1	878
200.903	1560.329	365.409	1850.000	.198E-04	1	879
603.045	740.000	817.901	909.206	.185E-04	1	880
0.000	933.286	162.205	1024.680	.816E-05	1	881
538.551	2445.789	706.407	2626.248	.138E-04	1	882
752.796	694.842	933.380	878.289	.615E-05	1	883
38.271	993.195	189.510	1263.500	.558E-05	1	884
332.767	3700.000	351.533	3733.580	.437E-05	1	885
346.396	0.000	413.417	55.008	.569E-05	1	886
649.657	1480.000	860.712	1732.933	.968E-05	1	887
27.166	1839.796	85.360	1945.134	.410E-04	1	888
769.426	1162.194	901.185	1234.150	.121E-04	1	889
455.789	3187.396	713.880	3328.155	.653E-05	1	890
0.000	2641.159	74.381	2778.768	.485E-05	1	891
103.191	0.000	188.094	157.583	.861E-05	1	892
925.533	1143.920	933.380	1158.533	.513E-05	1	893
932.331	747.201	933.380	747.964	.761E-05	1	894
764.591	603.049	933.380	774.671	.218E-04	1	895
40.639	2490.516	174.944	2614.668	.609E-05	1	896
0.000	756.784	65.645	790.589	.663E-05	1	897
639.722	2878.953	847.855	2985.405	.519E-05	1	898
16.083	1707.370	144.263	1772.107	.104E-04	1	899
13.433	2140.875	107.324	2187.460	.412E-05	1	900
6.751	640.349	215.339	743.499	.798E-05	1	901
282.009	926.188	370.003	1110.000	.104E-04	1	902
121.868	38.667	262.395	195.145	.104E-04	1	903
666.503	1816.146	699.096	1886.589	.125E-04	1	904
286.296	1850.000	455.117	2220.000	.100E-04	1	905
831.951	578.152	933.380	654.236	.410E-05	1	906
769.427	750.685	908.220	1065.251	.672E-05	1	907
0.000	3621.547	137.011	3733.580	.532E-05	1	908
865.415	1841.160	933.380	1869.870	.740E-05	1	909
271.886	2231.520	611.452	2372.693	.534E-05	1	910
788.800	3662.241	816.185	3733.580	.311E-05	1	911
25.560	2208.087	297.405	2312.438	.714E-05	1	912
795.962	0.000	902.735	40.986	.409E-05	1	913


```

724.999 1386.839 880.857 1575.299 .763E-05 1 914
0.000 2909.649 386.771 3058.116 .129E-04 1 915
460.371 236.884 678.054 320.444 .564E-05 1 916
894.867 672.778 933.380 687.561 .105E-04 1 917
WELLS
466.000 20.000 10875.000 0.330 1 10875.000
466.000 3730.000 0.330 1
END WELLS

```

A1.3 LDF File

*TITLE: Example Layer Description *** Imaginary Data to get program Running! ****

GRID Dimensions: Y X # of Layers

2 2 1

LAYER 1 TOP:

10875.0 10875.0

10875.0 10875.0

LAYER 1 BOTTOM:

11016.5 11016.5

11016.5 11016.5

LAYER 1 POROSITY:

0.04 0.04

0.04 0.04

LAYER 1 PERMEABILITY:

0.000055 0.000055

0.000055 0.000055

A1.4 BHP File

Calculation of Bottom-Hole Flowing Pressures by
Method of Cullender and Smith

ID Header (<= 80 characters)

joachim

WELL Number (for NFflow)

1

True vertical DEPTH to middle of reservoir (feet)

10875

DISTANCE down hole to middle of producing zone (feet)

10875

Equivalent inside DIAMETER of tubing or casing (inches)

6.625

Pipe ROUGHNESS FACTOR (Fr; SPE Pet. Eng. Handbook Tables 33.10 & 33.11)

0.0007837

WELLHEAD & RESERVOIR TEMPERATURES (F)

60.0 285.0

Gas SPECIFIC GRAVITY (air = 1.0)

0.621

PSEUDOCRITICAL TEMPERATURE (Rankine) & PRESSURE (psia)

353.8 672.9

RESULTS

day (d)	Qg (Mscf/d)	Ptf (psia)	Pwf(psia)
0.00	5800.00		3600.00
5.00	5710.48		3576.50
10.00	5686.35		3527.37
15.00	5641.16		3435.33
20.00	5638.54		3294.15
25.00	5367.65		3074.58
30.00	5215.93		2982.88
35.00	5085.75		2870.71
40.00	4745.58		2609.69
45.00	4720.53		2580.59
50.00	4373.32		2370.39
55.00	4288.12		2298.38
60.00	4040.34		2215.51
65.00	3895.01		2157.38
70.00	3690.95		2079.06
75.00	3687.85		2078.32
80.00	3492.22		1994.44
85.00	3239.95		1906.87
90.00	3237.79		1906.24
95.00	2944.26		1813.32
100.00	2844.36		1758.23
105.00	2748.87		1738.35
110.00	2573.08		1697.67
115.00	2522.58		1688.12
120.00	2419.39		1939.23
125.00	2389.31		1719.66
130.00	2358.08		1757.94
135.00	2336.84		1837.43
140.00	2324.60		1672.77
145.00	2299.82		1793.37
150.00	2258.87		1931.80
155.00	2237.62		1633.82
160.00	2163.49		1616.04
165.00	2077.88		1602.80
170.00	1980.48		1704.92
175.00	1968.26		1750.68
180.00	1963.43		1846.17
185.00	1960.27		1571.69
190.00	1930.49		1556.28
195.00	1910.76		1534.93
200.00	1876.51		1525.17
205.00	1735.35		1584.51
210.00	1708.39		1611.94
215.00	1687.45		1588.53
220.00	1658.05		1575.39
225.00	1609.12		1557.57
230.00	1583.37		1463.57
235.00	1575.50		1534.20
240.00	1561.17		1498.76

245.00	1560.78	1495.06
250.00	1558.26	1565.69
255.00	1553.20	1565.79
260.00	1542.57	1605.20
265.00	1542.43	1606.85
270.00	1366.53	1750.85
275.00	1366.93	1852.76
280.00	1380.28	1856.58
285.00	1635.10	1346.89
290.00	1681.01	1350.34
295.00	1549.93	1370.56
300.00	1465.82	1429.35
305.00	1456.34	1449.10
310.00	1432.32	1480.53
315.00	1415.37	1715.87
320.00	1407.40	1578.67
325.00	1418.89	1355.15
330.00	1446.21	1417.98
335.00	1446.92	1428.72
340.00	1447.03	1645.48
345.00	1447.17	1433.77
350.00	1447.34	1433.84
355.00	1434.44	1433.85
360.00	1404.76	1245.66

A1.5 RES File (Rate controlled)

TITLE

Well GU#3, Abbreviated Simulation

LDF FILE: C:\N\GoodResults\Uniform5\gu32.ldf

PG_DATUM DATUM

7000.0 10875.0

TSC PSC TRES

60.0 14.7 285.0

PG ZG UG

300.0 .986 0.0138

600.0 .974 0.0142

900.0 .963 0.0146

1200.0 .956 0.0150

1500.0 .950 0.0154

1800.0 .948 0.0159

2100.0 .948 0.0163

2400.0 .950 0.0168

2700.0 .954 0.0173

3000.0 .961 0.0178

3300.0 .970 0.0183

3600.0 .980 0.0189

3900.0 .992 0.0194

4200.0 1.006 0.0200

4500.0 1.020 0.0206

4800.0 1.035 0.0212

5100.0	1.052	0.0218
5400.0	1.069	0.0224
5700.0	1.086	0.0230
6000.0	1.105	0.0236
6300.0	1.123	0.0243
6600.0	1.143	0.0249
6900.0	1.162	0.0256
7200.0	1.182	0.0263
7500.0	1.202	0.0269
7800.0	1.222	0.0276
8100.0	1.243	0.0283
8400.0	1.263	0.0289
8700.0	1.284	0.0296
9000.0	1.305	0.0302
9300.0	1.326	0.0309
9600.0	1.347	0.0315
9900.0	1.369	0.0321
10200.0	1.390	0.0327
10500.0	1.411	0.0333
10800.0	1.432	0.0338
11100.0	1.454	0.0344
11400.0	1.475	0.0349
11700.0	1.497	0.0354
12000.0	1.518	0.0358
12300.0	1.539	0.0362

END PVT

NETWORK

NODES

DATA FOR WELL 1 IN FILE C:\N\GoodResults\Uniform5\Eagle2.bhp

TIME 0.0

OMEGA = 1.97

LOG = 6

DT = 15

OUTPUT WELL AT 5.00 EVERY 5.00 W/GRAPHICS

OUTPUT RES AT 30.00 EVERY 30.00 W/GRAPHICS NUMBERS TYPE

PRODUCE 1 AT 5800 MCF/D

TIME 5.00

PRODUCE 1 AT 5710 MCF/D

TIME 10.00

PRODUCE 1 AT 5686 MCF/D

TIME 15.00

PRODUCE 1 AT 5641 MCF/D

TIME 20.00

PRODUCE 1 AT 5638 MCF/D

TIME 25.00

PRODUCE 1 AT 5367 MCF/D

TIME 30.00

PRODUCE 1 AT 5215 MCF/D

TIME 35.00

PRODUCE 1 AT 5085 MCF/D

TIME 40.00

PRODUCE 1 AT 4745 MCF/D

TIME 45.00

*PRODUCE 1 AT 4720 MCF/D
TIME 50.0
PRODUCE 1 AT 4373 MCF/D
TIME 55.00
PRODUCE 1 AT 4288 MCF/D
TIME 60.00
PRODUCE 1 AT 4040 MCF/D
TIME 65.00
PRODUCE 1 AT 3895 MCF/D
TIME 70.00
PRODUCE 1 AT 3690 MCF/D
TIME 75.00
PRODUCE 1 AT 3687 MCF/D
TIME 80.00
PRODUCE 1 AT 3492 MCF/D
TIME 85.00
PRODUCE 1 AT 3239 MCF/D
TIME 90.00
PRODUCE 1 AT 3237 MCF/D
TIME 95.00
PRODUCE 1 AT 2944 MCF/D
TIME 100.00
PRODUCE 1 AT 2844 MCF/D
TIME 105.00
PRODUCE 1 AT 2748 MCF/D
TIME 110.00
PRODUCE 1 AT 2573 MCF/D
TIME 115.00
PRODUCE 1 AT 2522 MCF/D
TIME 120.00
PRODUCE 1 AT 2419 MCF/D
TIME 125.00
PRODUCE 1 AT 2389 MCF/D
TIME 130.00
PRODUCE 1 AT 2358 MCF/D
TIME 135.00
PRODUCE 1 AT 2336 MCF/D
TIME 140.00
PRODUCE 1 AT 2324 MCF/D
TIME 145.00
PRODUCE 1 AT 2299 MCF/D
TIME 150.00
PRODUCE 1 AT 2258 MCF/D
TIME 155.00
PRODUCE 1 AT 2237 MCF/D
TIME 160.00
PRODUCE 1 AT 2163 MCF/D
TIME 165.00
PRODUCE 1 AT 2077 MCF/D
TIME 170.00
PRODUCE 1 AT 1980 MCF/D
TIME 175.00
PRODUCE 1 AT 1968 MCF/D*

TIME 180.00
PRODUCE 1 AT 1963 MCF/D
TIME 185.00
PRODUCE 1 AT 1960 MCF/D
TIME 190.00
PRODUCE 1 AT 1930 MCF/D
TIME 195.00
PRODUCE 1 AT 1910 MCF/D
TIME 200.00
PRODUCE 1 AT 1876 MCF/D
TIME 205.00
PRODUCE 1 AT 1735 MCF/D
TIME 210.00
PRODUCE 1 AT 1708 MCF/D
TIME 215.00
PRODUCE 1 AT 1687 MCF/D
TIME 220.00
PRODUCE 1 AT 1658 MCF/D
TIME 225.00
PRODUCE 1 AT 1609 MCF/D
TIME 230.00
PRODUCE 1 AT 1583 MCF/D
TIME 235.00
PRODUCE 1 AT 1575 MCF/D
TIME 240.00
PRODUCE 1 AT 1561 MCF/D
TIME 245.00
PRODUCE 1 AT 1560 MCF/D
TIME 250.00
PRODUCE 1 AT 1558 MCF/D
TIME 255.00
PRODUCE 1 AT 1553 MCF/D
TIME 260.00
PRODUCE 1 AT 1542 MCF/D
TIME 265.00
PRODUCE 1 AT 1542 MCF/D
TIME 270.00
PRODUCE 1 AT 1366 MCF/D
TIME 275.00
PRODUCE 1 AT 1366 MCF/D
TIME 280.00
PRODUCE 1 AT 1380 MCF/D
TIME 285.00
PRODUCE 1 AT 1635 MCF/D
TIME 290.00
PRODUCE 1 AT 1681 MCF/D
TIME 295.00
PRODUCE 1 AT 1549 MCF/D
TIME 300.00
PRODUCE 1 AT 1465 MCF/D
TIME 305.00
PRODUCE 1 AT 1456 MCF/D
TIME 310.00

PRODUCE 1 AT 1432 MCF/D
 TIME 315.00
 PRODUCE 1 AT 1415 MCF/D
 TIME 320.00
 PRODUCE 1 AT 1407 MCF/D
 TIME 325.00
 PRODUCE 1 AT 1418 MCF/D
 TIME 330.00
 PRODUCE 1 AT 1446 MCF/D
 TIME 335.00
 PRODUCE 1 AT 1446 MCF/D
 TIME 340.00
 PRODUCE 1 AT 1447 MCF/D
 TIME 345.00
 PRODUCE 1 AT 1447 MCF/D
 TIME 350.00
 PRODUCE 1 AT 1447 MCF/D
 TIME 355.00
 PRODUCE 1 AT 1434 MCF/D
 TIME 360.00
 PRODUCE 1 AT 1404 MCF/D
 STOP

A1.6 RES File (Pressure controlled)

TITLE

Well GU#3, Abbreviated Simulation

LDF FILE: C:\N\GoodResults\Uniform5\Gu3.ldf

PG_DATUM DATUM

4200.0	10875.0		
<i>TSC</i>	<i>PSC</i>	<i>TRES</i>	
60.0	14.7	285.0	
<i>PG</i>	<i>ZG</i>	<i>UG</i>	
300.0	.986	0.0138	
600.0	.974	0.0142	
900.0	.963	0.0146	
1200.0	.956	0.0150	
1500.0	.950	0.0154	
1800.0	.948	0.0159	
2100.0	.948	0.0163	
2400.0	.950	0.0168	
2700.0	.954	0.0173	
3000.0	.961	0.0178	
3300.0	.970	0.0183	
3600.0	.980	0.0189	
3900.0	.992	0.0194	
4200.0	1.006	0.0200	
4500.0	1.020	0.0206	
4800.0	1.035	0.0212	
5100.0	1.052	0.0218	
5400.0	1.069	0.0224	

5700.0	1.086	0.0230
6000.0	1.105	0.0236
6300.0	1.123	0.0243
6600.0	1.143	0.0249
6900.0	1.162	0.0256
7200.0	1.182	0.0263
7500.0	1.202	0.0269
7800.0	1.222	0.0276
8100.0	1.243	0.0283
8400.0	1.263	0.0289
8700.0	1.284	0.0296
9000.0	1.305	0.0302
9300.0	1.326	0.0309
9600.0	1.347	0.0315
9900.0	1.369	0.0321
10200.0	1.390	0.0327
10500.0	1.411	0.0333
10800.0	1.432	0.0338
11100.0	1.454	0.0344
11400.0	1.475	0.0349
11700.0	1.497	0.0354
12000.0	1.518	0.0358
12300.0	1.539	0.0362

END PVT

NETWORK

NODES

DATA FOR WELL 1 IN FILE C:\N\GoodResults\Uniform5\Eagle2.bhp

TIME 0.0

OMEGA = 1.97

LOG = 6

DT = 15

OUTPUT WELL AT 5.00 EVERY 5.00 W/GRAPHICS

OUTPUT RES AT 30.00 EVERY 30.00 W/GRAPHICS NUMBERS TYPE

PRODUCE 1 AT 3600 PSI

TIME 5.00

PRODUCE 1 AT 3576 PSI

TIME 10.00

PRODUCE 1 AT 3527 PSI

TIME 15.00

PRODUCE 1 AT 3435 PSI

TIME 20.00

PRODUCE 1 AT 3294 PSI

TIME 25.00

PRODUCE 1 AT 3074 PSI

TIME 30.00

PRODUCE 1 AT 2982 PSI

TIME 35.00

PRODUCE 1 AT 2870 PSI

TIME 40.00

PRODUCE 1 AT 2609 PSI

TIME 45.00

PRODUCE 1 AT 2580 PSI

TIME 50.0

*PRODUCE 1 AT 2370 PSI
TIME 55.00
PRODUCE 1 AT 2298 PSI
TIME 60.00
PRODUCE 1 AT 2215 PSI
TIME 65.00
PRODUCE 1 AT 2157 PSI
TIME 70.00
PRODUCE 1 AT 2079 PSI
TIME 75.00
PRODUCE 1 AT 2078 PSI
TIME 80.00
PRODUCE 1 AT 1994 PSI
TIME 85.00
PRODUCE 1 AT 1906 PSI
TIME 90.00
PRODUCE 1 AT 1905 PSI
TIME 95.00
PRODUCE 1 AT 1813 PSI
TIME 100.00
PRODUCE 1 AT 1758 PSI
TIME 105.00
PRODUCE 1 AT 1738 PSI
TIME 110.00
PRODUCE 1 AT 1697 PSI
TIME 115.00
PRODUCE 1 AT 1688 PSI
TIME 120.00
PRODUCE 1 AT 1938 PSI
TIME 125.00
PRODUCE 1 AT 1719 PSI
TIME 130.00
PRODUCE 1 AT 1757 PSI
TIME 135.00
PRODUCE 1 AT 1837 PSI
TIME 140.00
PRODUCE 1 AT 1672 PSI
TIME 145.00
PRODUCE 1 AT 1793 PSI
TIME 150.00
PRODUCE 1 AT 1931 PSI
TIME 155.00
PRODUCE 1 AT 1633 PSI
TIME 160.00
PRODUCE 1 AT 1616 PSI
TIME 165.00
PRODUCE 1 AT 1602 PSI
TIME 170.00
PRODUCE 1 AT 1704 PSI
TIME 175.00
PRODUCE 1 AT 1750 PSI
TIME 180.00
PRODUCE 1 AT 1846 PSI*

TIME 185.00
PRODUCE 1 AT 1571 PSI
TIME 190.00
PRODUCE 1 AT 1556 PSI
TIME 195.00
PRODUCE 1 AT 1534 PSI
TIME 200.00
PRODUCE 1 AT 1252 PSI
TIME 205.00
PRODUCE 1 AT 1584 PSI
TIME 210.00
PRODUCE 1 AT 1611 PSI
TIME 215.00
PRODUCE 1 AT 1588 PSI
TIME 220.00
PRODUCE 1 AT 1575 PSI
TIME 225.00
PRODUCE 1 AT 1557 PSI
TIME 230.00
PRODUCE 1 AT 1463 PSI
TIME 235.00
PRODUCE 1 AT 1534 PSI
TIME 240.00
PRODUCE 1 AT 1498 PSI
TIME 245.00
PRODUCE 1 AT 1495 PSI
TIME 250.00
PRODUCE 1 AT 1565 PSI
TIME 255.00
PRODUCE 1 AT 1566 PSI
TIME 260.00
PRODUCE 1 AT 1605 PSI
TIME 265.00
PRODUCE 1 AT 1606 PSI
TIME 270.00
PRODUCE 1 AT 1750 PSI
TIME 275.00
PRODUCE 1 AT 1852 PSI
TIME 280.00
PRODUCE 1 AT 1856 PSI
TIME 285.00
PRODUCE 1 AT 1346 PSI
TIME 290.00
PRODUCE 1 AT 1350 PSI
TIME 295.00
PRODUCE 1 AT 1370 PSI
TIME 300.00
PRODUCE 1 AT 1429 PSI
TIME 305.00
PRODUCE 1 AT 1449 PSI
TIME 310.00
PRODUCE 1 AT 1480 PSI
TIME 315.00

*PRODUCE 1 AT 1715 PSI
TIME 320.00
PRODUCE 1 AT 1578 PSI
TIME 325.00
PRODUCE 1 AT 1355 PSI
TIME 330.00
PRODUCE 1 AT 1417 PSI
TIME 335.00
PRODUCE 1 AT 1428 PSI
TIME 340.00
PRODUCE 1 AT 1645 PSI
TIME 345.00
PRODUCE 1 AT 1433 PSI
TIME 350.00
PRODUCE 1 AT 1434 PSI
TIME 355.00
PRODUCE 1 AT 1435 PSI
TIME 360.00
PRODUCE 1 AT 1245 PSI
STOP*

APPENDIX 2

A2.1 Case 1 Preliminary Calculation

A2.1.1 Fracture Length

When varying the fracture length to ensure that the 2d fracture density is kept constant by recalculating the values of the density of fracture center point such that only one parameter is varied at any point. The relationship between the density of fracture center points and the 2d-fracture density is given as

$$D_i * L_i = D_{fi} \tag{A1}$$

Table A2.1: Case 1 fracture length FracGen input calculation

D_i	$L_i(\text{ft})$	$D_{fi} (\text{ft}/\text{ft}^2)$
0.0002	280	0.056
0.000267	210	0.056
0.0004	140	0.056
0.00016	350	0.056
0.000133	420	0.056

A2.1.2 Fracture Density

When varying the fracture density to ensure that the 2d fracture density is varied and not the density of fracture center point since it represents the fracture density. Using the same relationship stated above **eqn. A1**.

Table A2.2: Case 1 fracture density FracGen input calculation

Di	Li(ft)	Dfi (ft/ft²)
0.0002	280	0.056
0.00015	280	0.042
0.0001	280	0.028
0.00025	280	0.07
0.0003	280	0.084

A2.2 Case 2 Preliminary Calculation

For this analysis the 2d fracture density (0.056 ft/ft²) obtained in case 1 was used as a known parameter subsequently other parameters needed was calculated from the 2d fracture density.

A2.2.1 Fracture Length

When varying the fracture length to ensure that the 2d fracture density is kept constant by recalculating the values of the density of fracture center point such that only one parameter is varied at any point.

The relationship between the two is shown in **eqn. A2**,

$$Dfi = 12 mi di (lci - li) li Dci \quad (A2)$$

where

m_i = exponential mean offset (or “spacing”) of fractures from their associated cluster axis (ft).

d_i = mean intra-cluster fracture center-point density (pts/ft²).

l_{ci} = mean length of clusters (ft).

l_i = mean fracture length (ft).

D_{ci} = cluster center-point density (pts/ft²).

$$d_i = D_{fi} / (12 m_i D_{ci} (l_{ci} - l_i) l_i) \quad (A3)$$

From **eqn. A2** we can compute the different cluster center-point density as the mean fracture length changes.

Table A2.3: Case 2 fracture length FracGen input calculation

	D_{fi}	m_i	d_i	l_{ci}	l_i	D_{ci}
Control	0.056	40	0.000059476	1500	280	0.000005742
-25%	0.056	40	0.000059476	1500	210	0.000007241
-50%	0.056	40	0.000059476	1500	140	0.000010302
25%	0.056	40	0.000059476	1500	350	0.000004874
50%	0.056	40	0.000059476	1500	420	0.000004324
100%	0.056	40	0.000059476	1500	560	0.000003726

A2.2.2 Fracture Density

When varying the fracture density some preliminary calculation was done to ensure that the 2d fracture density varied accurately by recalculating the values of the density of fracture center point, for this analysis the mean intra-cluster fracture center-point density was kept constant. The relationship between these parameters is **eqn. A2**,

Also rearranging equation A2 we have

$$D_{ci} = D_{fi} / (12 m_i d_i (l_{ci} - l_i) l_i) \quad (A4)$$

From **eqn. A4** we can compute the density of fracture center point as the mean fracture length is kept constant.

Table A2.4: Case 2 fracture density FracGen input calculation

	Dfi	mi	di	lci	li	Dci
Control	0.056	40	0.000059476	1500	280	0.000005742
-25%	0.042	40	0.000059476	1500	280	0.000004307
-50%	0.028	40	0.000059476	1500	280	0.000002871
25%	0.07	40	0.000059476	1500	280	0.000007178
50%	0.084	40	0.000059476	1500	280	0.000008614
100%	0.112	40	0.000059476	1500	280	0.000011485

A2.3 Case 3 Preliminary Calculation

A2.3.1 Fracture Length

In this case we have 2 uniformly distributed fracture sets, the primary and secondary fracture sets. The 2d-fracture density of the primary is made 75% of the value in case 1, which is 0.042 ft/ft². The 2d-fracture density of the secondary fracture set is then 0.014 ft/ft² and it is kept constant throughout the study. When varying the fracture length of the primary fracture set, to ensure that the 2d fracture density is kept constant the values of the density of fracture center point is recalculated such that only one parameter is varied at any point. The relationship between the density of fracture center points and the 2d-fracture density is given as **eqn. A1** above

Table A2.5: Case 3 fracture length FracGen input calculation

Di	Li(ft)	Dfi (ft/ft²)
0.00015	280	0.042
0.0002	210	0.042
0.0003	140	0.042
0.00012	350	0.042
0.0001	420	0.042

A2.3.2 Fracture Density

When varying the fracture density of the primary fracture set to ensure that the 2d fracture density is varied and not the density of fracture center point since it represents the fracture density. Using the same relationship stated above we have that;

Table A2.6: Case 3 fracture density FracGen input calculation

Di	Li(ft)	Dfi (ft/ft²)
0.0002	280	0.042
0.00015	280	0.028
0.0001	280	0.014
0.00025	280	0.056
0.0003	280	0.07

A2.4 Case 4 Preliminary Calculation

In this case we have 2 fracture sets, where one is clustered and the other is uniformly distributed, the primary and secondary fracture sets. The clustered fracture network is the primary while the uniform fracture network is the secondary. The 2d-fracture density

of the primary is made 75% of the value in case 1, which is 0.042 ft/ft². The 2d-fracture density of the secondary fracture set is then 0.014 ft/ft² and it is kept constant throughout the study. The 2d fracture density and other were used as known parameters subsequently other parameters needed was calculated from the relationship.

A2.4.1 Fracture Length

When varying the fracture length of the primary fracture set to ensure that the 2d fracture density is kept constant by recalculating the values of the density of fracture center point such that only one parameter is varied at any point.

The relationship between the two is **eqn. A5**.

$$d_i = D_{fi} / (12 m_i D_{ci} (l_{ci} - l_i) l_i) \quad (\text{A5})$$

From **eqn. A5** we can compute the different cluster center-point density as the mean fracture length changes.

Table A2.7: Case 4 fracture length FracGen input calculation

	D_{fi}	m_i	d_i	l_{ci}	l_i	D_{ci}
Control	0.042	40	0.000059476	1500	280	0.000004307
-25%	0.042	40	0.000059476	1500	210	0.000005431
-50%	0.042	40	0.000059476	1500	140	0.000007727
25%	0.042	40	0.000059476	1500	350	0.000003655
50%	0.042	40	0.000059476	1500	420	0.000003243
100%	0.042	40	0.000059476	1500	560	0.000002795

A2.4.2 Fracture Density

When varying the fracture density of the primary fracture set some preliminary calculation was done to ensure that the 2d fracture density varied accurately by recalculating the values of the density of fracture center point, for this analysis the mean intra-cluster fracture center-point density was kept constant. The relationship between these parameters is **eqn. A4**.

From **eqn. A4** we can compute the density of fracture center point as the mean fracture length is kept constant.

Table A2.8: Case 4 fracture density FracGen input calculation

	Dfi	mi	di	lci	li	Dci
Control	0.042	40	0.000059476	1500	280	0.000004307
-25%	0.0315	40	0.000059476	1500	280	0.000003230
-50%	0.021	40	0.000059476	1500	280	0.000002153
25%	0.0525	40	0.000059476	1500	280	0.000005383
50%	0.063	40	0.000059476	1500	280	0.000006460
100%	0.084	40	0.000059476	1500	280	0.000008614

VITA

Name: Joachim Nwabunwanne Ogbechie

Address: Dept. of Petroleum Engineering, Texas A&M University.

Email Address: Joachim.ogbechie@pe.tamu.edu

Education: B.Eng., Electrical/Electronic Engr., University of Benin, 2004
M.S., Petroleum Engineering, Texas A&M University, 2011